8-9-2014

SIX1 OVEREXPRESSION PROMOTES EPITHELIAL–MESENCHYMAL TRANSITION AND MALIGNANT PROGRESSION IN MODELS OF CERVICAL AND COLON CANCER

Hanwen Xu
University of South Carolina - Columbia

SIX1 OVEREXPRESSION PROMOTES EPITHELIAL–MESENCHYMAL TRANSITION AND MALIGNANT PROGRESSION IN MODELS OF CERVICAL AND COLON CANCER

By

Hanwen Xu

Bachelor of Science
China Pharmaceutical University, 2005

Master of Science
Nanjing University, 2008

Submitted in Partial Fulfillment of the Requirements

For the Degree of Doctor of Philosophy in

Pharmaceutical Sciences

College of Pharmacy

University of South Carolina

2014

Accepted by:

Kim E. Creek, Major Professor

Campbell McInnes, Committee Member

Lucia A. Pirisi-Creek, Committee Member

Sondra Berger, Committee Member

Sherine Chan, Committee Member

Lacy Ford, Vice Provost and Dean of Graduate Studies

DEDICATION

To my husband Zhang Yu, without whose love and support this accomplishment would never have been possible.

ACKNOWLEDGEMENTS

I would like to thank my mentor, Dr. Kim E. Creek for his constant support and encouragement. Thanks for willing to listen, discuss and inspire my crazy ideas, and giving me freedom to explore new directions. Thanks also for taking me as a student when my former mentor left. I would also like to express my gratitude to Dr. Lucia Pirisi-Creek for her guidance and experience. The wisdom, decency and warmth they showed me do and will continue to make me not only a better scientist but a better person.

I would also like to thank the members of my dissertation committee, Dr. Campbell McInnes, Dr. Sondra Berger and Dr. Sherine Chan for their valuable suggestions and criticisms.

I would like to thank Dr. Maria M. Peña and her lab group for supporting all my animal experiments. Thanks to Drs. Yuxun Wang and Bin Huang for teaching me cloning techniques. Thanks to Ms. Rupa Velidandla and Ms. Susannah Kassler for being my English teachers. Thanks to Dr. Diego Altomare and for helping with my Microarray. Thanks to all the members in the lab.

Last but not least, I am deeply grateful to my parents, my husband and my daughter for their endless and unconditional love. They are always my most priceless treasure.

ABSTRACT

Inappropriate expression of embryonic genes, particularly homeodomain transcription factors, contributes to tumorigenesis and tumor progression. The overexpression of Six1, a member of the Six family of homeodomain transcription factors, has been found in various human cancers, and is associated with tumor progression and metastasis. We have previously determined that the expression of SIX1 mRNA increased during *in vitro* progression of human papillomavirus type 16 (HPV16)-immortalized human keratinocytes (HKc/HPV16) toward a differentiation-resistant (HKc/DR) phenotype. However, the mechanism(s) of how Six1 promotes HPV16-mediated transformation remain unknown. In this study, we explored the role of Six1 at early stages and late stages of HPV16-mediated transformation by overexpressing Six1 in HKc/HPV16 and HKc/DR. We found that HKc/HPV16 and HKc/DR overexpressing Six1 exhibited a more mesenchymal phenotype compared to vector controls, as characterized by a fibroblastic appearance and increased invasion. We utilized Whole Human Genome Microarrays to explore the gene expression changes associated with Six1 overexpression in HKc/HPV16 and HKc/DR. Using a combination of KEGG pathway analysis, realtime PCR, and Western blotting, we determined that overexpression of Six1 downregulated epithelial-related genes and upregulated mesenchymal-related genes, which suggests that Six1 overexpression induces epithelial-mesenchymal transition (EMT). In addition, we observed alterations in the transforming

growth factor-beta (TGF-β) pathway and activation of the Mitogen-activated protein kinase (MAPK) pathway in response to Six1 overexpression, indicating that Smad-independent pathways of TGF-β signaling may be involved in Six1-mediated EMT. Moreover, the overexpression of Six1 in HKc/HPV16 resulted in resistance to serum and calcium-induced differentiation, which is the hallmark of the HKc/DR phenotype; while Six1 overexpression in HKc/DR resulted in malignant conversion and increased the cancer stem cell (CSC)-like population. The activation of MAPK is linked to Six1-mediated resistance to calcium-induced differentiation in HKc/HPV16 and Six1-associated features of CSCs in HKc/DR. Finally, we used a series of MAPK inhibitors to further demonstrate the important role MAPK activation plays in Six1-induced EMT and CSCs properties. Taken together, this study determined that Six1 overexpression resulted in differentiation resistance and promoted EMT at early stages of HPV16-mediated transformation, and Six1 overexpression promotes EMT, CSCs properties, and malignant conversion at late stages of HPV16-mediated transformation of HKc.

We also used an orthotopic mouse model and a splenic injection metastasis model to investigate the role of Six1 overexpression in colorectal cancer (CRC) progression and metastasis. We found that overexpression of Six1 dramatically promoted CRC tumor growth and metastasis *in vivo*, increased features of cancer stem cells (CSCs), and stimulated angiogenesis by up-regulating the expression of vascular endothelial growth factor (VEGF). Moreover, we determined that Six1 overexpression results in the recruitment of tumor-associated macrophages (TAM) by increasing the expression of macrophage-specific colony-stimulating factor-1 (CSF-1), chemokine (C-C motif) ligand 2/5 (CCL2/5) and VEGF, which further facilitates CRC tumor growth and metastasis.

Furthermore, we determined that Six1 activated ERK and p38 MAPK signaling in MC38 CRC cells. In summary, our studies strongly suggest that Six1 overexpression promotes malignant progression in models of cervical and colon cancer, and MAPK activation may play a pivotal role in Six1-associated tumor progression.

TABLE OF CONTENTS

DEDICATION iii

ACKNOWLEDGEMENTS iv

ABSTRACT v

LIST OF TABLES x

LIST OF FIGURES xi

LIST OF ABBREVIATIONS xiv

CHAPTER 1 INTRODUCTION 1

1.1 SIX1 AND ITS ROLE IN TUMORIGENESIS 1

1.2 EPITHELIAL-MESENCHYMAL TRANSITION (EMT) 5

1.3 THE ROLES OF TRANSFORMING GROWTH FACTOR-BETA (TGF-B) SIGNALING IN CANCER 8

1.4 HUMAN PAPILLOMAVIRUS (HPV) AND CERVICAL CANCER 14

1.5 *IN VITRO* MODEL OF HPV16-MEDIATED TRANSFORMATION 16

1.6 SUMMARY AND GOAL OF MY DISSERTATION RESEARCH 19

CHAPTER 2 MATERIALS AND METHODS 20

CHAPTER 3 SIX1 PROMOTES EPITHELIAL-MESENCHYMAL TRANSITION AND MALIGNANT CONVERSION IN HKC/DR 34

3.1 INTRODUCTION 34

3.2 RESULTS 36

3.3 DISCUSSION 53

CHAPTER 4 SIX1 OVEREXPRESSION IN HPV16-IMMORTALIZED HUMAN KERATINOCYTES PROMOTES DIFFERENTIATION RESISTANCE AND EMT 58

4.1 INTRODUCTION 58

4.2 RESULTS 59

4.3 DISCUSSION 72

CHAPTER 5 SIX1 PROMOTES COLORECTAL CANCER GROWTH AND METASTASIS BY STIMULATING ANGIOGENESIS AND RECRUITING TUMOR-ASSOCIATED MACROPHAGES....76

5.1 INTRODUCTION....76

5.2 RESULTS. 77

5.3 DISCUSSION 94

REFERENCES 99

LIST OF TABLES

Table 2.1 Primer sequences used in RT-PCR.....23

Table 3.1 Expression of EMT-associated Genes Targeted by TGF-β in HKc/DR.....42

LIST OF FIGURES

Figure 1.1 Schematic representations of the mouse Six proteins showing their characteristic structural features 2

Figure 1.2 Human Six1 gene and protein 3

Figure 1.3 The morphologic and genetic changes during epithelial-mesenchymal transition (EMT) 6

Figure 1.4 EMT facilitates tumor metastasis 7

Figure 1.5 Smad-dependent (canonical) TGF-β signaling....9

Figure 1.6 Smad-independent (noncanonical) TGF-β signaling....11

Figure 1.7 Progression of cervical lesions to cervical cancer 16

Figure 1.8 *In vitro* model system of HPV16-mediated transformation 18

Figure 3.1 The expression of Six1 increases during in vitro progression of HPV16-immortalized human keratinocytes 36

Figure 3.2 Six1 overexpression in HKc/DR induces EMT-like characteristics 38

Figure 3.3 Six1 overexpression induces markers of EMT in HKc/DR 40

Figure 3.4 Immunofluorescent staining of E-cadherin, β-catenin and fibronectin in HKc/DR-Ctrl HKc/DR-Six1 41

Figure 3.5 Six1 overexpression in HKc/DR increases the expression of TβRs....43

Figure 3.6 Six1 overexpression in HKc/DR activates Smad-independent pathways 45

Figure 3.7 Six1 overexpression in HKc/DR activates p38-TβRII signaling 47

Figure 3.8 Six1 overexpression promotes tumorigenesis 49

Figure 3.9 Cells isolated from HKc tumors 50

Figure 3.10 Six1 overexpression in HKc/DR and HeLa increases CSC properties 51

Figure 3.11 TβRII-MAPK signaling is critical for Six1-induced CSC properties 52

Figure 4.1 Six1 overexpression in HKc/HPV16 changes cell morphology and increases cell proliferation, invasion and migration.....60

Figure 4.2 Six1 overexpression induces EMT in HKc/HPV16 62

Figure 4.3 Western blot for Six1 in HKc/HPV16-low passage, HKc/HPV16-high passage, HKc/GFI and HKc/DR that were derived HKc/HPV16 lines 64

Figure 4.4 Six1 overexpression in HKc/HPV16 results in resistance to serum and calcium-induced differentiation.....65

Figure 4.5 Six1 overexpression in HKc/HPV16 does not impact the redistribution of adhesion junctions when cultured in high calcium media 66

Figure 4.6 Western blot of p-PI3-kinase p85 (p-PI3K) and p-AKT in HKc/HPV16-Ctrl and HKc/HPV16-Six1 66

Figure 4.7 Six1 overexpression in HKc/HPV16 alters TGF-β signaling 68

Figure 4.8 Six1 overexpression in HKc/HPV16 modulates MAPK signaling.....69

Figure 4.9 Western blot analysis for E-cadherin, fibronectin and β-actin.....70

Figure 4.10 Inhibition of ERK and p38 reverses Six1-meditated EMT 71

Figure 5.1 mRNA levels of Six1 increases during APCMin/+ mice tumorigenesis 78

Figure 5.2 Six1 overexpression increases CRC tumor growth and metastasis *in vivo*.....79

Figure 5.3 Six1 overexpression in MC38 cells increases CSC characteristics.....82

Figure 5.4 Six1 overexpression promotes angiogenesis.....84

Figure 5.5 Six1 overexpression in MC38 increases migration and invasion *in vitro*.....85

Figure 5.6 The overexpression of Six1 activates ERK and p38 MAPK in human and mouse CRC cell lines.....87

Figure 5.7 Six1 overexpression does not induce systemic inflammation.....89

Figure 5.8 MC38 cells overexpressing Six-1 recruit macrophages to tumors.....91

Figure 5.9 Immunofluorescent staining of VEGF, F4/80 and merged with nuclei in MC38-Six1 derived tumors.....92

Figure 5.10 Six1 overexpression in MC38 increases the expression of molecules that induce chemotaxis of TAM 92

Figure 5.11 mRNA expressions of VEGF, CCL2, CCL5, CSF-1 and CSF-2 were detected by real time PCR in HCT116-Ctrl and HCT116-Six1, and HT29-Ctrl and HT29-Six1 ...94

List of Abbreviations

ALDH1 ..... Aldehyde dehydrogenase 1

bHLH .....basic Helix-loop-helix

BPE .....Bovine pituitary extract

CCL 2..... Chemokine (C-C motif) ligand 2

CCL 5..... Chemokine (C-C motif) ligand 5

CDK .....Cyclin-dependent kinase

CIN.....Cervical intraepithelial neoplasia

CRC..... Colorectal cancer

CSC .....Cancer stem cell

CSF-1 .....Macrophage colony-stimulating factor

CSF-2 .....Granulocyte-macrophage colony-stimulating factor-2,

CSF-3 ..... Granulocyte colony stimulating factor-3

DAPI .....4', 6-diamidino-2-phenylindole

DMEM .....Dulbecco's Modification of Eagle's Medium

DMSO ..... Dissolved in dimethyl sulfoxide

DR ..... Differentiation resistant

EGF ..... Epidermal growth factor

EGFR ..... Epidermal growth factor receptor

EMT .....Epithelial-mesenchymal transition

FBS .....Fetal bovine serum

GFI ..... Growth factor independent

H&E ..... Hematoxylin and eosin

HCC ..... Hepatocellular carcinomas

HKc ..... Human keratinocytes

HPV ..... Human papillomavirus

HRP ..... Horseradish peroxidase

HSV2 ..... Herpes Simplex Virus 2

IL-1β ..... Interleukin 1 beta

IL-6 ..... Interleukin 6

LOX ..... Lysyl oxidase

MAPK ..... Mitogen-activated protein kinase

MMP2 ..... Matrix metalloproteinases 2

MMP9 ..... Matrix metalloproteinases 9

PI3K Phosphatidylinositol-3-kinase

S6K ..... S6 kinase 1

SBE ..... Smad binding element

Shc ..... Src homology domain 2 containing

SME ..... Smad mutated element

TAK1 ..... Transforming growth factor-beta-activated kinase 1

TAM ..... Tumor-associated macrophages

TGF-β ..... Transforming growth factor-beta

TNF-α ..... Tumor necrosis factor alpha

TRAF6 ..... Tumor necrosis factor receptor associated factor 6

TβRI ..... Transforming growth factor-beta receptor type I

TβRII ..... Transforming growth factor-beta receptor type II

TβRIIDN ..... Dominant-negative TβRII plasmid

TβRIII ..... Transforming growth factor-beta receptor type III

uPA ..... Urokinase plasminogen activator

VEGF ..... Vascular endothelial growth factor

α-SMA ..... Alpha-smooth muscle actin

CHAPTER 1

INTRODUCTION

1.1 SIX1 AND ITS ROLE IN TUMORIGENESIS

Six1 (sine oculis homeobox 1) is a member of the Six family of homeodomain transcription factors. The Six family members are homologous to *Drosophila* sine oculis (*So*), *Optix* and *Dsix4* genes. Six family genes have been identified in many species, including human, mouse, chicken, frog and fish, but no homologues have been found in unicellular organisms such as yeast. Six1 family proteins are characterized by the presence of two conserved domains: Six-type homeodomain (HD, 60 amino acids) and Six1-domain (SD, 110-115 amino acids). Based on the amino acid sequence similarities of HDs and SDs, the Six family can be classified into three subfamilies: Six1/Six2 (*So*), Six3/Six6 (*Optix*), and Six4/Six5 (*Dsix4*) in vertebrates (Figure 1.1). HDs generally contain a helix-turn-helix (HTH) motif and mediate DNA binding. The consensus binding site for mammalian Six1/2/4/5 is TCAGGTTC, which is similar to the sequence that is bound by *Drosophila So*. The binding sites for Six family proteins in flies and worms are TGATAC and GGGTATCA. In contrast, the binding site for Six3/6 contains the conserved homeobox binding core sequence ATTA, thus it is significantly different from the DNA sequences bound by other subfamilies. The SDs are critical for mediating protein-protein interactions. The first identified interaction between a Six protein and a transcriptional co-activator is the physical interaction between *Drosophila So* and Eyes

Absent (Eya). Loss-of-function mutations in either gene cause the complete loss of the retina. In addition, Six proteins can interact with Gro or DACH to suppress/silence downstream targets (Kawakami et al., 2000; Kumar, 2009; Larder et al., 2011).

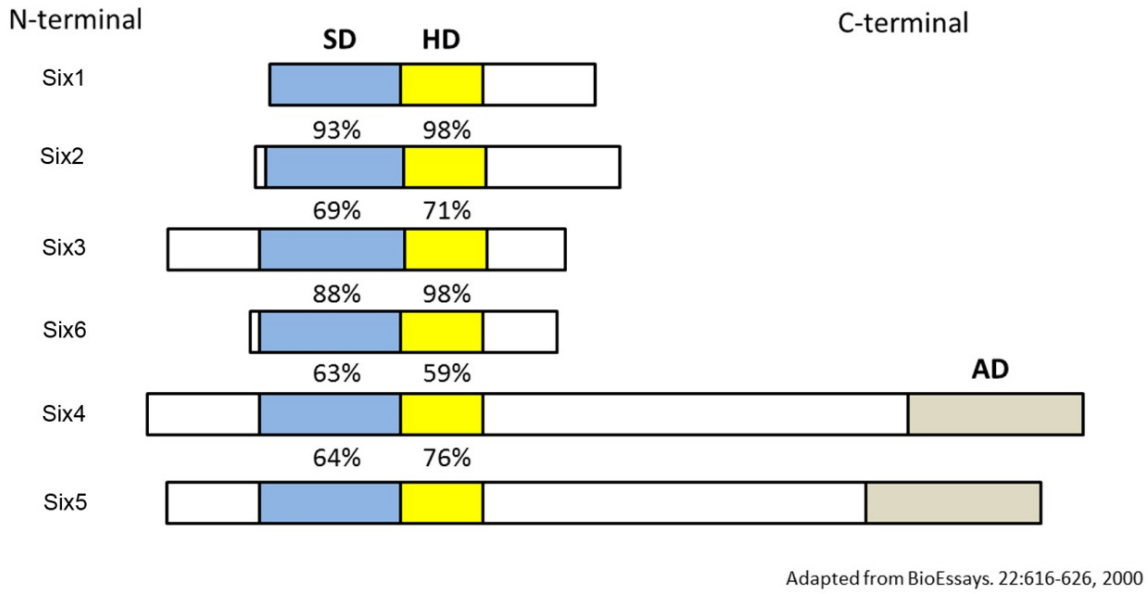

Figure 1.1 Schematic representations of the mouse Six proteins showing their characteristic structural features: the Six domain (SD, blue) and the Six-type homeodomain (HD, yellow). The numbers indicate the percentage of amino acid identity between the SDs and between the HDs. The transcription activation domains (AD) of Six4 and Six5 have been marked as gray shading in the C-terminal.

The human Six1 gene is located on chromosome 14q23.1 and in composed of 2 exons and one intron. The transcript length is 1,376 base pairs, which codes for a protein of 284 amino acids with a mass of 32,210 Daltons (Figure 1.2) (GenBank accession no NM_005982, (Sanggaard et al., 2007). Six1 is broadly expressed in various tissues and organs, and plays a critical role in tissue and organ development, including muscle (Laclef et al., 2003a), the auditory system (Zheng et al., 2003), olfaction (Ikeda et al., 2010), and kidney (Xu et al., 2003). Six1-/- mice die at birth and show multiple organ developmental defects, including rib defects, muscle hypoplasia, absence of kidneys and

thymus, craniofacial defects, and ear and nose defects (Laclef et al., 2003b). Six1 +/- mice show partial hearing loss because of a failure of sound transmission in the middle ear (Zheng et al., 2003). Six1 activates the expression of target genes by binding to MEF3, SRE1 and other putative DNA–binding sequences (Liu et al., 2012). For instance, Six1 regulates the expression of Myogenin by binding to a conserved MEF3 site in the promoter, which regulates myogenesis (Spitz et al., 1998). Six1 utilizes co-factors, coactivators and corepressors, to regulate the transcription of target genes. For example, the formation of an Eya1-Six1 complex is essential for auditory system development (Ruf et al., 2004), and the phosphatase activity of Eya3 switches the function of Six1-Dach from repression to transcriptional activation through recruitment of the co-activator CBP (Li et al., 2003).

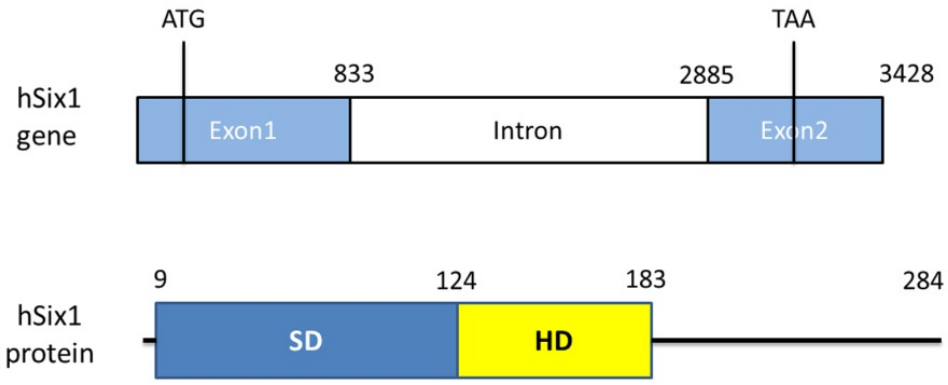

Figure 1.2 Human Six1 gene and protein. Upper panel: the human Six1 gene is composed of 2 exons that are 833 and 543 base pairs (bp) respectively, and a 2052-bp intron. The start and stop codons are shown. Lower panel: the human Six1 protein (total length of 284 amino acids) that contains an N-terminal SD (115 amino acids) and a C-terminal HD (60 amino acids) domain.

Many studies have shown that inappropriate expression of embryonic genes, particularly homeodomain transcription factors, contributes to tumorigenesis and/ or

tumor progression (Abate-Shen, 2002). Six1 overexpression has been found in various adult human cancers including breast (Coletta et al., 2008), ovarian (Behbakht et al., 2007), cervical (Wan et al., 2008; Zheng et al., 2010), colorectal (Ono et al., 2012) and hepatocellular carcinomas (HCC) (Ng et al., 2010), as well as pediatric malignancies such as rhabdomyosarcomas (Yu et al., 2004) and Wilms' tumors (Li et al., 2002). The overexpression of Six1 is associated with increased tumor progression and decreased survival (Christensen et al., 2008). For example, Six1 is overexpressed in 50% of primary mammary carcinomas and 90% of metastatic lesions (Reichenberger et al., 2005). The expression of SIX1 mRNA was detected in about 85% of hepatocellular carcinomas (HCC), while expression was observed in only 8.3% of HCC non-tumor adjacent liver tissue and 10% of normal liver tissue. Consistently, Six1 protein was detected in about 60% of tumor tissue while no Six1 protein was found in adjacent non-tumor liver tissues and normal liver. The elevated Six1 expression in HCC patients is related to advanced stage and poor overall survival (Ng et al., 2006). Six1 is also overexpressed in cervical cancer cell lines and cervical cancer tissues, and the extent of Six1 overexpression is correlated to increased malignancy and lymph node metastasis (Tan, Zhang, and Qian, 2011; Wan et al., 2008; Zheng et al., 2010).

Among these cancers, the functions of Six1 in breast cancer are the most extensively investigated. The major roles Six1 plays in breast cancer include: (1) Six1 overexpression increases cell proliferation in breast cancer by directly up-regulating cyclin A1 transcription (Coletta et al., 2004); (2) The overexpression of Six1 in immortalized and nontumorigenic mammary epithelial cells induces genomic instability and malignant transformation, leading to highly aggressive and invasive tumors in nude

mice (Coletta et al., 2008); (3) Six1-overexpresstion in human breast cancer cell lines promotes epithelial-mesenchymal transition (EMT) and enhances metastasis *in vitro* and *in vivo* [27,28]; (4) EMT resulting from Six1 overexpression is associated with Smad-dependent transforming growth factor-beta (TGF-β) signaling and increased expression of TGF-β receptor type I (TβRI) (Micalizzi et al., 2009; Micalizzi et al., 2010); and (5) Six1 induces lymphangiogenesis and distant metastasis in breast cancer by up-regulating VEGF-C, a specific lymphangiogenic factor (Wang et al., 2012). Besides cyclin A1, other pro-tumorigenic genes can be regulated by Six1, such as cyclin D1, c-Myc, and Ezrin (Yu et al., 2006). For instance, Six1 promotes cell cycle progression and proliferation in pancreatic cancer cells by upregulating cyclin D1 expression (Li et al., 2013). Ezrin is responsible for Six1-induced metastasis in a series of representative pediatric cancers (Yu et al., 2006).

1.2 EPITHELIAL-MESENCHYMAL TRANSITION (EMT)

EMT is a dynamic process that allows immotile and highly polarized epithelial cells acquire a motile, apolar and fibroblastic phenotype (Figure 1.3). In normal physiology, EMT is required for proper tissue organization, normal embryonic development, wound healing, and in the repair of damaged tissue. EMT is also considered a critical step in mediating the acquisition of metastasis. EMT allows tumor cells to migrate from the primary tumor into surrounding tissue, intravasate into the vasculature and lymphatics, and extravasate at a secondary site, leading to tumor cell dissemination and colonization of distant organs (Figure 1.4) (Christiansen and Rajasekaran, 2006).

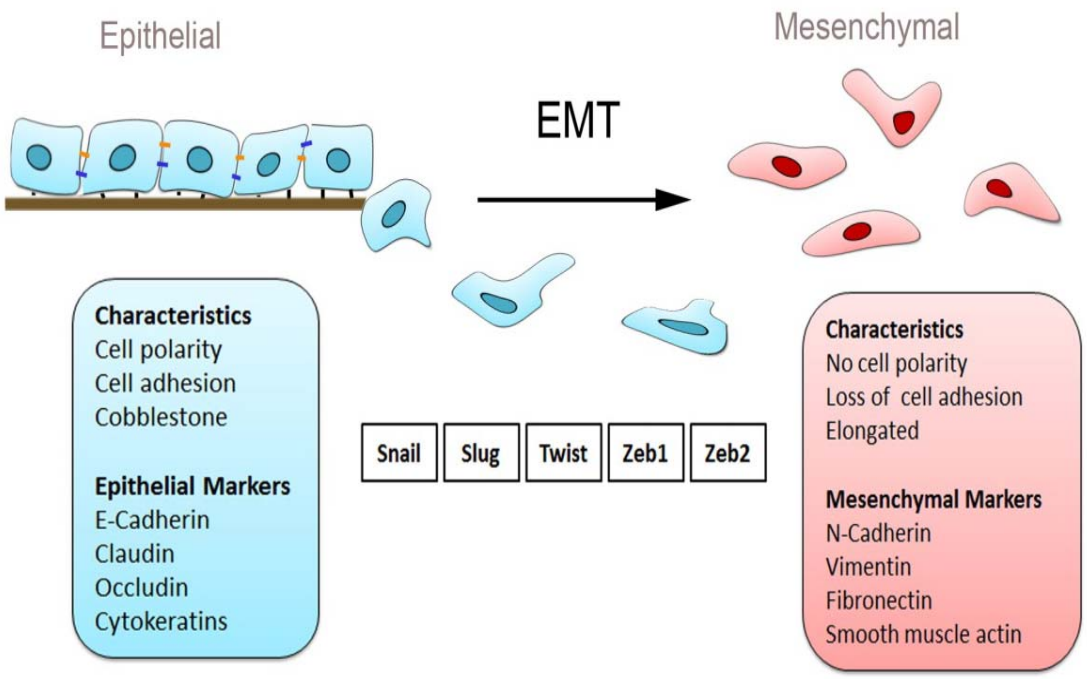

Figure 1.3 The morphologic and genetic changes during epithelial-mesenchymal transition (EMT).

EMT is defined by the morphologic and genetic transition of epithelial cells to mesenchymal-like cells (Figure 1.3). In response to the initiation of EMT, cell-cell junctions disassemble and filamentous actin is redistributed to stress fibers. Molecular alterations underlying EMT including the decreased expression of cell-cell junction proteins such as E-cadherin, claudins and occludins, and increased expression of mesenchymal markers such as N-cadherin, fibronectin, vimentin and α-smooth muscle actin (α-SMA). In addition, numerous transcription factors are upregulated by EMT inducers in variety of cancers, such as snail1, snail2, twist, ZEB1 and ZEB2 (Wendt, Allington, and Schiemann, 2009).

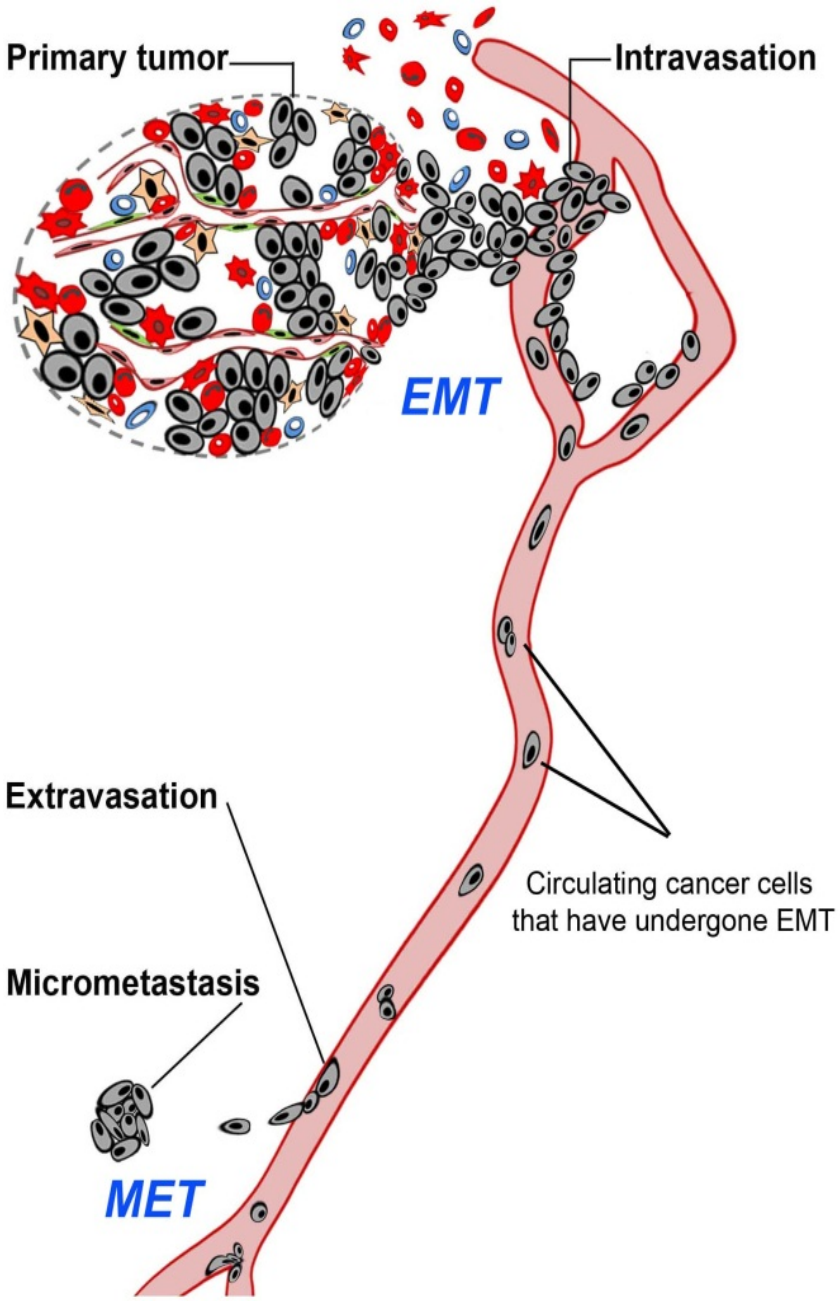

Figure 1.4 EMT facilitates tumor metastasis. Primary tumor cells undergo EMT to invade into surrounding tissue, intravasate into the vasculature and lymphatics, extravasate at a secondary site, leading to metastasis. At the distant site the cells can undergo mesenchymal-epithelial transition (MET).

The induction of EMT in response of Six1 overexpression has been observed in various cancers. Six1 induces human mammary carcinoma cells to undergo EMT by

enhancing TGF-β signaling (Micalizzi et al., 2009). In colorectal cancer, Six1 promotes EMT through posttranscriptional ZEB1 activation and transcriptional repression of the miR-200-family (Ono et al., 2012). A recent study indicates a possible role of Six family members in regulating developmental EMT and maintaining mesenchymal progenitor renewal (Grifone et al., 2005; Self et al., 2006). In all, Six family proteins are critical regulators of EMT in both development and tumor progression.

1.3 THE ROLES OF TRANSFORMING GROWTH FACTOR-BETA (TGF-β) SIGNALING IN CANCER.

TGF-β is a multifunctional cytokine that is involved in many aspects of cell development, differentiation and homeostasis. TGF-β contains three isoforms: TGFβ1, TGFβ2, and TGFβ3. TGF-β dimers mediate signaling by binding to three high-affinity receptors, called TGF-β receptor type I (TβRI), type II (TβRII) and type III (TβRIII). TβRIII is the most abundant TGF-β receptor and its function is to assist TGF-β binding to TβRII. TβRI and TβRII both have intrinsic Ser/Thr protein kinase activity in their cytoplasmic domains. In Smad-dependent (canonical) TGF-β signaling, the binding of TGF-β to TβRII recruits and then phosphorylates TβRI, leading to the phosphorylation of Smad2/3 proteins and induction of canonical Smad2/3-dependent signaling. Once activated, Smad2/3 form heterocomplexes with Smad4 and shuttle into the nucleus, where the complex regulates the transcription of a large number of target genes (Figure 1.5).

Each step in TGF-β signaling is highly regulated. First of all, the phosphorylation of Smads is reversed by phosphatases, which forming a rapid activation-deactivation

cycle. Secondly, activated Smad2/3 can be targeted by ubiquitin E3 ligases for degradation. Thirdly, the interaction between Smad2 and Smad4 is disrupted by mono-ubiquitination of Smad4. In addition, the inhibitory Smads (I-Smads) are transcriptionally induced upon activation of TGF-β signaling (Derynck and Zhang, 2003; Meulmeester and Ten Dijke, 2011).

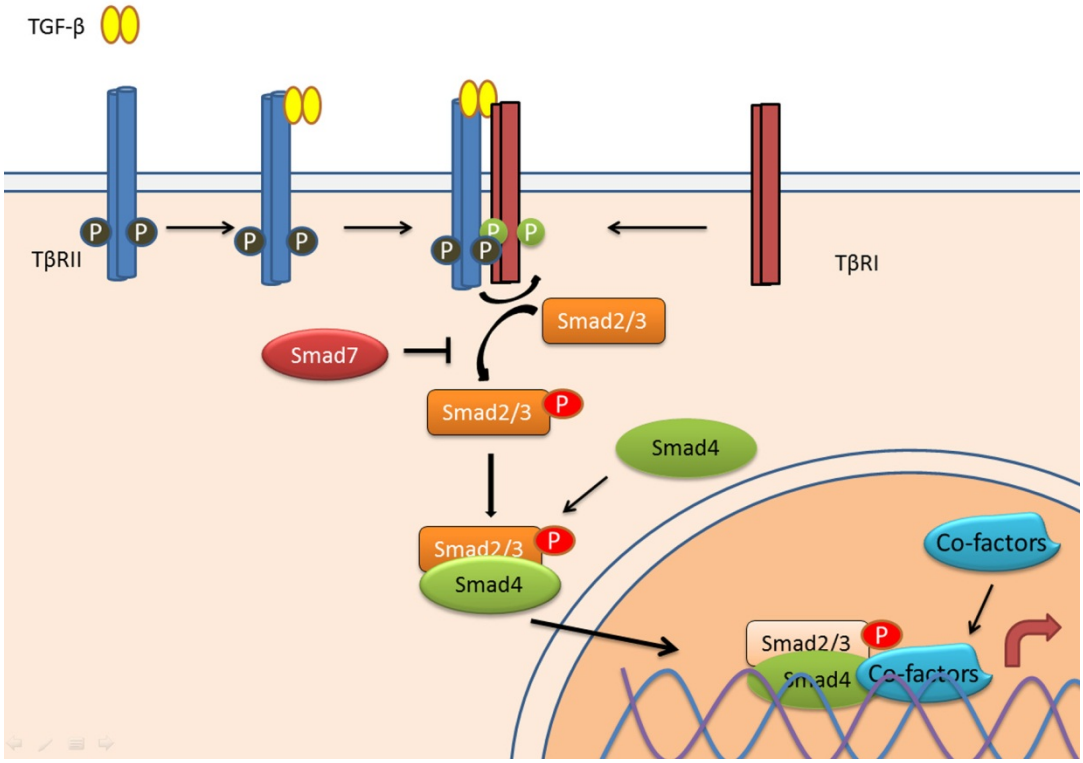

Figure 1.5 Smad-dependent (canonical) TGF-β signaling.

Besides Smad-dependent signaling, there are a variety of Smad-independent (noncanonical) signaling pathways, including the mitogen-activated protein kinase (MAPK) pathway, the phosphatidylinositol-3-kinase (PI3K)/AKT pathway and Rho-like GTPase signaling pathway (Figure 1.6). Below is a description of each of these non-Smad signaling pathways.

The ERK non-Smad pathway: TGF-β induces phosphorylation of TβRI/II and Shc (Src homology domain 2 containing) (Lee et al., 2007), which enables the recruitment of the Grb2/SOS complex and the sequential activation of Ras, Raf, and the ERK MAPK cascade (Hartsough and Mulder, 1995). ERK regulates target gene transcription through its downstream transcription factors (such as AP-1 family members) in conjunction with Smads to promote EMT, which mediates tumor invasiveness and metastasis (Davies et al., 2005; Zhang, Feng, and Derynck, 1998). ERK can also phosphorylate and inhibit the activity of the receptor-activated Smads (Smads 2/3), which may explain how oncogenic Ras overrides TGF-β-mediated growth arrest in cancer cells (Kretzschmar et al., 1999).

The JNK/p38 non-Smad pathway: JNK/p38 MAPK signaling is the best-characterized non-Smad pathway. Tumor necrosis factor receptor associated factor 6 (TRAF6) associates with TβRII and TβRI through the C-terminal TRAF domain and forms lysine-63 (K63)-linked polyubiquitin chains (Yamashita et al., 2008). Unlike K48-linked polyubiquitination, which generally targets proteins for degradation, K63-linked polyubiquitin chains serve as scaffolds to assemble protein complexes and mediate their activation (Haglund and Dikic, 2005). Polyubiquitinated TRAF6 recruits and activates TGF-β-activated kinase 1 (TAK1), enabling the activation of downstream JNK or p38 MAPK via MKK4 or MKK3/MKK6 respectively (Sorrentino et al., 2008; Yamaguchi et al., 1995). Interestingly, TRAF6 can be pulled down by TβRII in TβRI-deficient cells but not by TβRI in TβRII-deficient cells, indicating that TRAF6-mediated JNK and p38 signaling is directly or indirectly through TβRII (Yamashita et al., 2008). Although TGF-β-induced JNK/p38 activation is independent from Smad activation, JNK/p38 cooperates

with Smads to regulate apoptosis (Yu, Hebert, and Zhang, 2002). The JNK/p38 non-Smad pathway also plays a very important role in TGF-β-mediated EMT. Inhibition of p38 activity using a p38 inhibitor blocked TGF-β-mediated changes in cell shape and reorganization of the actin cytoskeleton (Bakin et al., 2002; Yu, Hebert, and Zhang, 2002).

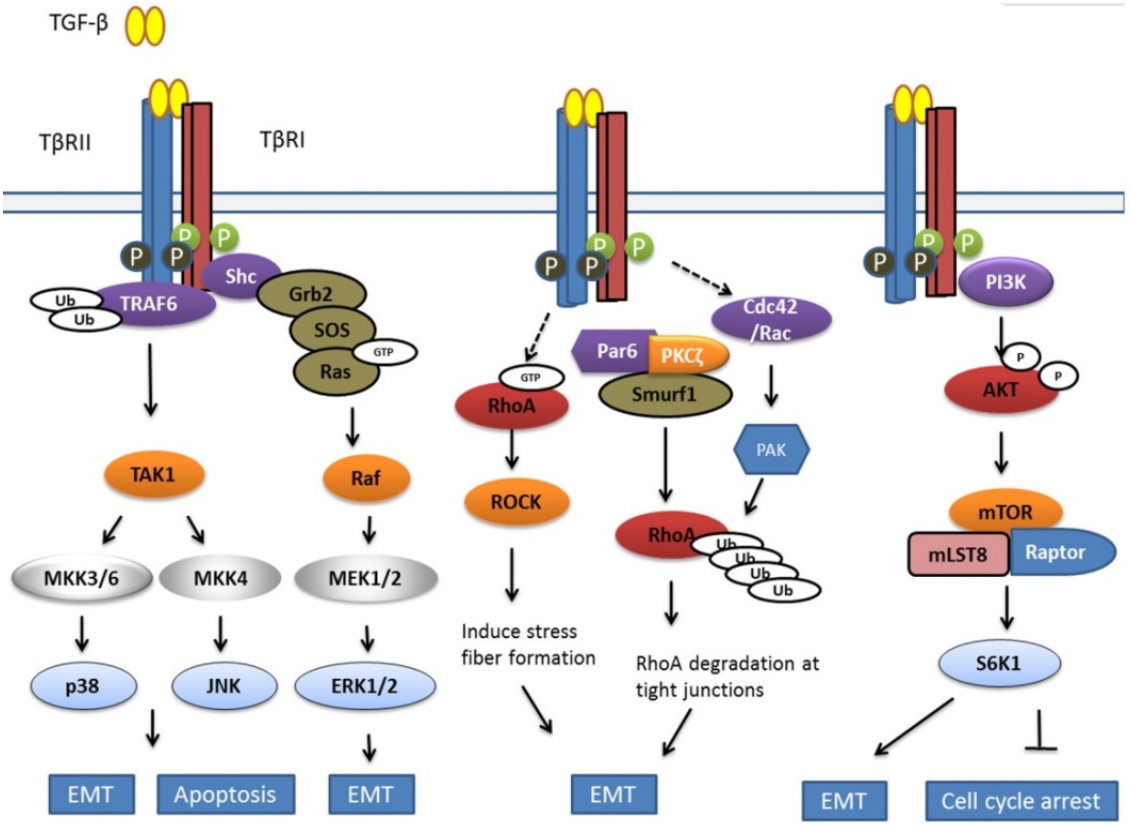

Figure 1.6 Smad-independent (noncanonical) TGF-β signaling. Left panel: TGF-β activates p38 MAPK and JNK signaling through the activation of TAK1 by TRAF6. TGF-β activates ERK signaling through recruitment and phosphorylation of Shc. Middle panel: TGF-β activates RhoA and induces ubiquitin-mediated RhoA degradation at tight junctions. Right panel: TGF-β induces PI3K/AKT signaling, leading to the activation of mTOR and S6K1, and consequently to increased translation.

The Small GTPase non-Smad pathway: The Rho-like GTPases, including RhoA, Rac and Cdc42, play important roles in cytoskeletal organization and cell motility

(Jaffe and Hall, 2005). In the small GTPase non-Smad pathway, RhoA is the key player in TGF-β-induced EMT. TGF-β regulates RhoA activity in two different ways to induce EMT: TGF-β initially induces a rapid activation of RhoA to induce actin stress fiber formation (Bhowmick et al., 2001a; Edlund et al., 2002). However, after prolonged signaling, TGF-β induces the assembly of TβRI-TβRII complexes at tight junctions, where TβRII phosphorylates Par6, a scaffold protein regulating epithelial cell polarity. Phosphorylated Par6 recruits Smurf1 to mediate localized ubiquitination and turnover of RhoA at tight junctions (Ozdamar et al., 2005). TGF-β can also induce activation of Cdc42 to induce morphological transformation in epithelial cells (Wilkes et al., 2003).

The PI3K/AKT non-Smad pathway: TGF-β has been shown to rapidly activate PI3K, leading to activation of AKT (Bakin et al., 2000; Wilkes et al., 2005). The p85 regulatory subunit of PI3K was found to be constitutively associated with TβRII and only associated with TβRI upon TGF-β stimulation (Yi, Shin, and Arteaga, 2005). The activated PI3K/AKT pathway controls translational responses through mTOR/ S6 kinase 1(S6K) (Lamouille and Derynck, 2007). Activation of S6K is required for snail expression, which works with Smad-mediated transcriptional responses during TGF-β-induced EMT (Pon et al., 2008). AKT can also directly interact with Smad3, resulting in the inhibition of Smad3-mediated transcription, inhibit nuclear localization of FoxO transcription factor thorough phosphorylation, and thereby protect cells from TGF-β-induced apoptosis and growth arrest (Chen et al., 1998; Conery et al., 2004; Seoane et al., 2004; Shin et al., 2001) (Summarized in (Zhang, 2009)).

TGF-β signaling plays a dual role in tumor progression. At early stages of tumorigenesis, TGF-β acts as a potent tumor suppressor due to its ability to inhibit the

proliferation of epithelial cells. Mechanistically, Smad3/Samd4 complexes induce the expression of cyclin-dependent kinase (CDK) inhibitors, such as p15 and p21 (Datto et al., 1995; Hannon and Beach, 1994). P15 arrests cell cycle progression at the G1 phase by abolishing the cyclin D-CDK4/6 interaction, while p21/p27 inhibits the cyclin E-CDK2 complex and stops the cell cycle at the G1-S boundary (Siegel and Massague, 2003). TGF-β also suppresses *c-Myc* oncogene expression, which results in reduced cell proliferation (Staller et al., 2001). TGF-β can also induce apoptosis in many cell types (Jang et al., 2002; Ohgushi et al., 2005). Furthermore, TGF-β can inhibit tumor progression by blocking the action of paracrine growth factors in the tumor stroma during the early stages of tumor development (Bhowmick et al., 2004). However, at late stages of tumorigenesis, tumors become resistant to the antiproliferative effects of TGF-β through multiple mechanisms, including mutation or deletion of components of the TGF-β signaling pathway (Grady et al., 1999; Markowitz et al., 1995; Myeroff et al., 1995). TGF-β can also promote tumor progression by inducing EMT and inactivating $CD4^+$ and $CD8^+$ T-cells, and thereby facilitating tumor metastasis and invasion (Elliott and Blobe, 2005; Meulmeester and Ten Dijke, 2011). Imbalances in the activation status of Smad-dependent versus Smad-independent TGF-β signaling might be the critical factor that results in the switch in TGF-β signaling from tumor suppression to tumor promotion (Zhang, 2009).

TGF-β is a potent inducer of EMT and treating various epithelial cells with TGF-β in culture is a common way to induce EMT. TGF-β can induce EMT through Smad-dependent and Smad-independent signaling. TGF-β induces the expression of EMT transcription factors, including the Snail, ZEB and basic helix-loop-helix (bHLH)

families, through a direct Smad-dependent mechanism or indirectly through activation of other transcription factors or relief of their repression by inhibitors. TGF-β also induces the expression of microRNAs (miRNAs) to promote EMT. For example, miRNA-155 and miR-181a can be up-regulated by TGF-β-Smad signaling, and contribute to EMT (Kong et al., 2008). EMT can also be induced by Smad-independent signaling pathways. Hence, understanding different mechanisms in response to TGF-β may facilitate the discovery of molecular targets in signaling leading to EMT. Identifying ways to suppress EMT might ultimately inhibit tumor progression and metastasis.

1.4 HUMAN PAPILLOMAVIRUS (HPV) AND CERVICAL CANCER

Cervical cancer is the second most common malignancy among women world-wide. Although screening is very effective in preventing cervical cancer, approximately 500,000 new cases of cervical cancer are diagnosed and 280,000 deaths from this disease occur annually (Peralta-Zaragoza et al., 2012). The main etiological agent for cervical cancer is an infection with human papillomavirus (HPV). HPVs are small non-enveloped viruses containing circular, double-stranded DNA (~ 8000 bps) that infect keratinocytes of the skin or mucous membranes (Faridi et al., 2011). The HPV genome encodes six early (E1, E2, E4, E5, E6 and E7) and two late (L1 and L2) proteins. The transcription of the early and late genes is controlled by a non-coding long control region (LCR) (Ganguly and Parihar, 2009). To date, more than 100 HPV types have been identified and 51 types infect the genital mucosa. HPVs can be classified into 3 subtypes according to their association with cervical cancer: high-risk (oncogenic) types (currently including types 16, 18, 31, 33, 35, 39, 45, 51, 52, 56, 58, 59, 68, 69, 73, 82), low-risk

(nononcogenic) types (6, 11, 40, 42, 43, 44, 54, 61, 70, 72, 81, and CP6108) and probable high-risk (26, 53, and 66) (Munoz et al., 2003; Schmitt et al., 2013). Most HPV infections are asymptomatic and are cleared naturally. However, over 10% of the population cannot clear high-risk HPV infections and this population stands to be at a high risk for developing cervical cancer in the future (Grainge et al., 2005). Cervical cancer is a slowly progressive disease. It starts with an infection to the genital mucosa by HPV which, when the infection remains persistent, can progress through several stages of dysplasia called Cervical Intraepithelial Neoplasia (CIN) before it develops into invasive cervical cancer (Figure 1.7) (Saslow et al., 2012). Currently, two vaccines are available to prevent infection by some HPV types: Gardasil (marketed by Merck) and Cervarix (marketed by GlaxoSmithKline). Cervarix protect against infection with HPV type 16 and 18, which cause 70% of cervical cancers. Gardasil protects against HPV type 16, 18 as well as 6 and 11, which cause 90% of genital warts (Toft et al., 2014).

It is now well accepted that a persistent cervical infection with high-risk HPV is necessary for the development of cervical cancer. HPV16 is the most carcinogenic HPV genotype, which accounts for 55%-60% of all cervical cancers; HPV18 is the second most carcinogenic HPV genotype, which accounts for 10–15% of cervical cancers. Approximately another 10 high-risk HPV genotypes contribute to the remaining 25–35% of cervical cancers (de Sanjose et al., 2010; Munoz et al., 2003; Walboomers et al., 1999). HPVs encode 8 genes, of which E6 and E7 are considered as oncoproteins and necessary for malignant conversion. High-risk HPV E6 binds to E6-associated protein (E6-AP), a cellular ubiquitin ligase, resulting in the ubiquitination and degradation of p53 (Werness, Levine, and Howley, 1990). E7 binds to the retinoblastoma protein (Rb) tumor

suppressor protein family which results in the release of the E2F transcription factor and promotes cell proliferation (Dyson et al., 1989).

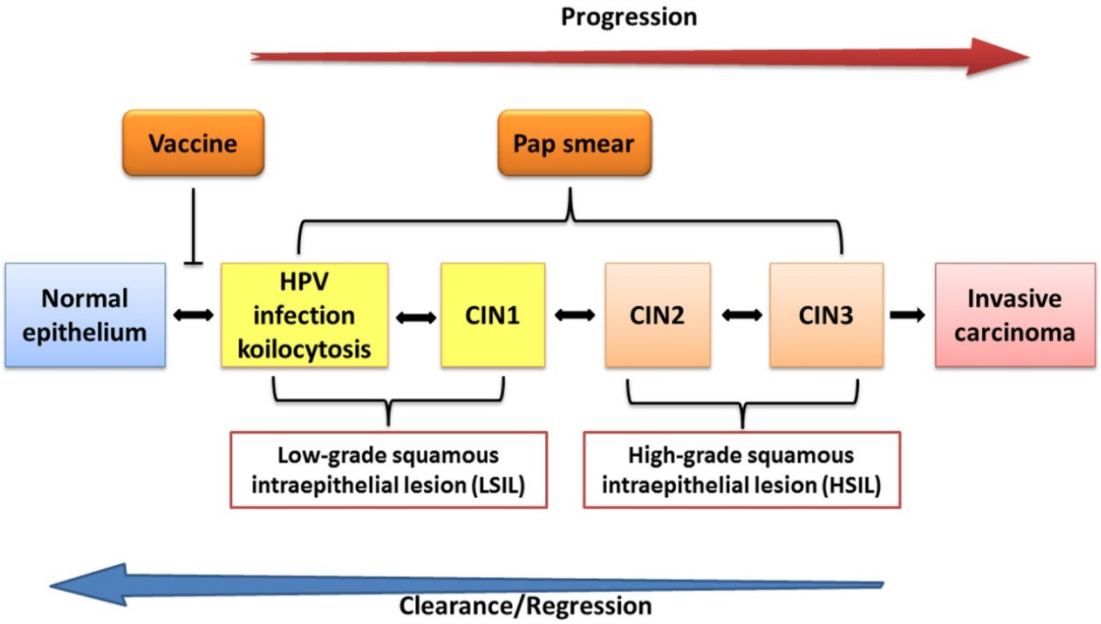

Figure 1.7 Progression of cervical lesions to cervical cancer. High risk HPV infection can be cleared by the host immune system or become a persistent infection. A persistent HPV infection can progress to LSIL, which can either regress or progress to HSIL. HSIL is pre-cancerous, and still can regress or progress to invasive cancer. Major early interventions include HPV vaccination and the Pap test. The HPV vaccine protects against initial infection with HPV16 and 18, while the Pap test detects abnormal cytology in exfoliated cervical cells.

1.5 *IN VITRO* MODEL OF HPV16-MEDIATED TRANSFORMATION

To explore the cellular and molecular events associated with HPV-mediated transformation, Pirisi *et al* established an *in vitro* model system to mimic the stages of premalignant progression. Briefly, normal human keratinocytes (HKc) were isolated from neonatal foreskin, and immortalized by transfection with a plasmid containing a head-to-tail dimer of HPV16 DNA (HKc/HPV16) and cultured in Keratinocyte serum-free medium supplemented with epidermal growth factor (EGF) and bovine pituitary extract

(BPE). Growth factor-independent HKc (HKc/GFI) were selected by culturing HKc/HPV16 in complete medium lacking EGF and BPE. Differentiation resistant cells (HKc/DR) were further selected from HKc/GFI in complete medium containing 1 mM calcium chloride and 5% fetal bovine serum (FBS) (Figure 1.8) (Pirisi et al., 1988; Pirisi et al., 1987). HKc/DR are not tumorigenic, but they form squamous carcinomas in nude mice upon transfection with activated Ras or Herpes Simplex Virus 2 (HSV2) DNA. HKc/GFI and HKc/DR share several characteristics with cancer cells. For example: HKc/GFI exhibit increased expression of the EGF receptor (EGFR) and constitutively activative EGFR signaling, which contributes to their autonomous growth (Akerman et al., 2001; Zyzak et al., 1994). HKc/DR are completely resistant to the antiproliferative effects of TGF-β1 and TGF-β2 treatment, while HKc/HPV16 are as sensitive as normal HKc to growth inhibition by TGF-β1 and TGF-β2 (Creek et al., 1995). The loss of sensitivity to growth inhibition by TGF-β in HKc/DR is due at least in part to a partial loss of TβRI (Mi et al., 2000). Smad activation induced by TGF-β in HKc/DR is about 50% of the maximum levels of activation observed in HKc/HPV16. However, TGF-β treatment of HKc/DR still results in EMT (Kowli et al., 2013). Retinoic acid (RA) suppresses HKc/HPV16 cell growth (Creek et al., 1994; Pirisi et al., 1992), but HKc/DR are resistant to RA-induced growth inhibition, and this resistance is linked to the loss of sensitivity to TGF-β (Borger et al., 2000).

This model system was established by selection *in vitro* of cells representing a more advanced transformed phenotype. Instead of radiation or treatment with carcinogens, we have selected for growth factor-independent (GFI) and differentiation resistant (DR) phenotypes using specialized culture conditions. This model represents

distinct stages of transformation, including immortality, lack of requirement for growth factors and lack of response to differentiation stimuli. It is valuable to identify genes whose altered expression may contribute to transformation and *in vitro* progression by comparing, using microarrays, gene expression profiles at the different stages. For example, we compared gene expression between normal HKc and HKc/HPV16 and between HKc/HPV16 and HKc/DR, and identified genes whose expression was altered during early and late stages of *in vitro* progression. Among these we selected some genes for further study, including, SIX1 (Wan et al., 2008). Thus, this *in vitro* model provides us an excellent platform to study the cellular and molecular role that certain genes may play during HPV16-mediated transformation.

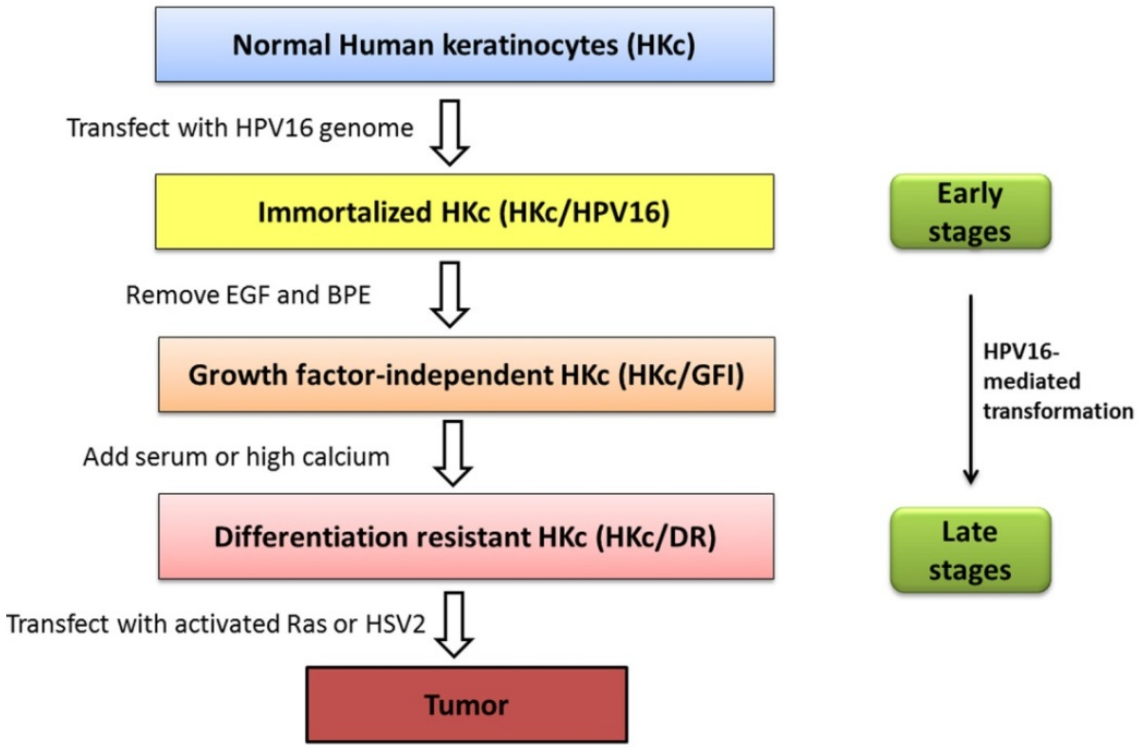

Figure 1.8 *In vitro* model system of HPV16-mediated transformation.

1.6 SUMMARY AND GOAL OF MY DISSERTATION RESEARCH.

Six1 overexpression has been found in various human cancers including tumors of the breast (Coletta et al., 2008), ovary (Behbakht et al., 2007), cervix (Wan et al., 2008; Zheng et al., 2010), colon (Ono et al., 2012) and liver (Ng et al., 2010). The overexpression of Six1 is associated with increased tumor progression and metastasis, and decreased survival (Christensen et al., 2008). For example, Six1 is overexpressed in cervical cancer cell lines, and that the extent of Six1 overexpression is correlated to increased tumor malignancy and lymph node metastasis (Tan, Zhang, and Qian, 2011; Wan et al., 2008; Zheng et al., 2010). Six1 overexpression has been found to be significantly associated with poorer overall survival in advanced-stage colorectal cancer (CRC) (Ono et al., 2012). We previous performed gene expression analyses of HKc/DR and HKc/HPV16, and determined that Six1 mRNA expression increased during *in vitro* progression of HPV16-immortalized cells and that Six1 was overexpressed in about 23% of cervical cancer samples in a tissue microarray (Wan et al., 2008). These findings strongly suggest that Six1 might be involved in the progression of cervical premalignant lesions to cervical cancer. However, the mechanism(s) by which Six1 promotes cervical carcinogenesis and progression is still to be determined.

The main goal of this study is to explore the role of Six1 at both the early and late stages of HPV16-mediated transformation by following the cellular and molecular changes associated with the overexpression of Six1 in HKc/HPV16 and HKc/DR. As an extension of these studies, we also investigated the role of Six1 on tumor progression and metastasis in mouse and human colorectal cancer cell lines.

CHAPTER 2

MATERIALS AND METHODS

Plasmid constructs

Total RNA was isolated from HKc/DR using the Total RNA Isolation Mini Kit (Agilent, Wilmington, DE) according to the manufacturer's protocol. The Six1 cDNA was amplified using the Titan One Tube RT-PCR System (Roche, Indianapolis, IN). The forward primer includes a *NheI* restriction site: 5'-GAC **GCT AGC** ATG TCG ATG CTG CCG TCG TTT G-3'; the reverse primer contains a *BamHI* site: 5'-TAC **GGA TCC** TGC TGC TCC AGG AAT CCC TTC G-3'. The restriction sites are shown in bold and underlined. Human Six1 cDNA was then cloned into the *NheI* and *BamHI* site of the mammalian expression vector pcDNA 3.1 (Invitrogen, Carlsbad, CA). The Six1 cDNA insert sequence was verified by direct sequencing of both DNA strands. This construct is referred to as pcDNA3.1-Six1. Mouse Six1 cDNA clone was purchased from Origene (Rockville, MD), and then cloned into the *EcoRI* and *NotI* site of pcDNA3.1. This construct is referred to as pcDNA3.1-mSix1.

HPV16-immortalized HKc cell lines and transfections

Normal HKc immortalized by transfection with HPV16 DNA (HKc/HPV16) were cultured in keratinocyte serum free medium supplemented with epidermal growth factor (EGF) and bovine pituitary extract (BPE) (Invitrogen) (Pirisi et al., 1987). This

medium is referred to as complete medium. Growth factor-independent HKc (HKc/GFI) cell lines were selected by culturing HKc/HPV16 in complete medium lacking EGF and BPE. Differentiation resistant cells (HKc/DR) were further selected from HKc/GFI and cultured in complete medium containing 1.0 mM calcium chloride and 5% fetal bovine serum (FBS) (Pirisi et al., 1988).

HKc/HPV16 and HKc/DR were transfected with pcDNA3.1 or pcDNA3.1-Six1 using TransFast (Promega, Madison, WI) following the manufacturer's instructions. Stable transfectants, named HKc/HPV16-Ctrl, HKc/HPV16-Six1, HKc/DR-Ctrl and HKc/DR-Six1 were selected in the presence of 50 μg/ml Zeocin (Invitrogen). HeLa cells were cultured in Dulbecco's Modification of Eagle's Medium (DMEM) with 4.5 g/L glucose (Mediatech, Manassas, VA) supplemented with 10% FBS (Atlanta Biologicals, Lawrenceville, GA), and were transfected with pcDNA3.1 or pcDNA3.1-Six1 using TransFast . Stable transfectants (HeLa-Ctrl and HeLa-Six1) were selected in the presence of 300 μg/ml Zeocin.

For microarray analysis, HKc/DR-Ctrl and HKc/DR-Six1 were switched to complete medium 48 h before RNA extraction. For cell differentiation resistance experiments, HKc/HPV16-Ctrl and HKc/HPV16-Six1 were cultured with either complete medium or complete medium supplemented with 1.0 mM calcium chloride or 5% FBS for the indicated time.

MAPK inhibitors were dissolved in dimethyl sulfoxide (DMSO) and then diluted in medium to a final concentration of 10 μM. Control cultures were exposed to equal concentrations of DMSO (0.1%) with no inhibitors. Cells were treated for 48 h. All cells were maintained in a humidified atmosphere of 5% CO2 and 95% air at 37 °C.

Colorectal cancer cell lines

The C57BL/6-derived mouse colon adenocarcinoma cell line MC38 and the human colon cancer cell lines HCT116, HT29 and SW80 were obtained from Dr. Maria M. Peña (University of South Carolina, Columbia, SC). MC38 was cultured in DMEM with 4.5 g/L glucose supplemented with 10% FBS. MC38 cells were transfected with pcDNA3.1 or pcDNA3.1-mSix1 using Lipofectamine 2000 (Invitrogen) following the manufacturer's instructions. Stable transfectants, named MC38-Ctrl and MC38-Six1, were selected in culture medium containing 300 μg/ml Zeocin.

HCT116, HT29 and SW480 were maintained in RPMI-1640 medium supplemented with 10% FBS. HT29 and SW480 human colon cancer cells were transfected with pcDNA3.1 or pcDNA3.1-Six1 using FuGENE 6 (Promega). Stable transfectants of HCT116 was selected in the presence of 200 μg/ml Zeocin, and referred to as HCT116-Ctrl and HCT116-Six1. Stable transfectants of HT29 was selected in the presence of 200 μg/ml Zeocin, and referred to as HT29-Ctrl and HT29-Six1. Stable transfectants of SW480 was selected in the presence of 100 μg/ml Zeocin, and referred to as SW480-Ctrl and SW480-Six1.

Real time PCR

Total RNA was isolated from cells using the Total RNA Isolation Mini Kit (Agilent, Wilmington, DE) according to manufacturer's protocol. Reverse transcription was carried out with 1μg of total RNA using the iScript cDNA Synthesis Kit (BioRad, Hercules, CA). Real time PCR was performed using iQ SYBR Green Supermix (BioRad) following the manufacturer's instructions. Primers are purchased from RealTimePrimers

(Elkins Park, PA) or Integrated DNA Technologies (Coralville, IA). The sequence of the primers used for real time PCR is shown in Table 2.1. β-actin was used as an internal control. All samples were assayed in triplicate.

Table 2.1 Primer sequences used in RT-PCR. Primer sequence 5'– 3'.

Genes	Forward	Reverse
human Six1	ATT CTC ACC TCC CCA AAG TC	ACT TAG GAC CCC AAG TCC AC
human E-cadherin	TGC TCT TGC TGT TTC TTC GG	TGC CCC ATT CGT TCA AGT AG
human fibronectin	ACC AAC CTA CGG ATG ACT CG	GCT CAT CAT CTG GCC ATT TT
human N-cadherin	ACA GTG GCC ACC TAC AAA GG	CCG AGA TGG GGT TGA TAA TG
human occludin	ATG ACA AGC GGT TTT ATC CA	CTC CAG CTC ATC ACA GGA CT
human vimentin	GAG AAC TTT GCC GTT GAA GC	TCC AGC AGC TTC CTG TAG GT
human snail	ACC CCA CAT CCT TCT CAC TG	TAC AAA AAC CCA CGC AGA CA
human TβRI	CTT AAT TCC TCG AGA TAG GC	GTG AGA TGC AGA CGA AGC
human TβRII	GGT TCC TGT GTG CCC TTA TT	TGC AAC CCA TGA AGG TAA AA
human TβRIII	CTG GCC AGC TAC AGA GAG AG	ACC CTC AGA CAC CAA AAA CA
human β-actin	CGT GGA CAT CCG CAA AGA C	AGG GTG TAA CGC AAC TAA G
human CCL2	CAG CCA GAT GCA ATC AAT GCC	TGG AAT CCT GAA CCC ACT TCT
human CCL5	ATC CTC ATT GCT ACT GCC CTC	GCC ACT GGT GTA GAA ATA CTC C
human CSF-1	CAG AAG GAG GAC CAG CAA GTG A	GAT CCC TCG GAC TGC CTC TC
human CSF-2	CTC AGA AAT GTT TGA CCT CCA G	TGA CAA GCA GAA AGT CCT TCA G
Human VEGF	GAG ATG AGC T TC CTA CAG CAC	TCA CCG CCT CGG CTT GTC ACA T
Mouse HIF1α	GGT TCC AGC AGA CCC AGT TA	AGG CTC CTT GGA TGA GCT TT
Mouse HIF1β	TTT ATC CCT AGA GAT GGG TAC AGG	CCA CAG GCT GGA CAG AAA CC
mouse β-actin	AAG AGC TAT GAG CTG CCT GA	TAC GGA TGT CAA CGT CAC AC
mouse CXCL1	CCT TGA CCC TGA AGC TCC CT	CGG TGC CAT CAG AGC AGT CT
mouse CCL5	GCA AGT GCT CCA ATC TTG CA	GAT GTA TTC TTG AAC CCA CTT CTT CTC
mouse CSF-1	CAT CTC CAT TCC CTA AAT CAA C	ACT TGC TGA TCC TCC TTC C
mouse VEGF	GAG GAT GTC CTC ACT CGG ATG	GTC GTG TTT CTG GAA GTG AGC AA

Western blot analysis

Whole cells lysates were prepared with RIPA buffer (Pierce, Rockford, IL). Antibodies against the following proteins were used: Six1, TβRI, TβRII, TβRIII,

aldehyde dehydrogenase 1 (ALDH1), β-catenin, cyclin E (1:1000, all from Santa Cruz Biotechnology, Santa Cruz, CA), E-cadherin, fibronectin (1:10,000, both from BD Biosciences, San Jose, CA), ERK, p-ERK, JNK, p-JNK, p38, p-p38, p-STAT3, cyclin D1, vimentin (1:3000, all from Cell Signaling Technology, Danvers, MA), matrix metalloproteinases (MMP)2, MMP9, proliferating cell nuclear antigen (PCNA), vascular endothelial growth factor (VEGF) (1:1000, all from Abcam, Cambridge, MA).

For Triton X-100-soluble and -insoluble protein fractionation experiments, cell extracts were prepared as previously described (Sadot et al., 1998). Briefly, HKc/HPV16-Ctrl and HKc/HPV16-Six1 were plated in 6-well plates and cultured in complete medium supplemented with 1.0 mM Ca^{2+} for the indicated times. The Triton X-100-soluble fraction was extracted at room temperature with 200 μl of 0.5% Triton X-100, 2.5 mM EGTA, 5 mM MgCl2, and 50 mM MES (pH 6.0) for 2 min. Then plates were washed twice with the same buffer. The Triton X-100-insoluble fraction was scraped into 200 μl of the same buffer. Equal volumes (20 μl) of cell fractionation extracts were separated by SDS-polyacrylamide gel electrophoresis (SDS-PAGE).

Sera from MC38-Ctrl- and MC38-Six1- tumor bearing mice were analyzed by Western blotting. Antibodies against the following proteins were used: MMP2, MMP9, VEGF, HGF, interleukin (IL)-1β, LOX (1:1000, Abcam), TNFα, and IL-6 (1:1000, Cell Signaling Technology).

The blots were incubated with primary antibody overnight at 4°C, washed three times with PBST, followed by incubation with horseradish peroxidase (HRP)-conjugated secondary antibody (1:10,000, Millipore, Temecula, CA). The blots were visualized with ECL Prime Western Blotting Detection System (GE Healthcare, Buckinghamshire, UK)

and exposed to BioMax light film (Kodak, Rochester, NY). As an internal control for equal protein loading, blots were stripped and reprobed with antibody against β-actin (Santa Cruz Biotechnology). Images were analyzed further using Image J software (NIH, Bethesda, MD) to obtain a semi-quantitative assessment of band intensities.

Microarray analysis

Total RNA was isolated using the Agilent Total RNA Isolation Mini Kit according to the manufacturer's protocol. RNA quality was assessed using an Agilent 2100 Bioanalyzer and RNA Integrity Numbers (RIN) ranged from 9.8 to 10.0. Microarray experiments were performed using the Agilent platform. Total RNA was amplified and dye labeled using Agilent's Low Input Quick Amp Labeling Kit (Agilent, Wilmington, DE) according to the manufacturer's instructions. Labeled RNA was then purified using Qiagen's RNeasy Mini Kit (Qiagen, Valencia, CA) and dye incorporation and cRNA yield were assessed. Labeled cRNA samples were hybridized to Agilent Whole Human Genome Microarrays 4x44K (Agilent, Wilmington, DE) using Agilent's Gene Expression Hybridization Kit (Agilent, Wilmington, DE) according to the manufacturer's instructions. Four vector control samples were hybridized against four Six1 overexpression samples in a dye swap design. One slide was hybridized for HKc/HPV16 and another slide for HKc/DR. After washes and drying, arrays were scanned for both the Cy3 and Cy5 channels at 5 μm resolution using a ProScanArray Express HT scanner (Perkin Elmer Life and Analytical Sciences) and the ScanArray Express SP3 software. The scanned images were saved as TIFF files and fluorescence intensities were quantitated using ImaGene 8.0.1 software (BioDiscovery). Raw

intensities for backgrounds and foregrounds (spots) were uploaded into limmaGUI (Wettenhall and Smyth, 2004) where features were background corrected using the Normexp method with offset equal to 50 (Ritchie et al., 2007). Subsequently, data were normalized within arrays using the locally weighted scatterplot smoothing (LOESS) algorithm and between the arrays performing scale normalization. Normalized data (M and A values) were exported from limmaGUI and normalized intensities for both Cy3 and Cy5 channel were calculated for all arrays by solving the equations for M and A, using M = log2(R/G) and A = 1/2 [log2(R) $^{+}$ log2(G)]. R = Cy5 channel intensity (Red), and G = Cy3 channel intensity (Green). In the final step, normalized intensities were uploaded and analyzed using GeneSifter software (Geospiza, Inc.).

Immunofluorescence studies

Cells were plated in Lab-Tek II chambers (Nalge Nunc International, Rochester, NY) for 24 h. Following fixation (with 4% paraformaldehyde in PBS, pH 7.2) and permeabilization (with 0.1% Triton X-100 in PBS), samples were incubated with antibodies against E-cadherin (1:200), β-catenin (1:100), fibronectin (1:200), TβRI (1:100), TβRII (1:100) or TβRIII (1:100) overnight at 4°C. Samples were then washed three times with PBST, followed by incubation with an Alexa 568-conjugated secondary antibody (1:1000, Invitrogen). Nuclei were stained with 1:20,000 dilution of 4', 6-diamidino-2-phenylindole (DAPI) (Invitrogen) before cells were mounted. Slides were viewed using either an Olympus X81 fluorescence microscope or a Zeiss LSM510 META confocal scanning laser microscope.

Cells were plated in Lab-Tek II chambers (Nalge Nunc International, Rochester, NY) for 24 h. Following fixation (with 4% paraformaldehyde in PBS, pH 7.2) and permeabilization (with 0.1% Triton X-100 in PBS), samples were incubated with antibodies against E-cadherin (1:200), β-catenin (1:100), fibronectin (1:200), TβRI (1:100), TβRII (1:100) or TβRIII (1:100) overnight at 4°C. Samples were then washed three times with PBST, followed by incubation with an Alexa 568-conjugated secondary antibody (1:1000, Invitrogen). Nuclei were stained with 1:20,000 dilution of 4', 6-diamidino-2-phenylindole (DAPI) (Invitrogen) before cells were mounted. Slides were viewed using either an Olympus X81 fluorescence microscope or a Zeiss LSM510 META confocal scanning laser microscope.

Cell invasion and migration assays (Transwell)

The invasive ability of HKc/HPV16-, HKc/DR- and MC38-Ctrl and their corresponding HKc/HPV16-, HKc/DR- and MC38-Six1 was measured using transwell chambers (24 well plate) (Costar, Cambridge, MA) with polycarbonate membranes (8.0-μm pore size) coated with 100 μl Matrigel (BD Biosciences, Franklin Lakes, NJ) on the top side of the membrane. The upper surface of the matrix was plated with 20,000 cells, and the cells were kept in basal medium containing 0.1% bovine serum albumin (BSA). The lower chamber contained complete medium. After 24 h the cells were fixed and stained with 0.1% crystal violet. Cells and Matrigel on the upper surface of the membrane were carefully removed with a cotton swab. Enumeration of the cells that invaded through the matrix was accomplished by visually counting cells in five randomly chosen areas. Alternatively, crystal violet was extracted with ethanol and the absorbance

determined in a spectrophotometer. The migration of cells was measured by directly counting the cells in lower chamber. Each experiment was performed in triplicate wells and repeated three times.

Wound healing (scratch) assay

MC38-Ctrl and MC38-Six1 cells were plated into 6-well plates and cultured until approximately 90% confluent. Cell monolayers were wounded with a sterile 200 µl pipet tip and then incubated with DMEM containing 1% FBS for 24 h or 48 h in a humidified atmosphere of 5% CO2 and 95% air at 37 °C. Representative areas of wounded monolayers containing wounds of the same width were marked and photographed under an inverted microscope at 40× magnification. After incubation, the same areas were photographed. The extent of wound repair was evaluated by measuring the area of the wound by computerized image analysis using Image J software (NIH). Each experiment was performed in triplicate wells and repeated three times.

Cell proliferation assay

To determine the growth rate of HKc/HPV16, HKc-Ctrl, HKc-Six1, HKc/DR, HKc/DR-Ctrl and HKc/DR-Six1, 50,000 cells in 2 ml of their respective media were plated per well in 6-well plates. Cells in triplicate wells were counted daily for up to 5 days of incubation at 37 °C, using a hemocytometer. For MC38, MC38-Ctrl and MC38-Six1, 20,000 cells per well in 2 ml of DMEM containing 10% FBS were plated in 6-well plates.

Luciferase assays

HKc/HPV16-Ctrl, HKc/HPV16-Six1, HKc/DR-Ctrl and HKc/DR-Six1 were seeded into 6-well plates. Transfections were performed using TransFast Transfection Reagent (Promega) according to the manufacturer's instructions. The luciferase construct p6SBE-luc, which contains six copies of the Smad binding element (SBE) and p6SME-luc, which contains Smad mutated elements (SME) were obtained from Dr. Scott Kern (Dai et al., 1998). For each well, cells were transfected with either p6SBE-luc (4 μg) or p6SME-luc (4 μg), along with pRL-SV40 (4 ng) (Promega, Madison, WI) *Renilla* luciferase as a control for transfection efficiency. Cells were treated with 40 pM TGF-β1 or vehicle 24 h after transfection. Both firefly and *Renilla* luciferase activity were measured using the Dual Luciferase Assay Kit (Promega, Madison, WI) 48 h after transfection. Firefly luciferase values were normalized to *Renilla* luciferase values.

Single-cell isolation from tumors

Tumors were dissected free of necrotic areas, connective tissue, and blood clots then rinsed 3 times with cold (4°C) DMEM containing 1% FBS and 2% Pen/Strep. Tumors were sliced into 1-3 mm3 fragments and then incubated in DMEM containing collagenase type I (200 units/ml), DNase (270 units/ml), and hyaluronidase type IV (35 NF units/ml) (Sigma, St. Louis, MO for 30 min at 37 °C. The resulting cell suspension was kept in wet ice, filtered through a 70 μm nylon cell strainer (BD Biosciences, Bedford, MA), and washed twice with PBS.

Flow cytometry analysis

HKc/DR-Ctrl and HKc/DR-Six1 were stained with FITC-conjugated anti-CD24 and PE-conjugated anti-CD44. MC38-Ctrl and MC38-Six1 were stained with FITC-conjugated anti-CD44 and PE-conjugated anti-CD166. Single-cell suspensions isolated from MC38-Ctrl or MC38-Six1 tumors were stained with eFluor450-conjugated anti-CD45, APC-conjugated CD11b, FITC-conjugated anti-Gr1 and PE-conjugated anti-F4/80. All the antibodies were purchased form eBioscience (San Diego, CA). One million cells were incubated with antibodies in 100 μl wash buffer (PBS containing 0.1% BSA) at 4 °C for 1 h. Cells were then washed twice with ice-cold wash buffer, and fixed with 1% paraformaldehyde. Flow cytomertry analysis was performed using a BD LSRII flow cytometer (BD Biosciences, San Jose, CA), and 30,000 cells were analyzed.

In vitro tumorsphere formation assay

HKc/HPV16-Ctrl, HKc/HPV16-Six1, HeLa-Ctrl, HeLa-Six1, MC38-Ctrl and MC38-Six1 (10,000 per well) were plated in ultra-low attachment 6-well plates (Corning, Tewksbury, MA) in 2 ml serum-free DMEM/F12 media (Invitrogen) supplemented with 20 ng/ml EGF (Sigma, St. Louis, MO), 10 ng/ml basic fibroblast growth factor (bFGF, Sigma), 5 μg/ml insulin (Sigma), 1×B27 supplement (Invitrogen) and 0.4% bovine serum albumin (BSA, Sigma). Cells were cultured under 5% CO2 at 37°C for 7 days.

Xenograft mouse model

Eight-week-old female athymic nude (nu/nu) mice were purchased from The Jackson Laboratory (Bar Harbor, Maine). Briefly, 5×10^6 HKc/DR-Ctrl or HKc/DR-Six1

cells were suspended in 100 μl of serum-free medium containing 50% Matrigel, and injected subcutaneously into the flank of nude mice. For HeLa, 3×10^6 HeLa-Ctrl or HeLa-Six1 were injected into each side of the flank of nude mice. Six weeks after implantation, mice were sacrificed and the tumor weights were measured.

Homograft mouse model

For the orthotopic model, MC38-Ctrl and MC38-Six1 were harvested and washed with PBS just prior to implantation. Eight-week-old male and female syngeneic C57BL/6 mice were anesthetized by inhalation of 2% isoflurane in oxygen. A midline incision was made to expose the cecum. Then, 10 μl of PBS containing 2×10^6 MC38-Ctrl or MC38-Six1 cells were injected into the cecum subserosa using a 33-gauge micro-injector (Hamilton Company, Reno, NV). The injection site was sealed with a tissue adhesive (3M, St. Paul, MN) and washed with 70% alcohol and PBS to eliminate the leakage of the cancer cells. The cecum was replaced in the peritoneal cavity, and the abdominal wall and skin closed with 6-0 polyglycolic acid sutures (CP Medical, Portland, OR). Six weeks after implantation, mice were sacrificed. Tumor weights were measured, and tumors were processed for further analysis.

For the subcutaneous model, 2×10^6 MC38-Ctrl or MC38-Six1 cells were suspended in 100 μl of PBS, and injected subcutaneously into the flank of C57BL/6 mice. Six weeks after implantation, mice were sacrificed and tumors were stripped and weighted.

For the splenic metastasis model, eight-week-old syngeneic C57BL/6 mice were anesthetized by inhalation of 2% isoflurane in oxygen. A lateral incision was made to

expose the spleen. Ten microliters of PBS containing 2×10^5 MC38-Ctrl or MC38-Six1 cells were injected into the spleen using a 33-gauge micro-injector. The injection site was pressed using a cotton swab to stop bleeding, sealed with a tissue adhesive and washed with PBS to eliminate the leaked cancer cells. The spleen was replaced and the abdominal wall and skin closed with 6-0 polyglycolic acid sutures. Three weeks after implantation, mice were sacrificed and spleens and livers were collected and weighted.

Histology and immunohistochemistry

Tumors were fixed and embedded in paraffin, 5 μm sections were obtained and stained with hematoxylin and eosin (H&E) (VWR, West Chester, PA) for visual examination.

Tumor sections were deparaffinized, rehydrated, then incubated in a microwave oven with 0.01 M citrate buffer, pH 6.0 for 10 min for antigen retrieval. Endogenous peroxidases were blocked with 3 % H_2O_2 for 15 min. Nonspecific epitopes were blocked with horse serum (Jackson ImmunoResearch, West Grove, PA) for 1 h. The sections were incubated overnight at 4°C with antibodies against one of the following proteins: PCNA (1:300, abcam), CD31, LOX, MMP9, α-SMA, VEGF, vascular endothelial growth factor receptor 1 (VEGFR1) (1:100, abcam), cleaved caspase 3 (1:100, Cell Signaling Technology), Six1, ALDH1, (1:100, Santa Cruz), and Ki67 (1:100, OriGene). After incubation with a HRP-conjugated secondary antibody (BioRad) for 1 h at room temperature, antigen signals were detected using the 2-Solution Diaminobenzidine (DAB) Kit (Invitrogen), counterstained with hematoxylin, mounted in Acrymount (StatLab, Mckinney, TX), and visualized under a light microscope.

Statistical Analysis

Data were expressed as the mean ± standard deviation (SD). Statistical analysis was performed using the students' t-test when only two value sets were compared, and one-way ANOVA followed by Dunnett's test when the data involved three or more groups. $P < 0.05$, $P < 0.01$ or $P < 0.001$ were considered statistically significant and indicated in the figures by *, ** or *** respectively.

CHAPTER 3

SIX1 PROMOTES EPITHELIAL-MESENCHYMAL TRANSITION AND MALIGNANT CONVERSION IN HKC/DR

3.1 INTRODUCTION

In our *in vitro* model for HPV-mediated carcinogenesis, normal human keratinocytes (HKc) immortalized by transfection with HPV16 DNA (HKc/HPV16) progress toward malignancy through growth factor-independent (HKc/GFI) and differentiation-resistant (HKc/DR) stages (Pirisi et al., 1988). Although immortalized and differentiation resistant, HKc/DR are not tumorigenic (Pirisi et al., 1988). Gene expression profiling studies determined that Six1 is overexpressed in HKc/DR. Furthermore, Six1 was overexpressed in 23% of cervical cancer samples in a tissue microarray (Wan et al., 2008). These findings prompted us to further investigate the role of Six1 overexpression in HPV16-mediated transformation.

The Six1 homeoprotein, a member of the Six family of homeodomain transcription factors, is essential for the development of numerous organs (Ikeda et al., 2010; Xu et al., 2003; Zheng et al., 2003). Six1 overexpression has been found in various human cancers including tumors of the breast (Coletta et al., 2008), ovary (Behbakht et al., 2007), cervix (Wan et al., 2008; Zheng et al., 2010) and liver (Ng et al., 2010). Six1 overexpression is associated with increased tumor progression and metastasis, and decreased survival (Christensen et al., 2008). For example, Six1 overexpression in human

breast cancer cell lines induced epithelial-mesenchymal transition (EMT) and metastasis, which was associated with Smad-dependent transforming growth factor-β (TGF-β) signaling and increased TGF-β receptor type I (TβRI) expression (Micalizzi et al., 2009; Micalizzi et al., 2010). SIX1 mRNA expression increased during *in vitro* progression of HPV16-immortalized cells and Six1 protein is overexpressed in cervical cancer tissues, which strongly suggests that Six1 might be involved in the progression of cervical premalignant lesions to cervical cancer (Wan et al., 2008). Six1 is also overexpressed in cervical cancer cell lines, and the extent of Six1 overexpression correlates to increased tumor malignancy and lymph node metastasis (Tan, Zhang, and Qian, 2011; Wan et al., 2008; Zheng et al., 2010). However, the mechanisms by which Six1 promotes cervical carcinogenesis and progression remain to be determined.

In this study we explored the functional consequences of Six1 overexpression in HKc/DR. HKc/DR overexpressing Six1 exhibited a more mesenchymal phenotype compared to vector controls, including a fibroblastic appearance and increased motility and invasion. Induction of EMT by overexpression of Six1 was associated with decreased activity of Smad-dependent signaling and activation of the mitogen-activated protein kinase (MAPK) pathway. In particular, we observed increased activity of p38 MAPK and increased expression of the TβRII upon Six1 overexpression. Moreover, we determined that overexpression of Six1 in HKc/DR resulted in malignant conversion which was associated with an increase in the population of cancer stem cell (CSC)-like cells. We conclude that Six1 overexpression in HKc/DR induces EMT and promotes tumorigenesis by activation of p38-TβRII signaling.

3.2 RESULTS

3.2.1 THE EXPRESSION OF SIX1 INCREASES DURING HPV16-MEDIATED TRANSFORMATION OF HKC

Previous studies in our laboratory using gene expression profiling discovered that SIX1 mRNA increased during *in vitro* progression of HKc/HPV16 toward the HKc/DR phenotype (Wan et al., 2008). To further validate overexpression of Six1 during *in vitro* progression of HPV16-immortalized HKc, we conducted both real time PCR and Western blot analysis for Six1 in three sets of HKc/HPV16 and HKc/DR lines (designated D1, D4 and D5), derived from normal HKc isolated from three different foreskins.

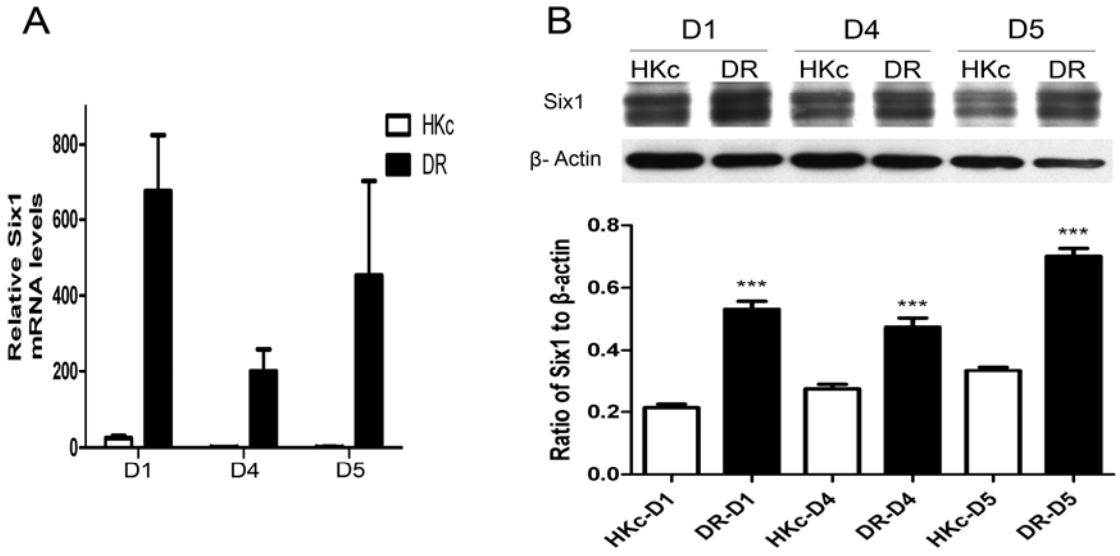

Figure 3.1 The expression of Six1 increases during *in vitro* progression of HPV16-immortalized human keratinocytes. (A) Real-time PCR analysis of Six1 mRNA in three independently derived HKc/HPV16 (HKc) lines (D1, D4 and D5) and their corresponding HKc/DR (DR) lines. Six1 expression was normalized to β-actin. (B) Top: western blot for Six1 in HKc/HPV16-D1, -D4 and -D5, (labeled as HKc) and their corresponding HKc/DR (labeled as DR). β-actin was used as control for equal protein loading. Bottom: the expression of Six1 protein was quantified by using ImageJ software. Bars indicate standard deviation (SD) and *** indicate statistically significant p value < 0.001.

The results showed that the expression of both Six1 mRNA (Figure 3.1A) and protein (Figure 3.1B) increased in HKc/DR compared to HKc/HPV16.

3.2.2 OVEREXPRESSION OF SIX1 INDUCES ALTERATIONS IN CELL MORPHOLOGY AND BEHAVIOR

HKc/DR stably overexpressing Six1 were established by transfection of HKc/DR (referred to as HKc/DR-Six1) with pcDNA3.1-Six1. Controls (referred to as HKc/DR-Ctrl) were HKc/DR transfected with pcDNA3.1. Western blots confirmed that HKc/DR-Six1 overexpressed Six1 protein (Figure 3.2A). HKc/DR-Six1 exhibited an elongated and fibroblastic appearance rather than the typical cobblestone epithelial-like morphology of HKc/DR-Ctrl (Figure 3.2B). The overexpression of Six1 in HKc/DR increased cell migration approximately 2.6-fold and cell invasion through Matrigel by 6.5-fold (Figure 3.2C). Six1 overexpression inhibited cell proliferation (Figure 3.2D). These data demonstrate that HKc/DR overexpressing Six1 exhibited a much more mesenchymal phenotype with increased migration and cell invasion properties compared to the vector-transfected controls.

3.2.3 SIX1 OVEREXPRESSION IN HKC/DR PROMOTES EMT

We next explored the effects of Six1 overexpression on global gene expression using Agilent Whole Human Genome Microarrays (4x44K). Paired comparisons of gene expression were made between four individual clones of HKc/DR-Ctrl and HKc/DR-Six1. We used Gene Sifter software to analyze the microarray results.

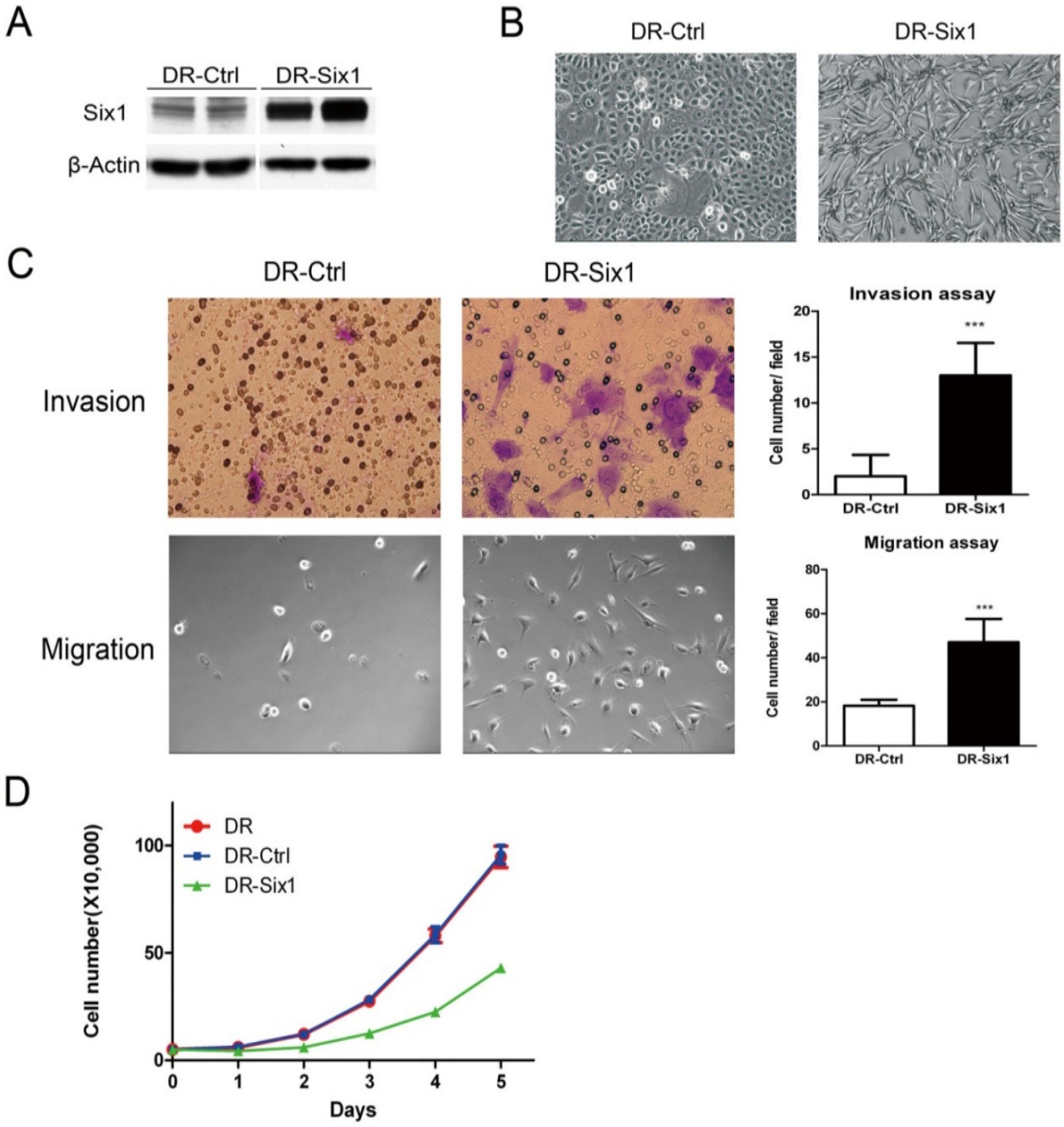

Figure 3.2 Six1 overexpression in HKc/DR induces EMT-like characteristics. (A) HKc/DR were stably transfected with either pcDNA3.1 (DR-Ctrl) or pcDNA3.1-Six1 (DR-Six1). Six1 protein levels in cell extracts were determined by western blotting. β-actin was used as a loading control. (B) Cell morphology of HKc/DR-Ctrl (DR-Ctrl) and HKc/DR-Six1 (DR-Six1). Images are shown at 100× magnification. (C) Invasion (upper panels) and migration (lower panels) assays for HKc/DR-Control (DR-Ctrl) and HKc/DR-Six1 (DR-Six1). Images for the invasion assay are shown at 400× and those for migration at 100× magnification. Quantification of the invasion assay and the migration assay are shown in the upper right and lower rights panels, respectively. Bars indicate SD, and *** indicate statistically significant p values < 0.001. (D) Cell proliferation was determined by directly counting cells at the days indicated in HKc/DR (DR), HKc/DR-Six1 (DR-Six1), and HKc/DR-Ctrl (DR-Ctrl).

To determine the differentially expressed genes in the pairwise comparisons we used a fold change greater than 1.5 and a p-value smaller than 0.05 as cutoff values. In addition, KEGG pathways analysis was performed on the differentially expressed genes. We noted that a number of EMT related genes were changed in SIX1-overexpressing HKc/DR. We used Cluster and TreeView software to analyze genes involved in cell-cell junctions and a series of markers associated with EMT in HKc/DR-Ctrl and HKc/DR-Six1 (Figure 3.3A). We found that, in response to Six1 overexpression, cell-cell junctions and EMT markers were altered, including decreased expression of epithelial-related genes, such as E-cadherin (CDH1) and occludin (OCLN), and increased expression of mesenchymal-related genes, such as fibronectin (FN1), N-cadherin (CDH2) and vimentin (VIM), as well as increased expression of transcription factors that promote EMT, such as snail (SNAI1), twist1 and ZEB2 (Figure 3.3A). These microarray data suggest that Six1 overexpression induces EMT in HKc/DR.

Real time PCR was used to confirm selected gene expression changes identified by microarrays. As shown in Figure 3.3B, the mRNA level of E-cadherin and occludin decreased by 86% and 84% respectively, while mRNA levels of fibronectin, N-cadherin, vimentin and snail increased by 5.1-, 10.5-, 10.6- and 4.0-fold respectively in HKc/DR-Six1 compared to HKc/DR-Ctrl. Furthermore, we examined the protein levels of E-cadherin (an epithelial maker) and fibronectin (a mesenchymal marker) by western blot analysis and immunofluorescence. The results showed changes in protein levels that corresponded with what we observed at the mRNA level (Fig 3.3C). We also investigated β-catenin, because it is a key component of adherens junctions in epithelial cells (Schock

and Perrimon, 2002), and we found that the expression of β-catenin decreased in cells overexpressing Six1 (Fig 3.3C).

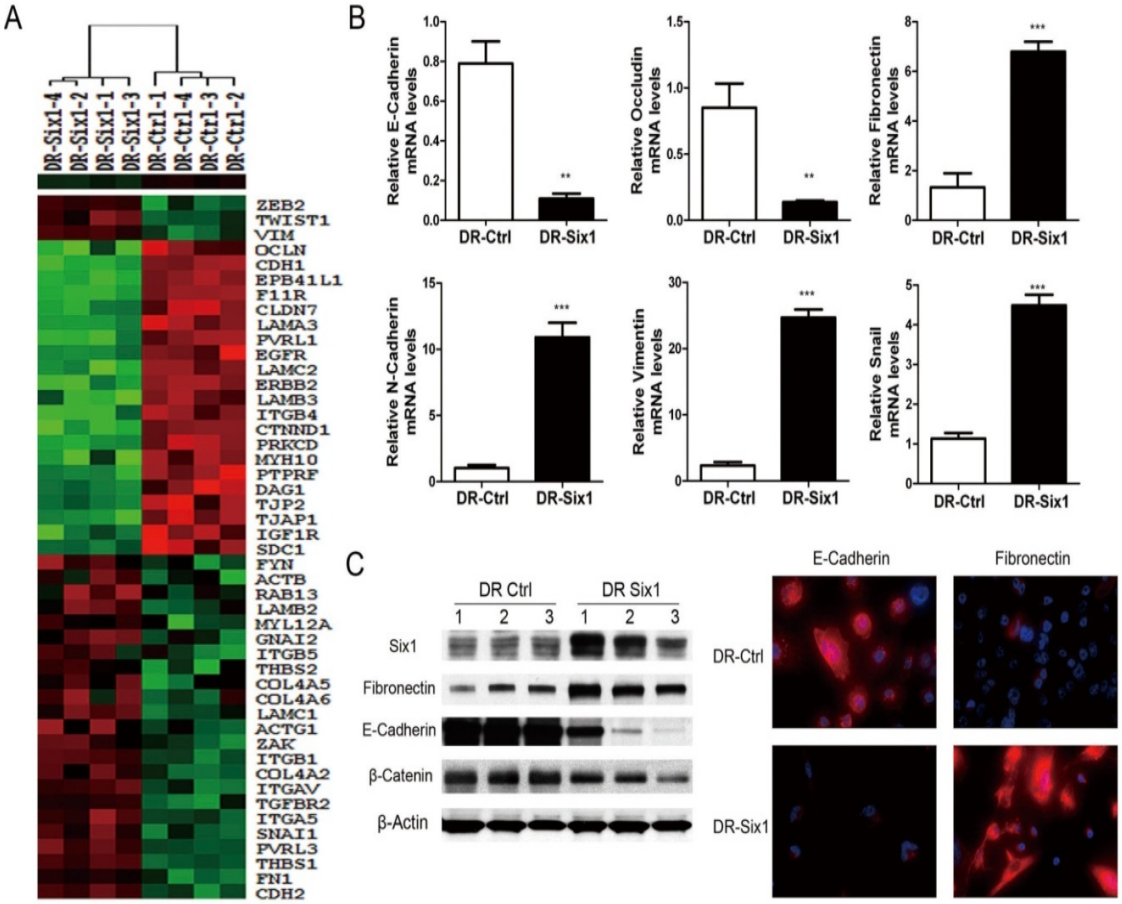

Figure 3.3 Six1 overexpression induces markers of EMT in HKc/DR. (A) Hierarchical clustering of differentially expressed genes involved in cell-cell junctions and EMT between HKc/DR-Ctrl (DR-Ctrl) and HKc/DR-Six1 (DR-Six1) was conducted using cluster and TreeView software. The color represents the expression level of a gene above (red), below (green), or at (black) the mean expression level of that gene across all samples. (B) Levels of mRNA expression of E-cadherin, occludin, fibronectin, N-cadherin, vimentin and snail were determined by Real time PCR in HKc/DR-Ctrl (DR-Ctrl) and HKc/DR-Six1 (DR-Six1). Data were normalized to β-actin expression. Bars indicate SD, and ** and *** indicate statistically significant p values < 0.01 and 0.001 respectively. (C) Left panel: western blot for Six1, fibronectin, E-cadherin and β-catenin in HKc/DR-Ctrl (DR-Ctrl) and HKc/DR-Six1 (DR-Six1). β-actin was used as loading control. Right panels: immunofluorescent staining of E-cadherin (red) and fibronectin (red) merged with nuclei (blue) in HKc/DR-Ctrl (DR-Ctrl) and HKc/DR-Six1 (DR-Six1). Images are shown at 400× magnification.

Since the distribution of E-cadherin and β-catenin is critical for functional organization of adherens junctions, we used confocal microscopy to compare cellular localization and overall levels of E-cadherin, β-catenin and fibronectin in HKc/DR-Six1 to that found in HKc/DR-Ctrl. The results show a dramatic downregulation of E-cadherin and β-catenin, and increased levels of fibronectin in HKc/DR-Six1, which is a hallmark of EMT (Figure 3.4). Taken together, our data show that Six1 overexpression promotes EMT at the late stage of HPV16-mediated transformation.

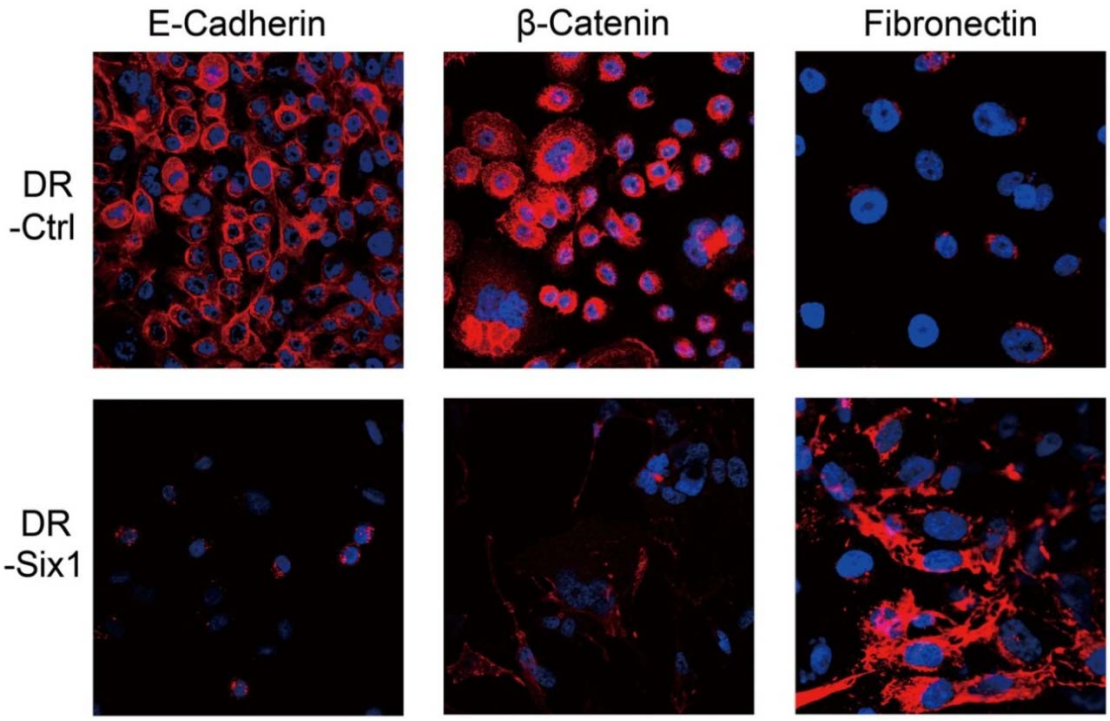

Figure 3.4 Immunofluorescent staining of E-cadherin, β-catenin and fibronectin (red) in HKc/DR-Ctrl (DR-Ctrl) and HKc/DR-Six1 (DR-Six1). Nuclei were stained with DAPI (blue). Images were taken using a confocal microscope and are shown at 400× magnification.

3.2.4 INCREASED LEVELS OF TGF-B RECEPTORS ARE ASSOCIATED WITH SIX1 OVEREXPRESSION

Since Six1 overexpression induced EMT in HKc/DR, we attempted to identify the signaling pathways regulated by Six1 that might be involved in promoting EMT. The TGF-β pathway has been found to be dysregulated at early stages of cervical cancer (Noordhuis et al., 2011), and TGF-β is a potent inducer of EMT in HKc/DR (Kowli et al., 2013). Numerous EMT-associated genes regulated by TGF-β have been identified (summarized in (Wendt, Allington, and Schiemann, 2009)). Therefore, we further analyzed our microarray data for those genes involved in TGF-β signaling. In response to Six1 overexpression, we observed altered expression of EMT associated genes targeted by TGF-β such as increased Dab2, Hic5, vimentin, N-cadherin, urokinase plasminogen activator (uPA), α-SMA, β3 integrin, and decreased E-cadherin, indicating that Six1-induced EMT may be associated with activation of TGF-β signaling (Table 3.1).

Table 3.1. Expression of EMT-associated Genes Targeted by TGF-β in HKc/DR

Genes	***Direction***	***Ratio***	***p-value***
E-cadherin	Down	6.00	0.0000318
β3 integrin	Up	3.29	0.000146
N-cadherin	Up	5.33	0.0000291
Vimentin	Up	11.68	0.000035
α-Smooth Muscle Actin	Up	1.65	0.000736
Fibronectin	Up	5.10	0.0000709
Urokinase Plasminogen Activator	Up	4.27	0.0000149
Dab2	Up	1.79	0.006232
Hic5	Up	1.57	0.001866

Three receptors, TGF-β receptor type I, type II and type III (TβRI, TβRII and TβRIII), are involved in TGF-β signaling (Meulmeester and Ten Dijke, 2011). Two of the TGF-β receptors were upregulated in HKc/DR overexpressing Six1. Real time PCR

showed upregulation of TβRII mRNA by about 2.4-fold and TβRIII expression by 6.6-fold in DR-Six1 compared to DR-Ctrl (Figure 3.5A). TβRI mRNA increased by about 1.7-fold in DR-Six1, but that change was not statistically significant (Figure 3.5A). Western blotting and immunofluorescence analysis determined increased protein levels of TGF-β receptors, consistent with the changes in mRNA levels (Figure 3.5B).

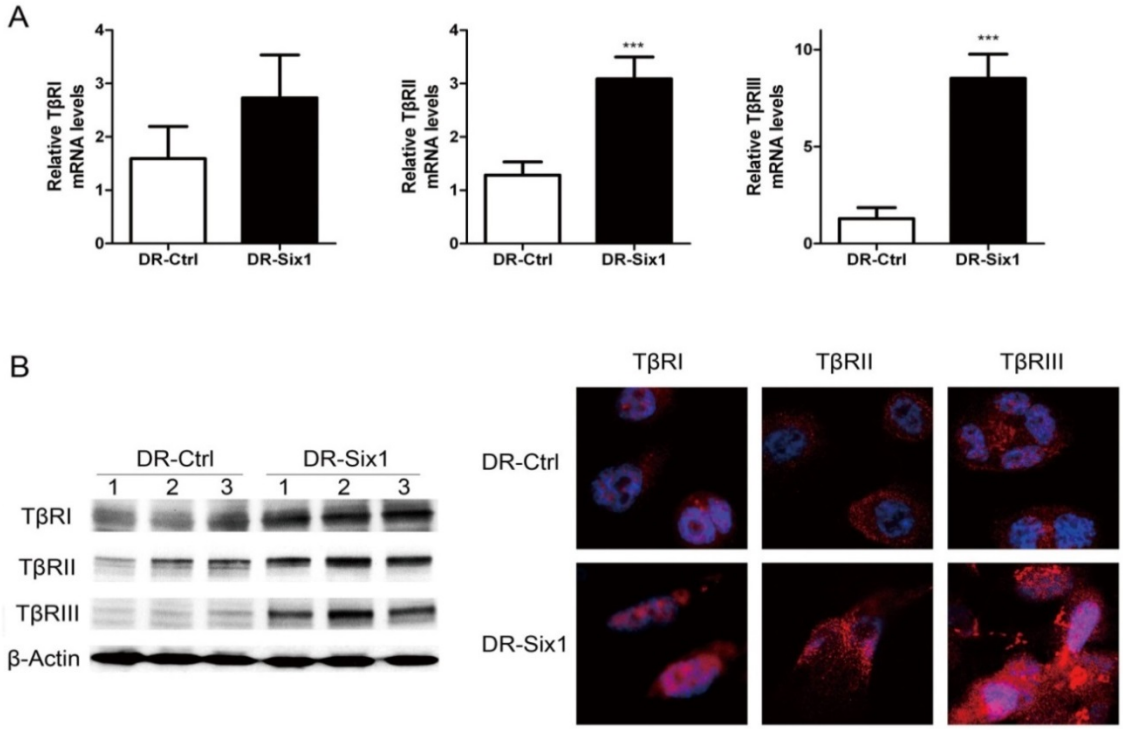

Figure 3.5 Six1 overexpression in HKc/DR increases the expression of TβRs. (A) Levels of mRNA expression of TβRI, TβRII and TβRIII were determined by real time PCR in HKc/DR-Ctrl (DR-Ctrl) and HKc/DR-Six1 (DR-Six1). Data were normalized to β-actin expression. Bars indicate SD and *** indicate statistically significant p values < 0.001. (B) Left panel: western blot analysis of TβRI, TβRII and TβRIII in HKc/DR-Ctrl (DR-Ctrl) and HKc/DR-Six1 (DR-Six1). β-actin was used as control for equal protein loading. Right panels: immunofluorescent staining of TβRI, TβRII and TβRIII (red) in HKc/DR-Ctrl (DR-Ctrl) and HKc/DR-Six1 (DR-Six1). Nuclei were stained with DAPI (blue). Images are shown at 630× magnification.

Taken together, our results show that Six1 overexpression leads to enhanced expression of the TGF-β receptors, especially TβRII and TβRIII, which might contribute to activation of TGF-β signaling.

3.2.5 SMAD-DEPENDENT TGF-B SIGNALING IS NOT ACTIVATED IN ASSOCIATION WITH SIX1

We next investigated whether increased TGF-β receptors are linked to enhanced canonical TGF-β signaling in DR-Six1. We analyzed basal phosphorylation of Smad2/3 in DR-Ctrl and DR-Six1 by western blotting. Smad2/3 phosphorylation was decreased in Six1 overexpressing cells, suggesting decreased basal canonical TGF-β signaling (Fig 3.6A). To further explore whether Six1 overexpression altered Smad-dependent signaling, we also compared the activity of a Smad-responsive luciferase reporter construct (p6SBE-Luc) in DR-Ctrl to DR-Six1. Overexpression of Six1 decreased somewhat the basal activity of the Smad-responsive luciferase reporter (Fig 3.6B Top Panel). There was also no difference in fold-induction of the Smad-dependent reporter construct between DR-Ctrl (Fig 3.6B Middle Panel) and DR-Six1 (Fig 3.6B Bottom Panel) in response to TGF-β1 treatment. These data suggest that Six1 neither increases endogenous Smad-dependent signaling, nor enhances the activation of Smad-dependent signaling in response to TGF-β1 treatment.

3.2.6 P38 MAPK SIGNALING CONTRIBUTES TO SIX1-INDUCED EMT

Besides Smad-dependent signaling, TGF-β acts through a variety of Smad-independent signaling pathways, including: (1) MAP kinase (MAPK) pathways, such as ERK1/2, p38 MAPK and JNK; (2) PI3K/AKT pathways; and (3) Rho-like GTPase signaling pathways (Zhang, 2009). Thus, we investigated Smad-independent TGF-β signaling in HKc/DR-Ctrl and HKc/DR-Six1 by Western blotting using phospho-specific antibodies for p-ERK, p-p38, p-JNK, p-AKT, and p-PI3K p85.

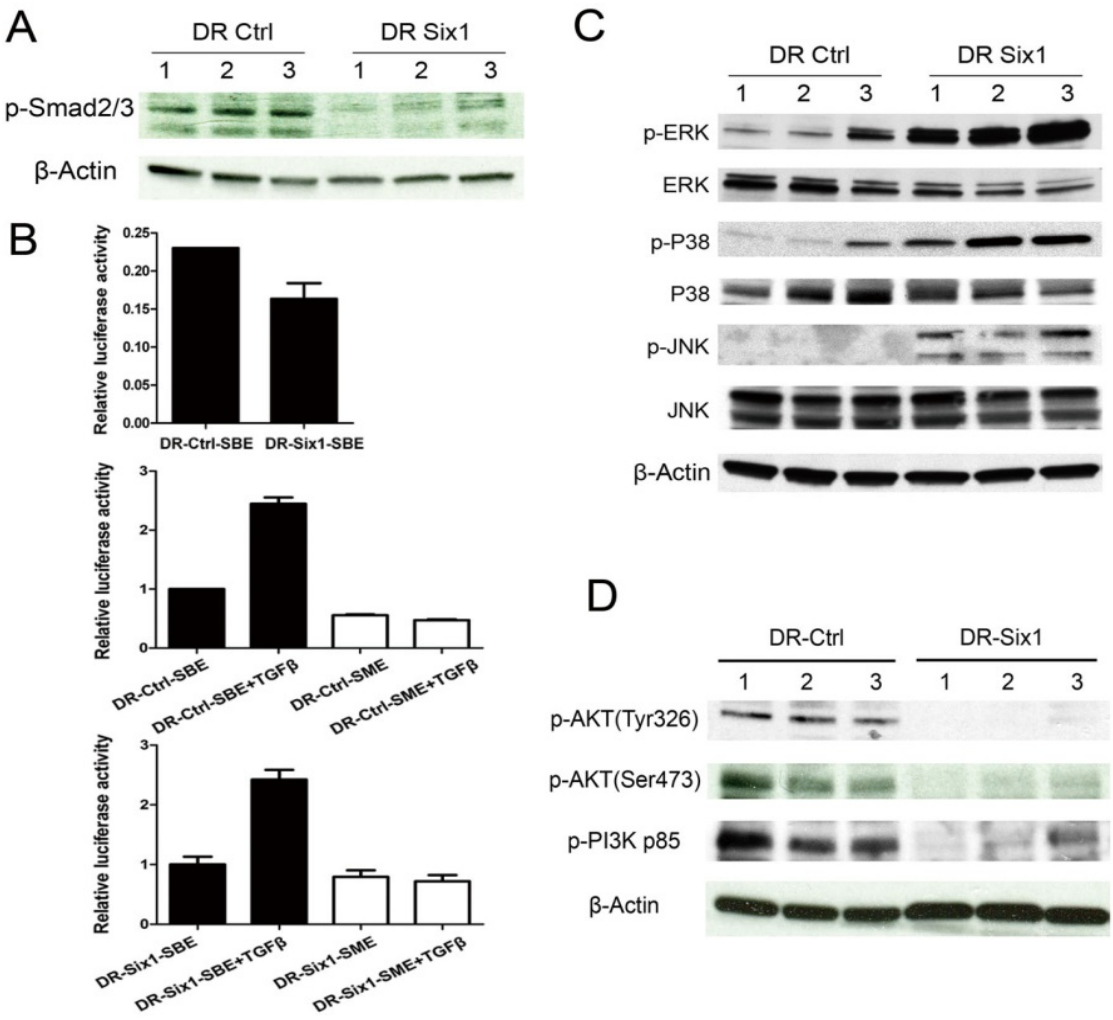

Figure 3.6 Six1 overexpression in HKc/DR activates Smad-independent pathways. (A) Phospho-Smad2/3 was detected by western blot analysis in cell extracts prepared from HKc/DR-Ctrl (DR-Ctrl) and HKc/DR-Six1 (DR-Six1). (B) Upper panel: HKc/DR-Ctrl and HKc/DR-Six1 were co-transfected with a TGF-β-inducible luciferase reporter (p6SBE-luc), which contains six tandem copies of the Smad binding element (SBE), and pRL-SV40 Renilla luciferase, as control for transfection efficiency. Luciferase activity was determined 48 h after transfection. Firefly luciferase values are normalized to Renilla luciferase. Bars indicate SD. Middle/Lower panels: HKc/DR-Ctrl or HKc/DR-Six1 were transfected with either p6SBE-luc or p6SME-luc, which contains mutated SBEs (SME). Twenty four h after transfection cells were treated with 40 pM TGF-β1 for 24 h and then luciferase activity was determined. Values are normalized to Renilla luciferase. Bars indicate SD. (C) Protein levels of p-ERK, ERK, p-p38, p38, p-JNK and JNK were determined by western blotting in HKc/DR-Ctrl (DR-Ctrl) and HKc/DR-Six1 (DR-Six1). (D) Western blot of p-AKT (Tyr326), p-AKT (Ser473) and p-PI3-kinase p85 (Tyr467/199) in HKc/DR-Ctrl (DR-Ctrl) and HKc/DR-Six1 (DR-Six1). β-actin was used as a loading control.

As shown in Figure 3.6C, Six1 overexpression resulted in a dramatic increase in phosphorylation of ERK, p38, and JNK in HKc/DR-Six1. In contrast, overexpression of Six1 resulted in decreased phosphorylation of AKT and PI3K p85, indicating Six1 overexpression in HKc/DR repressed the PI3K/AKT pathway (Figure 3.6D). Collectively, these data suggest activation of MAPKs but not PI3K/AKT upon Six1 overexpression in HKc/DR. ERK1/2, JNK and p38 activation has been reported to induce EMT in various cancers (Zhang, 2009). We next investigated which MAPK played a dominant role in Six1-induced EMT by treating HKc/DR-Six1 with MAPK inhibitors. Treatment of HKc/DR-Six1 with the p38 inhibitor SB202190 blocked several markers of Six1-induced EMT, increasing E-cadherin mRNA and reducing mRNA levels of fibronectin and snail (Figure 3.7A). In contrast, treatment of HKc/DR-Six1 with the ERK inhibitor U0126 did not block Six1 modulation of mRNA markers of EMT, and the JNK inhibitor SP600125 increased mRNA levels of E-cadherin, but did not decrease fibronectin or snail mRNA (Figure 3.7A).

Similar to what was observed at the mRNA level, SB202190, but not U0126 or SP600125, decreased fibronectin protein expression and slightly increased E-cadherin protein level in HKc/DR-Six1 (Figure 3.7B). Moreover, inhibition of p38 by SB202190 treatment in HKc/DR-Six1 decreased the expression of TβRII mRNA by about 38%, but had no effect on the expression of TβRI or TβRIII mRNA (Figure 3.7C). HKc/DR-Six1 treated with SB202190, but not U0126 or SP600125, lost some of their fibroblastic appearance (Figure 3.7D).

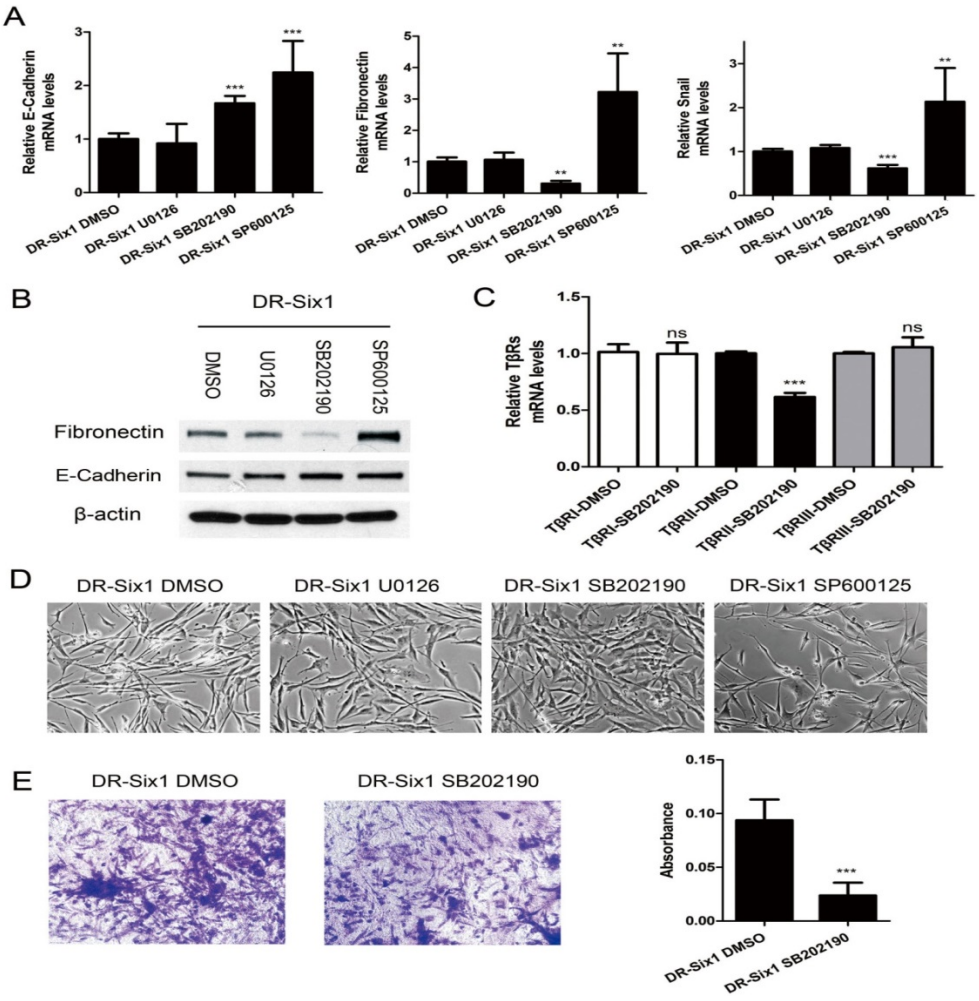

Figure 3.7 Six1 overexpression in HKc/DR activates p38-TβRII signaling. (A) HKc/DR-Six1 were treated with the ERK inhibitor U0126 (10 μM), the p38 inhibitor SB202190 (10 μM), the JNK inhibitor SP600125 (10 μM) or DMSO for 48 h. mRNA expression of E-cadherin, fibronectin and snail was then determined by real time PCR. Data were normalized to β-actin expression. (B) Western blot analysis for E-cadherin, fibronectin and β-actin (loading control) after treatment of HKc/DR-Six1 for 48 h with U0126 (10 μM), SB202190 (10 μM), SP600125 (10 μM) or DMSO. (C) mRNA levels of TβRI, TβRII and TβRIII were determined by real time PCR after treatment of HKc/DR-Six1 with 10 μM SB202190 for 48 h. Data were normalized to β-actin expression. Bars indicate SD, and ** and *** indicate p values < 0.01 and < 0.001 respectively. (D) Phase-contrast photographs of HKc/DR-Six1 treated with U0126 (10 μM), SB202190 (10 μM), SP600125 (10 uM) or DMSO for 48 h. Images are shown at 200× magnification. (E) Invasion assays for HKc/DR-Six1 treated with DMSO or SB202190 (10 μM for 24 h). Cell invasion was determined by a Matrigel invasion assay. Images are shown at 100× magnification. The number of invading cells was quantified after crystal violet staining. Quantification of the invasion assay is presented in the bar graph next to the photographs. Each column represents the mean of three repeats.

Lastly, HKc/DR-Six1 treated with SB202190 exhibited a decreased ability to invade through Matrigel (Figure 3.7E). These results support the conclusion that p38 MAPK signaling plays an important role in promoting EMT in Six1 overexpressing HKc/DR.

3.2.7. OVEREXPRESSION OF SIX1 RESULTS IN MALIGNANT CONVERSION IN HKC/DR AND LARGER TUMORS IN HELA

Next, we tested whether overexpression of Six1 in the non-tumorigenic HKc/DR resulted in malignant conversion. We found that HKc/DR-Six1 formed tumors in nude mice (7 out of 10 mice), whereas HKc/DR-Ctrl failed to form tumors (0 out of 10 mice) (Figure 3.8A). Histologic examination indicated high-grade squamous cell carcinoma, characterized by poor differentiation and high mitotic activity (Figure 3.8B). We detected by immunohistochemistry the expression of Six1 in the tumors as well as Ki67 and PCNA (markers of cell proliferation) (Figure 3.8B). We also dissected the tumor tissue, isolated tumor cells and then cultured the tumor cells *in vitro*: these cells exhibited similar fibroblastic-like morphology as HKc/DR-Six1 (Figure 3.9A), and showed even higher levels of Six1 mRNA than HKc/DR-Six1 (Figure 3.9B).

We also used the human cervical cancer cell line HeLa to explore the enhanced tumorigenic properties associated with Six1 overexpression. We found that HeLa stably overexpressing Six1 (HeLa-Six1) formed larger tumors in nude mice as compared to vector controls (HeLa-Ctrl) (Figure 3.8C). Since the increased tumor size may be caused by increased proliferation or decreased apoptosis, we compared the cell proliferation marker Ki67 and the apoptosis marker cleaved caspase 3 in HeLa-Ctrl and HeLa-Six1.

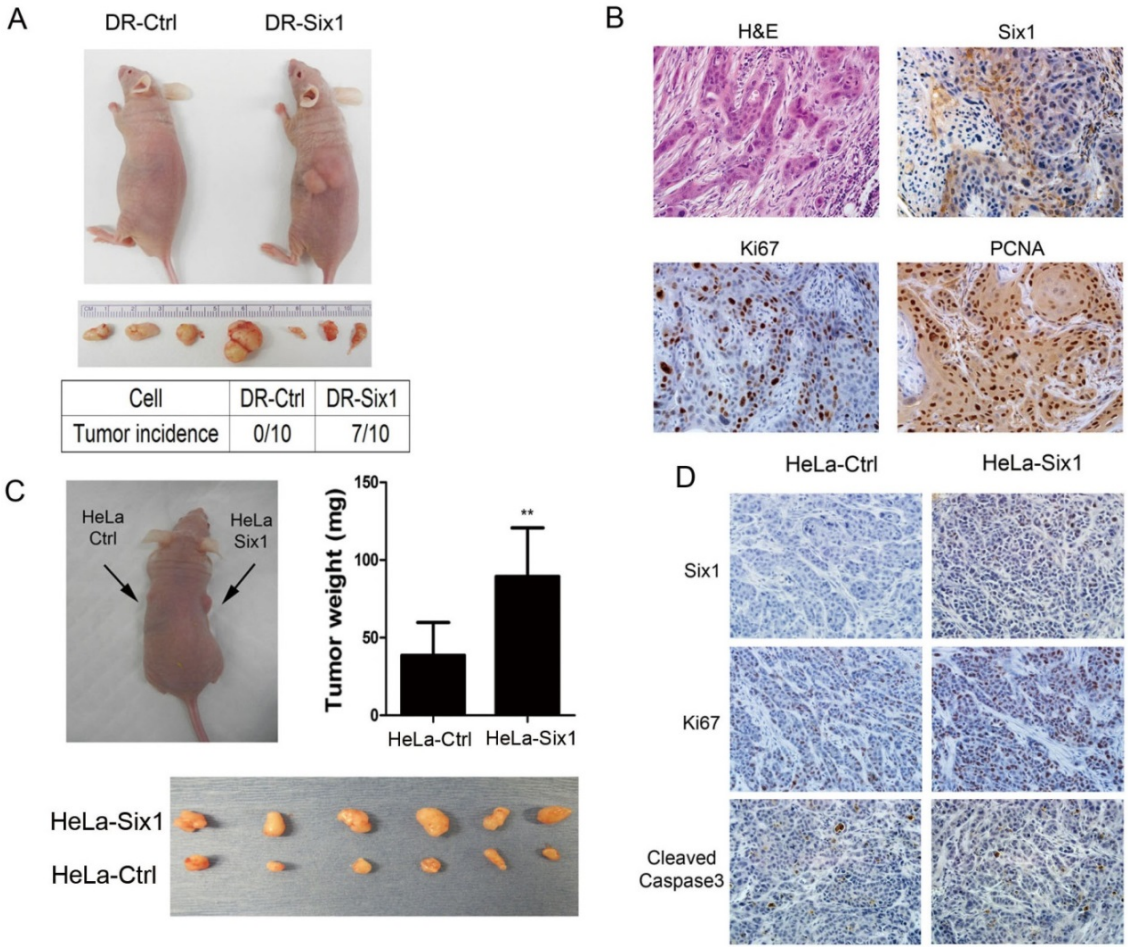

Figure 3.8 Six1 overexpression promotes tumorigenesis. (A) Six1-overexpressing HKc/DR form aggressive tumors in vivo. Upper panel: Six1-overexpressing HKc/DR (DR-Six1) or controls (DR-Ctrl) were injected into the flank of nude mice for 6 weeks. Tumors arose in HKc/DR-Six1, but not in HKc/DR-Ctrl. Middle panel: Six1-induced tumors. Lower panel: tumor incidence rates in HKc/DR-Six1 and HKc/DR-Ctrl groups (n=10). (B) Histology of tumors formed by Six1-overexpressing HKc/DR. H&E-stained sections of HKc/DR-Six1 tumors (upper left), the expression of Six1 (Upper right), Ki67 (lower left) and PCNA (lower right) in DR-Six1 tumors by immunohistochemistry (X400). (C) Upper panel: Six1-overexpressing HeLa (HeLa-Six1) were injected into the right flank of nude mice, and vector controls (HeLa-Ctrl) were injected into the left flank for 6 weeks. The weight of tumors in HeLa-Six1 group increases as compared to that in HeLa-Ctrl group. Lower panel: tumors formed from HeLa-Six1 (upper) and HeLa-Ctrl (lower). (D) The expression of Six1, Ki67 and cleaved caspase 3 in tumors from HeLa-Ctrl and HeLa-Six1. (X400)

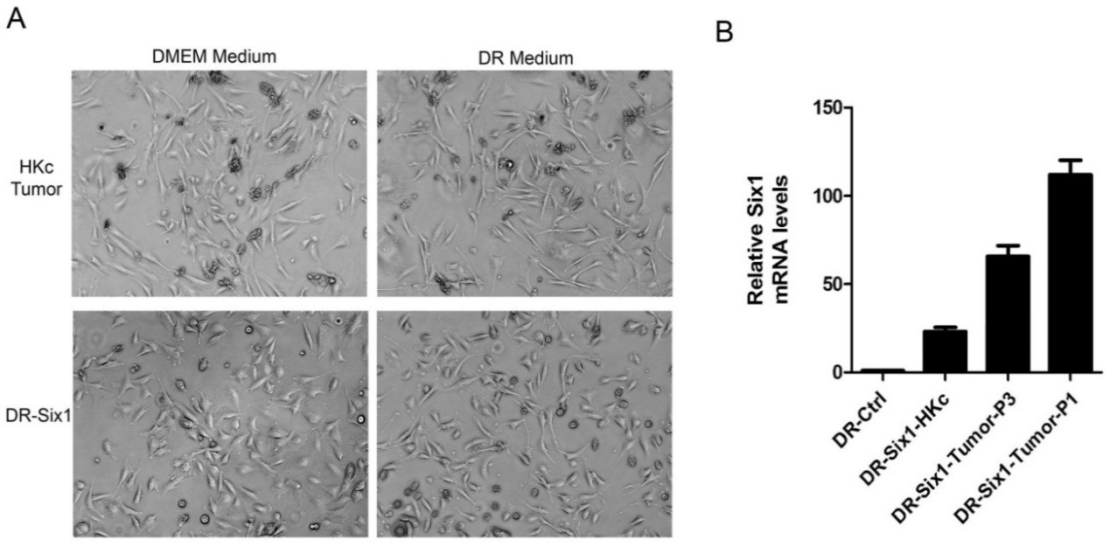

Figure 3.9 Cells isolated from HKc tumors. (A) Cell morphology of HKc/DR-Six1 (DR-Six1) and cells isolated from tumors (HKc tumor) cultured in DR medium or DMEM medium. Images are shown at 100× magnification. (B) mRNA expression of Six1 in HKc/DR-Ctrl (DR-Ctrl), HKc/DR-Six1 cultured in HKc/DR medium (DR-Six1-HKc), cells isolated form HKc/DR-Six1 tumor that cultured in HKc/DR medium (passage 3) (DR-Six1-Tumor-P3) and cells isolated form HKc/DR-Six1 tumor that cultured in HKc/DR medium (passage 1) (DR-Six1-Tumor-P1) was determined by real time PCR.

Tumors overexpressing Six1 (HeLa-Six1) showed a greater percentage of Ki67 positive cells compared to controls (HeLa-Ctrl) (Figure 3.8D), indicating Six1 enhanced tumor cell proliferation *in vivo*. There was no marked difference in the expression of cleaved caspase 3 between tumors from HeLa-Six1 and HeLa-Ctrl (Figure 3.8D), suggesting the effect of Six1 on tumor growth is associated with increased cell proliferation rather than alterations in apoptosis.

3.2.8 SIX1 OVEREXPRESSION INDUCES FEATURES OF CANCER STEM CELLS

Cancer stem cells (CSCs) are proposed to drive tumor onset and maintain tumor progression. TGF-β signaling has been known to play a vital role in regulating CSCs by induction of EMT (Mani et al., 2008). Therefore, we analyzed CSC markers in HKc/DR-

Ctrl and HKc/DR-Six1. Cell surface antigens $CD44^+/CD24^-$ have been widely used as breast and ovarian cancer CSCs markers (Meng et al., 2012; Sheridan et al., 2006), and have recently been identified as cervical CSCs markers (Gu et al., 2011). Another important stem cell marker is aldehyde dehydrogenase 1 (ALDH1) (Rao et al., 2012; Yao et al., 2011). We thus measured $CD44^+/CD24^-$ populations and the expression level of ALDH1 in HKc/DR-Ctrl and HKc/DR-Six1 by flow cytometry. HKc/DR-Six1 had a markedly increased $CD44^+/CD24^-$ population (86% in HKc/DR-Six1 versus 11% in HKc/DR-Ctrl) (Figure 3.10A) and increased ALDH1 expression as compared to HKc/DR-Ctrl (Figure 3.10B). To determine whether Six1 also enhances characteristics of CSCs in HeLa, we examined tumorsphere formation ability of HeLa-Ctrl and HeLa-Six1. As shown in Figure 3.10C, increased tumorsphere formation ability was observed in HeLa-Six1 as compared to HeLa-Ctrl. Taken together, our study demonstrates that Six1 overexpression increases the cancer stem cell-like cell population in HKc/DR and HeLa.

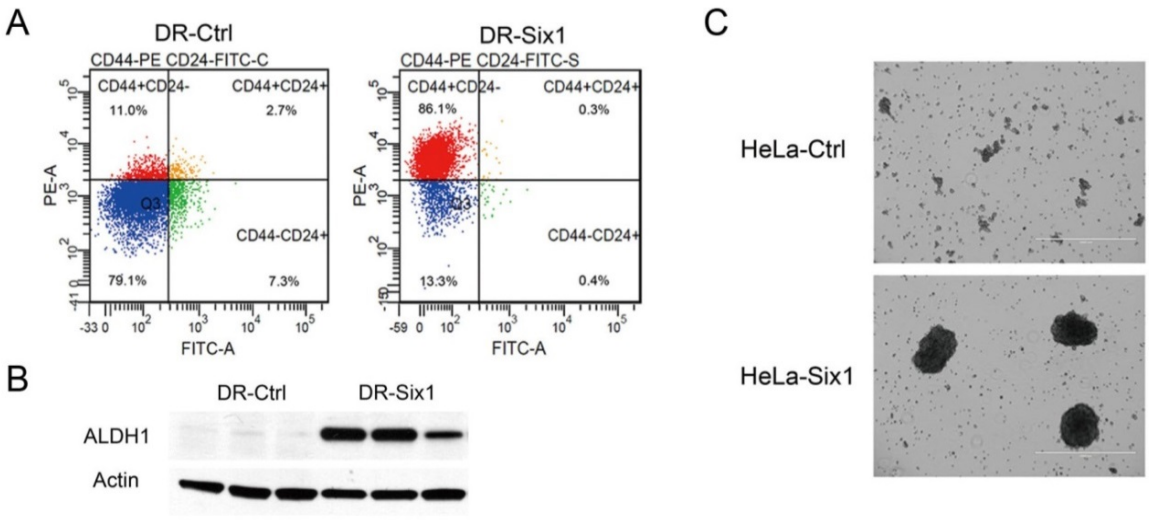

Figure 3.10 Six1 overexpression in HKc/DR and HeLa increases CSC properties. (A) Analysis of CD24 and CD44 expression in Six1-overexpressing HKc/DR (DR-Six1) or HKc/DR controls (DR-Ctrl) by flow cytometry. (B) Western blot of ALDH1 in HKc/DR-Six1 and HKc/DR-Ctrl. β-actin was used as a loading control. (C) Tumorsphere formation ability in HeLa-Ctrl and HeLa-Six1.

Next, we determined if MAPK activation is associated with the increased CSC population that was induced by Six1 overexpression. We examined the expression of ALDH1 by Western Blotting in HKc/DR-Six1 treated with the ERK inhibitor U0126 (10 μM), the p38 inhibitor SB202190 (10 μM), the JNK inhibitor SP600125 (10 μM) or DMSO for 48 h. The inhibition of p38 and JNK significant decreased ALDH1 protein levels, indicating a decreased CSC population (Figure 3.11). Moreover, to test whether TβRII-mediated signaling is necessary for Six1-induced CSC properties, we transfected HKc/DR-Six1 with a dominant-negative TβRII plasmid (TβRIIDN). TβRIIDN lacks the cytoplasmic tail and therefore cannot activate downstream signaling. As expected, TβRIIDN decreased the expression of ALDH1 (Figure 3.11). Overall, our data indicate that MAPK activation and TβRII signaling are critical for Six1-induced CSC properties.

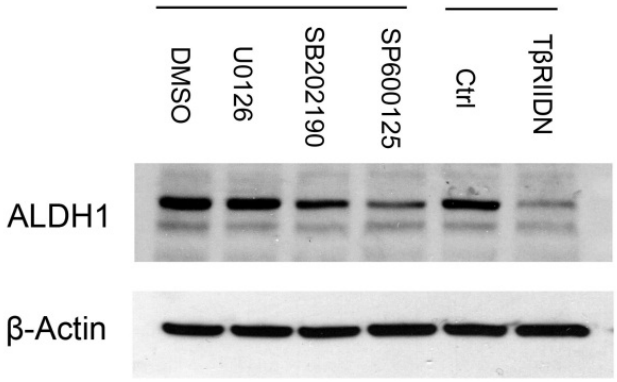

Figure 3.11 TβRII-MAPK signaling is critical for Six1-induced CSC properties. HKc/DR-Six1were treated with the ERK inhibitor U0126 (10 μM), the p38 inhibitor SB202190 (10 μM), the JNK inhibitor SP600125 (10 μM) or DMSO for 48 h; or HKc/DR-Six1were transfected with Ctrl or TβRIIDN for 48 h. Western blot analysis for ALDH1 and β-actin (loading control) was then conducted.

3.3 DISCUSSION

The Six1 homeoprotein is essential for the development of numerous organs, but also contributes to cancer cell proliferation and survival. Six1 overexpression has been found in various human cancers, and is associated with increased tumor progression and metastasis, and poor prognosis (Christensen et al., 2008). Although overexpression of Six1 had been observed in cervical cancer cell lines and tissues (Tan, Zhang, and Qian, 2011; Wan et al., 2008; Zheng et al., 2010), the role of Six1 in the progression of HPV-mediated cancer was unknown. We demonstrate here that Six1 overexpression promotes EMT at a late premalignant stage of HPV16-mediated transformation (HKc/DR). We further show that increases in TβRII and TβRIII and activation of Smad-independent TGF-β signaling are associated with Six1 overexpression and that p38 MAPK activation is pivotal in Six1-induced EMT in HPV16-immortalized cells. Finally, we show that Six1 overexpression increases the CSC-like cell population in HKc/DR and results in malignant conversion.

Previous studies showed that Six1 promotes cell proliferation and cell cycle progression in breast cancer by up-regulating cyclin A1 (Coletta et al., 2004; Coletta et al., 2008). Six1 promotes proliferation of pancreatic cancer cells by upregulation of cyclin D1 expression (Li et al., 2013). However, in our study, we found decreased cell growth in Six1-overexpressing HKc/DR as compared to controls *in vitro*. We did not observe significant cell cycle changes in response to Six1 overexpression in HKc/DR. The *in vitro* growth rate of Six1 overexpressing HeLa is comparable to the vector control, but *in vivo* Six1 overexpressing HeLa form larger tumors. Clinically, Six1 overexpression is associated with cervical cancer metastasis but not with tumor size (Zheng et al., 2010),

indicating that Six1 is not critical for the regulation of tumor cell growth in cervical cancer. Therefore, Six1-induced cell proliferation is context dependent, and cell cycle-associated growth promotion is not the main mechanism by which increased Six1 expression leads to enhanced aggressiveness and poor prognosis in cervical cancer.

Dysregulation of TGF-β signaling has been related to cervical cancer progression and metastasis (Baritaki et al., 2007; Noordhuis et al., 2011). At early stages of tumorigenesis, TGF-β acts as a potent tumor suppressor, strongly inhibiting the proliferation of epithelial cells. However, at late stages of tumorigenesis, tumors become resistant to growth inhibition by TGF-β and exploit TGF-β signaling to promote EMT, thereby facilitating tumor metastasis and invasion (Meulmeester and Ten Dijke, 2011). To date, several studies showed that imbalances in the activation status of canonical and noncanonical TGF-β signaling may underlie the ability of TGF-β to induce EMT in normal and malignant cells, and might be critical in the switch in TGF-β signaling from tumor suppression to tumor promotion (Zhang, 2009). Therefore, we analyzed both signaling pathways in response to Six1 overexpression in HKc/DR, and observed significant MAPK activation, including ERK1/2, JNK and p38 MAPK. By using inhibitors, we identified p38 MAPK as the primary mediator of Six1-induced EMT. The activation of p38 MAPK by TGF-β, which induces EMT in normal and malignant cells, requires the expression and activity of either β1 or β3 integrin, and the involvement of TβRII (Bhowmick et al., 2001; Galliher and Schiemann, 2007). Based on our microarray data, β1 integrin increased 2.3-fold and β3 integrin increased 3.3-fold in DR/Six1. Our finding that the inhibition of p38 MAPK in HKc/DR-Six1 decreases the expression of TβRII is consistent with the finding that TβRII is induced by a transcriptional mechanism

involving p38 activation in breast cancer (Buck and Knabbe, 2006). The activation of ERK1/2 and JNK may be due to increased expression of TβRII, or the dramatically enhanced fibronectin expression, which activates ERK1/2 and JNK (Jiang, Jia, and Cohen, 2002). Taken all together, these data suggest for the first time that Six1 augments the p38-TβRII pathway, and thus promotes EMT during HPV16-mediated transformation of human epithelial cells.

TGF-β-induced EMT is also thought to drive cells towards a more "cancer stem cell-like" phenotype. Although very few studies demonstrate the role of TGF-β-induced EMT on regulating CSCs in cervical cancer, it has been reported that induction of EMT by TGF-β1 or its downstream targets, Snail or Twist, promoted the expression of cell surface markers associated with CSCs ($CD44^+/CD24^-$ phenotype) and tumorsphere forming features in breast cancer (Mani et al., 2008). Interestingly, the specific activation of TGF-β signaling in $CD44^+/CD24^-$ breast cancer cells is due to the dramatically increased expression of TβRII in these cells as compared to the corresponding $CD44^-/CD24^+$ population (Shipitsin et al., 2007). Moreover, non-Smad TGF-β effectors β1 and β3 integrin can induce CSC-like properties in breast cancer cells (Galliher and Schiemann, 2006; Galliher and Schiemann, 2007). We found that overexpression of Six1 promotes EMT and enhances features of CSCs in HKc/DR, including promoting tumorigenesis *in vivo*, augmenting the population of $CD44^+/CD24^-$ and increasing expression of ALDH1. Importantly, we found increased expression of TβRII, β1 integrin and β3 integrin, which are consistent with TGF-β-induced CSCs in breast cancer. Furthermore, by using MAPK inhibitors and expressing TβRIIDN, we determined the essential role of MAPK activation and TβRII-mediated signaling in Six1-induced CSC phenotype. These findings

strongly suggest that Six1 promotes tumor progression by inducing characteristics of CSCs, and TGF-β-associated-EMT plays an important role in this process.

The precise role that the p38 MAPK pathway plays in tumor initiation and progression is somewhat controversial. For example, p38 MAPK activation is implicated in the suppression of tumorigenesis because it can inhibit cell growth by decreasing the expression of cyclin D1 (Lavoie et al., 1996) However, p38 is essential for the expression of vascular endothelial growth factor (VEGF), which promotes tumor angiogenesis (Yoshino et al., 2006). P38 kinase is also important in promoting H-ras-specific cell invasion and migration in human breast epithelial cells (Kim et al., 2003). The inhibition of p38 kinase suppresses the proliferation of human ER-negative breast cancer cells (Chen et al., 2009). In addition, it has been reported that an increased cancer stem cell population found under hypoxia conditions and serum depletion is the result of activation of p38 signaling (Lin et al., 2012). We determined that p38 MAPK plays an important role in Six1-induced EMT and activation of noncanonical TGF-β signaling. To date, a large number of small-molecule p38 MAPK inhibitors have been developed, some of which are in clinical trials (Wagner and Nebreda, 2009). Based on our studies, p38 inhibitors might prove effective in the treatment of Six1 overexpressing malignancies.

In summary, we demonstrate that Six1 overexpression alters the TGF-β signaling network, induces EMT, promotes malignant progression, and increases the CSC population during HPV16-mediated transformation of HKc. We further establish a link between Six1 overexpression and an activated p38-TβRII pathway, which contributes to Six1-associated EMT and CSC characteristics. Recent studies have identified genes related to organ specific metastasis, and suggested that tumor progression and metastasis

is determined by the genetic characteristics of early-stage transformed cells (Bos et al., 2009; Minn et al., 2007; Minn et al., 2005). Therefore, the pathways of Six1-induced EMT and malignant conversion we uncovered in HKc/DR are likely to be relevant to cancer progression and metastasis in general. This work provides a rationale for future studies targeting the p38-TβRII pathway for the treatment of cancers overexpressing Six1.

CHAPTER 4

SIX1 OVEREXPRESSION IN HPV16-IMMORTALIZED HUMAN KERATINOCYTES PROMOTES DIFFERENTIATION RESISTANCE AND EMT

4.1 INTRODUCTION

Six1 is a member of the Six family of homeodomain transcription factors and is essential for the development of numerous organs (Ikeda et al., 2010; Xu et al., 2003; Zheng et al., 2003). Six1 overexpression has been found in various human cancers including cervical cancer (Behbakht et al., 2007; Coletta et al., 2008; Ng et al., 2010; Zheng et al., 2010). The overexpression of Six1 is associated with increased tumor progression and metastasis, and decreased survival (Christensen et al., 2008). Six1 is overexpressed in cervical cancer cell lines and cervical cancer tissues, and Six1 overexpression is correlated to increased tumor malignancy and lymph node metastasis (Tan, Zhang, and Qian, 2011; Zheng et al., 2010). While our initial work determined that the expression of SIX1 mRNA increased in HKc/DR compared to HKc/HPV16 (Wan et al., 2008), we more recently reported that overexpression of Six1 in HKc/DR resulted in increased cell motility and invasion by inducing epithelial-mesenchymal transition (EMT) (Chapter 3) (Xu et al., 2014). Furthermore, induction of EMT by Six1 overexpression was associated with activation of transforming growth factor beta receptor type 2 (TβRII)-p38 signaling (Chapter 3) (Xu et al., 2014). The fact that Six1 expression increased during *in vitro* progression of HPV16-immortalized cells and Six1 was

overexpressed in cervical cancer tissues (Wan et al., 2008; Zheng et al., 2010), strongly suggests that Six1 might be involved in the cervical premalignant progression.

Therefore, in this study, we explored the role of Six1 during the early stages of HPV16-mediated transformation by overexpressing Six1 in HKc/HPV16. We found that Six1 overexpression in HKc/HPV16 increased cell proliferation and induced cell migration and invasion by promoting EMT. Importantly, the overexpression of Six1 in HKc/HPV16 resulted in resistance to serum and calcium-induced differentiation. Finally, we found that activation of MAPK signaling is linked to resistance to calcium-induced differentiation in HKc/HPV16 overexpressing Six1. Overall our results support the conclusion that Six1 overexpression promotes differentiation resistance and EMT at early stages of HPV16-mediated transformation of HKc.

4.2 RESULTS

4.2.1 SIX1 INCREASES PROLIFERATION, MIGRATION AND INVASION IN HKC/HPV16

To further explore the function of Six1 in HKc/HPV16, we cloned a full-length human Six1 cDNA into the expression plasmid pcDNA3.1 (pcDNA3.1-Six1). HKc/HPV16-Six1 were established by stable transfection of HKc/HPV16 with pcDNA3.1-Six1. HKc/HPV16-Ctrl were HKc/HPV16 transfected with the pcDNA3.1 expression plasmid alone. Western blots confirmed the overexpression of Six1 in HKc/HPV16-Six1 (Figure 4.1A). HKc/HPV16-Six1 exhibited an elongated and fibroblastic appearance (Figure 4.1B), and increased cell proliferation (Figure 4.1C) compared to HKc/HPV16-Ctrl.

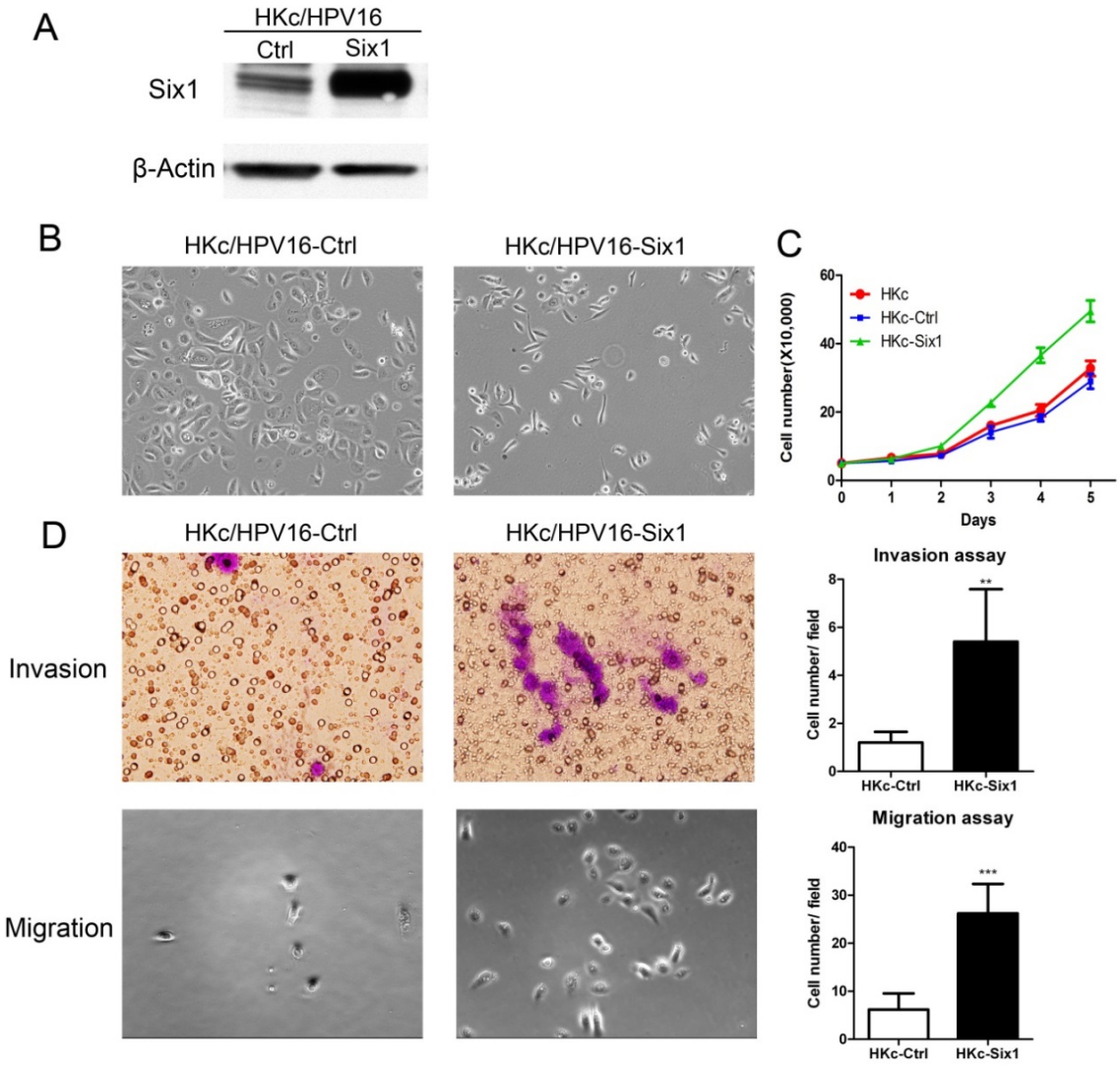

Figure 4.1 Six1 overexpression in HKc/HPV16 changes cell morphology and increases cell proliferation, invasion and migration. (A) HKc/HPV16 were stably transfected with either pcDNA3.1 (Ctrl) or pcDNA3.1-Six1 (Six1). Six1 protein levels in cell extracts were determined by western blotting. β-actin was used as a loading control. (B) Cell morphology of HKc/HPV16-Ctrl and HKc/HPV16-Six1. Images are shown at 100× magnification. (C) Proliferation in HKc/HPV16-Six1 (HKc-Six1) compared to HKc/HPV16-Ctrl (HKc-Ctrl) and HKc/HPV16 (HKc). Cell numbers were determined by manually counting cells on the days indicated. (D) Invasion (upper panels) and migration (lower panels) assays for HKc/HPV16-Ctrl (HKc-Ctrl) and HKc/HPV16-Six1 (HKc-Six1). Cell invasion was determined by a Matrigel invasion assay, and cell migration was determined by a transwell migration assay. Images for the invasion assay are shown at 400× and those for the migration assay at 100× magnification. Quantification of the invasion assay and the migration assay are shown in the upper right and lower right panels, respectively. Each column represents the mean of five different fields. Bars indicate SD, and ** and *** indicate statistically significant p values < 0.01 and 0.001 respectively.

Moreover, Six1 overexpression in HKc/HPV16 increased cell invasion by 4.5-fold and cell migration approximately 4.2-fold (Figure 4.1D). These data demonstrate that HKc/HPV16 overexpressing Six1 exhibited a more mesenchymal phenotype with increased cell growth, migration and invasion compared to HKc/HPV16-Ctrl.

4.2.2 SIX1 PROMOTES EMT

Due to the changes in cell morphology, growth and invasion associated with Six1 overexpression, we next explored the expression of EMT related genes upon Six1 overexpression in HKc/HPV16. As shown in Figure 4.2A, the overexpression of Six1 induced an increased expression of mesenchymal markers and decreased expression of epithelial markers. For example, the mRNA level of E-cadherin and occludin decreased by about 81% and 76%, while mRNA levels of vimentin and snail increased by approximately 2.0-, and 4.3-fold respectively in HKc/HPV16-Six1 when compared with HKc/HPV16-Ctrl (Figure 4.2A). Moreover, we examined the protein levels of E-cadherin and fibronectin by western blot analysis and immunofluorescence. The overexpression of Six1 in HKc/HPV16 led to decreased E-cadherin and slightly increased fibronectin (Figure 4.2B, C). We also investigated β-catenin, a key component of adherens junctions in epithelial cells (Gumbiner, 2005), and we found that protein levels of β-catenin decreased dramatically in Six1-overexpressing HKc/HPV16 (Figure 4.2B). Taken together, our data show that Six1 overexpression promotes EMT in HKc/HPV16.

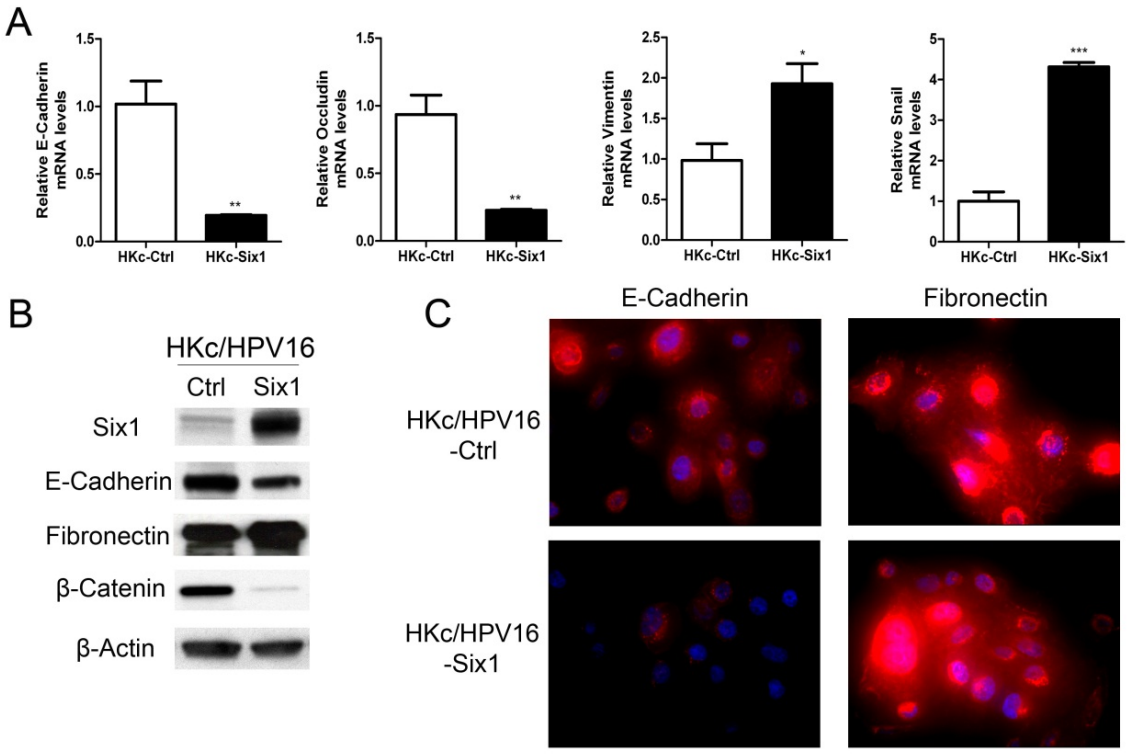

Figure 4.2 Six1 overexpression induces EMT in HKc/HPV16. (A) Levels of mRNA expression of E-cadherin, occludin, vimentin and snail were determined by Real-time PCR in HKc/HPV16-Ctrl (HKc-Ctrl) and HKc/HPV16-Six1 (HKc-Six1). Data were normalized to β-actin expression. Bars indicate SD, and *, ** and *** indicate statistically significant p values < 0.05, 0.01 and 0.001 respectively. (B) Western blot for Six1, E-cadherin, fibronectin and β-catenin in HKc/HPV16-Ctrl (Ctrl) and HKc/HPV16-Six1 (Six1). β-actin was used as loading control. (C) Immunofluorescent staining of E-cadherin (red) and fibronectin (red) in HKc/HPV16-Ctrl and HKc/HPV16-Six1. Nuclei were stained with DAPI (blue). Images are shown at 400× magnification.

4.2.3 THE OVEREXPRESSION OF SIX1 IN HKC/HPV16 RESULTS IN RESISTANCE TO SERUM AND CALCIUM-INDUCED DIFFERENTIATION

We determined protein levels of Six1 at the various stages of our *in vitro* model for HPV16-mediated transformation. A large increase in Six1 expression was observed in the final HKc/DR stage compared to the earlier HKc/HPV16 and HKc/GFI stages (Figure 4.3). Unlike most other cell types, normal HKc and HKc/HPV16 can be

propagated in serum-free media and under low Ca^{2+} conditions (i.e. 30 μM), and media containing high-calcium (i.e.1 mM) or serum triggers the initiation of terminal squamous differentiation (Boyce and Ham, 1983; Pirisi et al., 1988; Pirisi et al., 1987). The hallmark of HKc/DR is resistance to serum and calcium-induced differentiation (Pirisi et al., 1988). Therefore, we explored if the overexpression of Six1 is associated with differentiation resistance. As shown in Figure 4.4A, HKc/HPV16-Ctrl stratified and expressed keratin 10, a differentiation marker, after being treated with 1mM Ca^{2+} or 5% FBS for 5 days. In contrast, HKc/HPV16-Six1 retained their proliferation, did not stratify and did not express keratin 10 in response to Ca^{2+} or FBS. The cell morphology change in HKc/HPV16-Ctrl could be observed as early as 24 h post 1mM Ca^{2+} or 5% FBS treatment (Figure 4.4B). Upon being cultured in complete medium supplemented with 1 mM calcium chloride or 5% FBS, HKc/HPV16-Six1 showed mixed morphology of enlarged cobblestone and spindle cells (Figure 4.4A, B). The enlarged/flat cobblestone appearance is similar to the morphology of HKc/DR. Consistently, we found that keratin 10 protein levels dramatically increased at day 5 in HKc/HPV16-Ctrl, but not in HKc/HPV16-Six1 (Figure 4.5A).

The E-cadherin-β-catenin complex at the plasma membrane plays a critical role on cell differentiation in HKc and knocking-down E-cadherin or β-catenin expression blocked calcium-induced keratinocyte differentiation (Xie and Bikle, 2007). We hence examined E-cadherin by immunofluorescence and we found that both Six1-overexpressing HKc/HPV16 and controls exhibited increased membrane-associated E-cadherin and intercellular junction formation when exposed in high Ca2+ medium (Figure 4.4A). Then, we used western blotting to detect protein levels of total E-cadherin,

fibronectin, as well as soluble (cytoplasmic) and insoluble (cytoskeletal-associated) E-cadherin after being exposed to 1mM Ca2+ for varying times (10 min to 5 days).

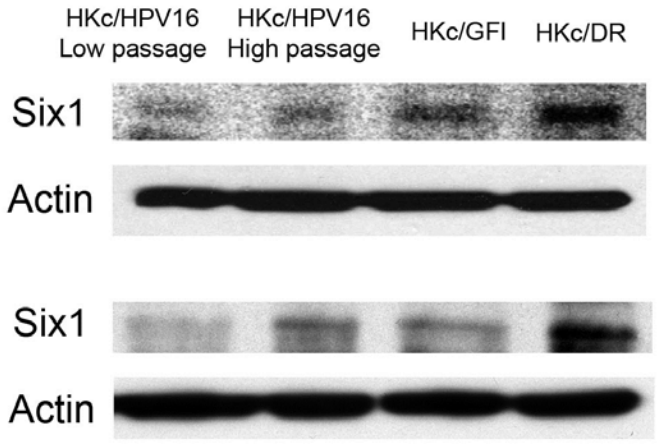

Figure 4.3 Western blot for Six1 in HKc/HPV16-low passage, HKc/HPV16-high passage, HKc/GFI and HKc/DR that were derived HKc/HPV16 lines (upper: D1, lower: D5). β-actin was used as a loading control.

We found that total E-cadherin remained unchanged and the expression of fibronectin decreased in both HKc/HPV16-Ctrl and Six1-overexpressing cells upon high calcium treatment (Figure 4.5A). Consistent with what we observed by immunofluorescence, HKc/HPV16-Six1 increased insoluble E-cadherin from 48 h after high calcium treatment, indicating the formation of intercellular junctions (Figure 4.5B). Phosphatidylinositol 3-kinase (PI3K)/AKT signaling can be activated by the E-cadherin complex and promotes early keratinocyte differentiation (Xie and Bikle, 2007). However, we did not observe any significant increase in phospho-PI3K or phospho-AKT in response to high calcium treatment (Figure 4.6). Taken together, our data strongly indicates that overexpression of Six1 in HKc/HPV16 results in resistance to Ca^{2+} or serum-induced differentiation.

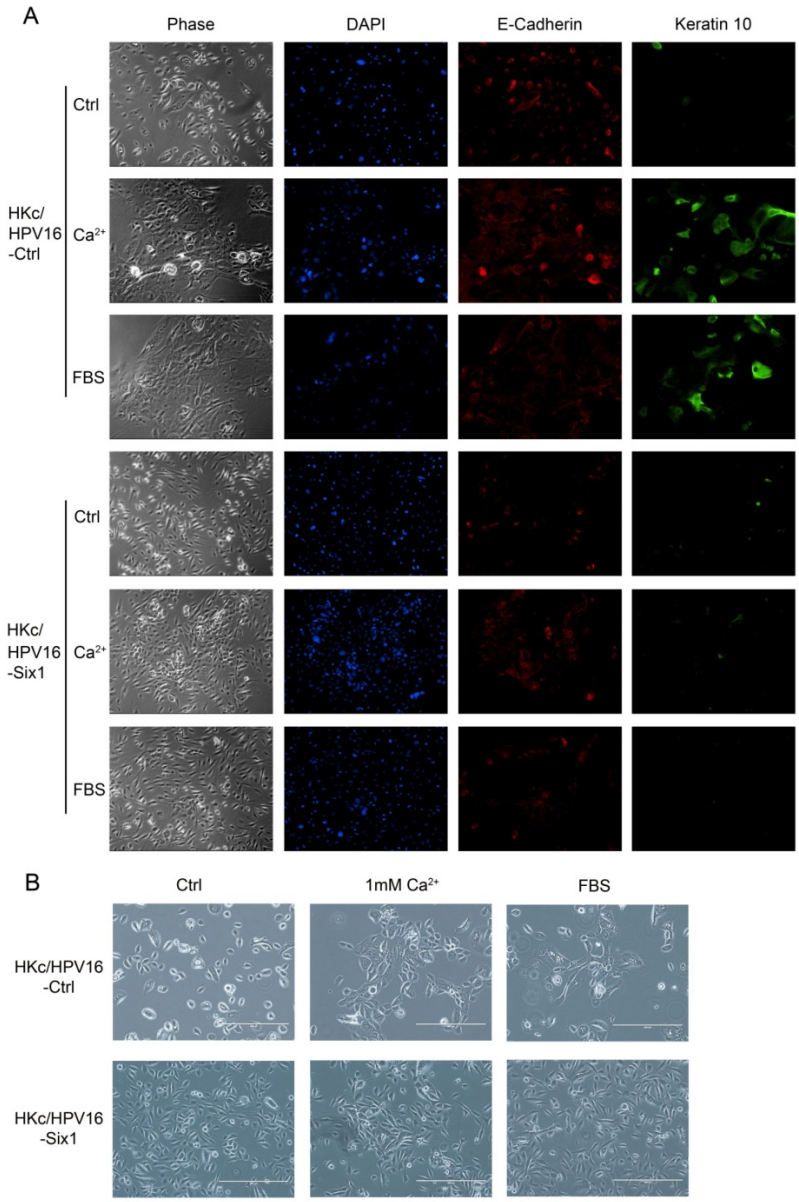

Figure 4.4 Six1 overexpression in HKc/HPV16 results in resistance to serum and calcium-induced differentiation. (A) HKc/HPV16-Ctrl and HKc/HPV16-Six1 were cultured with either complete medium or complete medium supplemented with 1 mM calcium chloride or 5% FBS for 5 days. Cell morphology of HKc/HPV16-Ctrl and HKc/HPV16-Six1 under the indicated treatment is shown in the first column (Phase). Immunofluorescent staining of nuclei (blue), E-cadherin (red) and keratin 10 (green) in HKc/HPV16-Ctrl (upper panels) and HKc/HPV16-Six1 (lower panels) is shown in columns 2-4. (B) Cell morphology of HKc/HPV16-Ctrl and HKc/HPV16-Six1 cultured in complete medium (Ctrl) or complete medium containing high calcium (1 mM Ca^{2+}) or serum (FBS) for 24 h. Images are shown at 100× magnification.

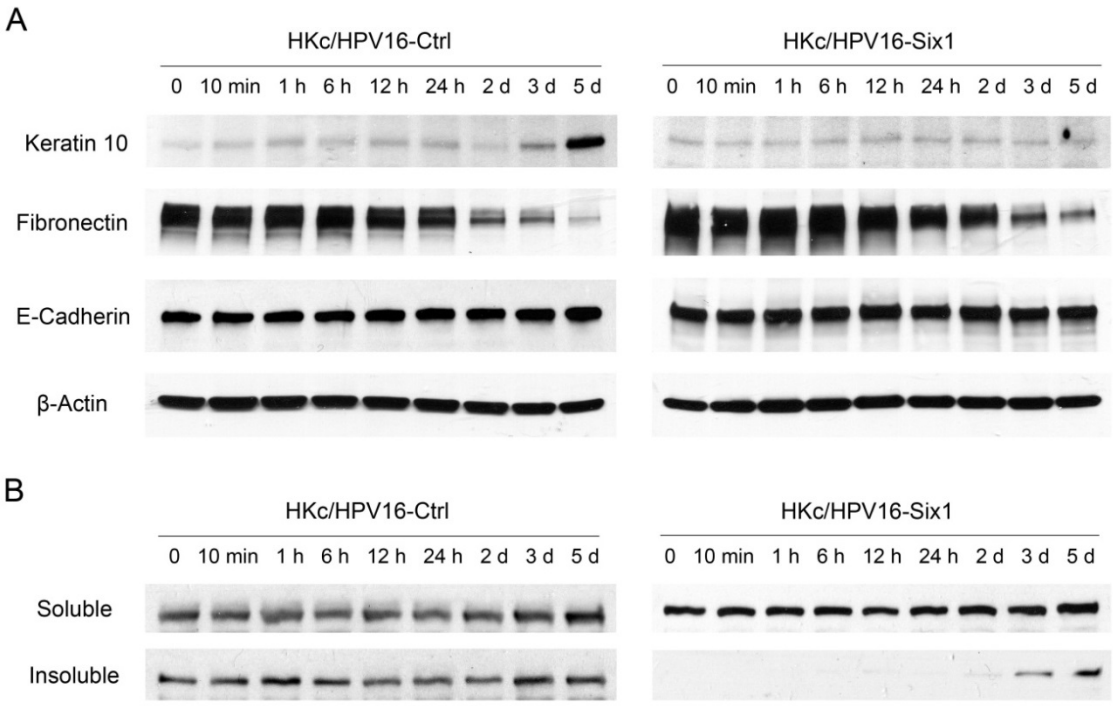

Figure 4.5 Six1 overexpression in HKc/HPV16 does not impact the redistribution of adhesion junctions when cultured in high calcium media. (A) Western blot of keratin 10, fibronectin and E-cadherin in whole cell lysate from HKc/HPV16-Ctrl and HKc/HPV16-Six1 that were treated with 1 mM Ca^{2+} for the indicated times. β-actin was used as a loading control. (B) The expression of E-cadherin in soluble (cytosolic) and insoluble (cytoskeleton-associated) fractions from HKc/HPV16-Ctrl and HKc/HPV16-Six1 that were treated with 1 mM Ca^{2+} for the indicated times. Fractions were analyzed by western blotting.

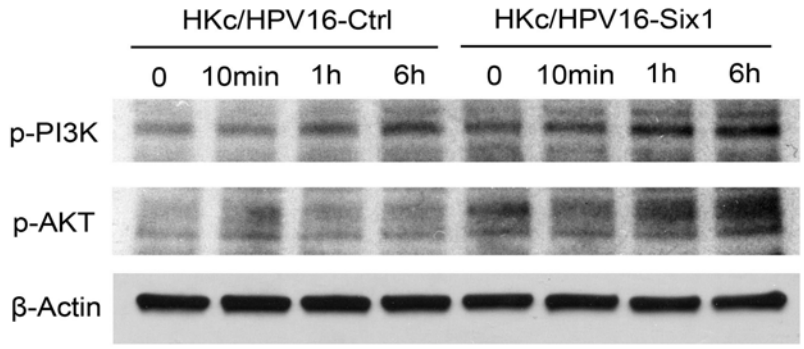

Figure 4.6 Western blot of p-PI3-kinase p85 (p-PI3K) and p-AKT in HKc/HPV16-Ctrl and HKc/HPV16-Six1. Cells were cultured in 1 mM Ca^{2+} medium for the indicated times. β-actin was used as a loading control.

4.2.4 SMAD-DEPENDENT TGF-B SIGNALING IS DECREASED IN ASSOCIATION WITH SIX1 OVEREXPRESSION

Next, we explored possible mechanisms of how Six1-overexpression in HKc/HPV16 leads to resistance to calcium/serum-induced differentiation. Cell cycle exit is one of the major processes involved in entering the terminally differentiated state (Missero et al., 1995; Missero et al., 1996). TGF-β-Smad2/3 signaling induces cell cycle withdrawal during keratinocyte terminal differentiation (Descargues et al., 2008), and TGF-β1 enhances differentiation of HKc under high Ca^{2+} conditions (Matsumoto et al., 1990). Moreover, TGF-β signaling is important in Six1-induced EMT (Micalizzi et al., 2009; Micalizzi et al., 2010). Compared to HKc/HPV16-Ctrl, mRNA levels of TβRII and TβRIII in HKc/HPV16-Six1 were increased 1.7-fold and 4.3-fold, respectively, while TβRI mRNA was slightly decreased (Figure 4.7A). In addition, increases in the protein levels of TβRII and TβRIII in HKc/HPV16-Six1 were detected by western blotting (Figure 4.7B). We next investigated whether Six1-induced EMT and differentiation resistance are linked to altered TGF-β-Smad2/3 signaling. We compared the both basal and TGF-β stimulated activity of a Smad-responsive luciferase reporter construct (p6SBE-Luc) in HKc/HPV16-Ctrl with HKc/HPV16-Six1. Six1 overexpression did not change the basal activity of the Smad-dependent reporter construct (Figure 4.7C). However, activation of Smad-dependent signaling in response to TGF-β1 treatment was attenuated by ~ 45% in HKc/HPV16-Six1 as compared with HKc/HPV16-Ctrl (Figure 4.7D). These data suggest that Six1overexpression decreases activation of Smad-dependent signaling in response to TGF-β1 treatment.

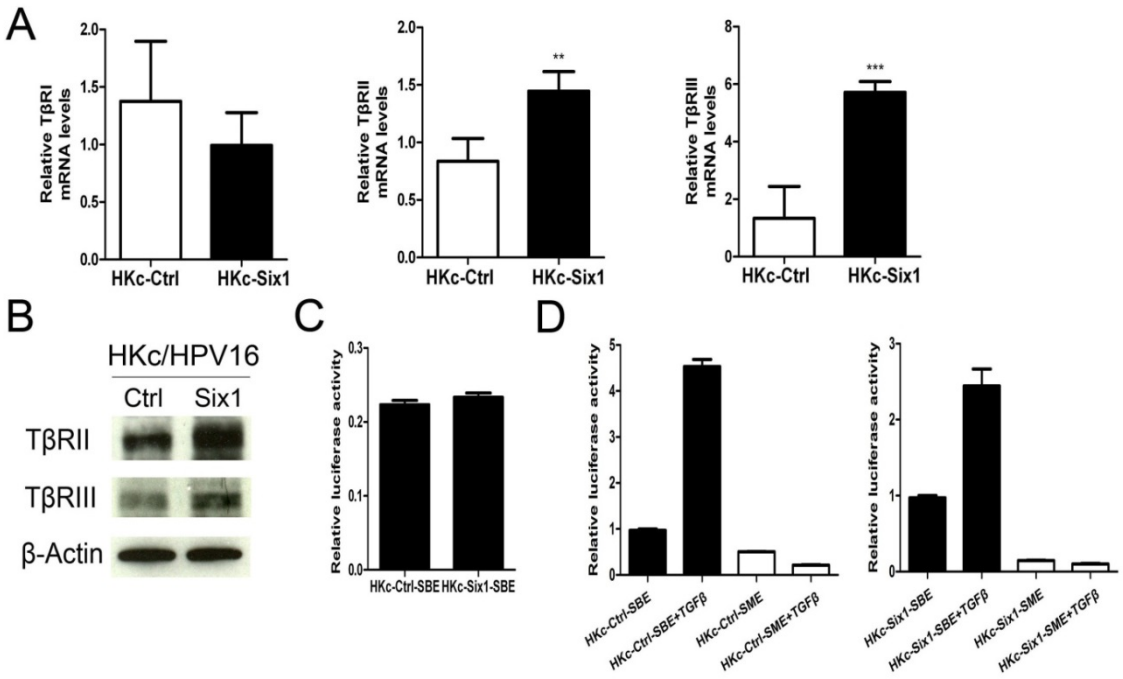

Figure 4.7 Six1 overexpression in HKc/HPV16 alters TGF-β signaling. (A) Levels of mRNA expression of TGF-β receptors TβRI, TβRII and TβRIII were determined by Real time PCR in HKc/HPV16-Ctrl (HKc-Ctrl) and HKc/HPV16-Six1 (HKc-Six1). Data were normalized to β-actin expression. (B) Western blot analysis of TβRII and TβRIII in HKc/HPV16-Ctrl and HKc/HPV16-Six1. β-actin was used as a control for equal protein loading. (C, D) HKc/HPV16-Ctrl (HKc-Ctrl) or HKc/HPV16-Six1 (HKc-Six1) were transfected with either p6SBE-luc or p6SME-luc. Twenty four h after transfection, cells were treated with 40 pM TGF-β1 or vehicle for 24 h and then luciferase activity determined. Values were normalized to Renilla luciferase. Bars indicate SD, and ** and *** indicate statistically significant p values < 0.01 and < 0.001 respectively.

4.2.5 SIX1 ACTIVATES ERK AND P38 MAPK SIGNALING

The Mitogen-Activated Protein Kinases (MAPKs) are central players in regulating keratinocyte differentiation (Eckert et al., 2002). MAPK signaling is one of the non-Smad TGF-β pathways (Zhang, 2009) and we have previously found that activation of MAPK is involved in Six1-induced EMT in HKc/DR (Xu et al., 2014). We compared MAPK activity in HKc/HPV16-Ctrl and HKc/HPV16-Six1 by conducting Western blots

using phospho-specific p-ERK, p-p38 and p-JNK antibodies. As shown in Figure 4.8A, phosphorylation of ERK and p38, but not JNK, was dramatically increased in response to Six1 overexpression in HKc/HPV16. After treatment of HKc/HPV16-Ctrl with 1mM Ca^{2+}, ERK was phosphorylated within 1 h, and increased phosphorylation of p38 was detected as soon as 10 min after Ca^{2+} treatment. In contrast, in HKc/HPV16-Six1, the phosphorylation of ERK and p38 was not further increased but rather decreased within 1 h after high Ca^{2+} treatment (Figure 4.8B). Signal transducer and activator of transcription 3 (STAT3) also plays an important roles in differentiation, migration and apoptosis of keratinocytes (Saeki et al., 2012). The phosphorylation of STAT3 increased in HKc/HPV16-Six1 compared to HKc/HPV16-Ctrl (Figure 4.8B). However, there is no STAT3 activation in HKc/HPV16-Ctrl following high Ca^{2+} treatment and the phosphorylation of STAT3 decreased in HKc/HPV16-Six1 following the addition of high Ca^{2+} medium (Figure 4.8B).

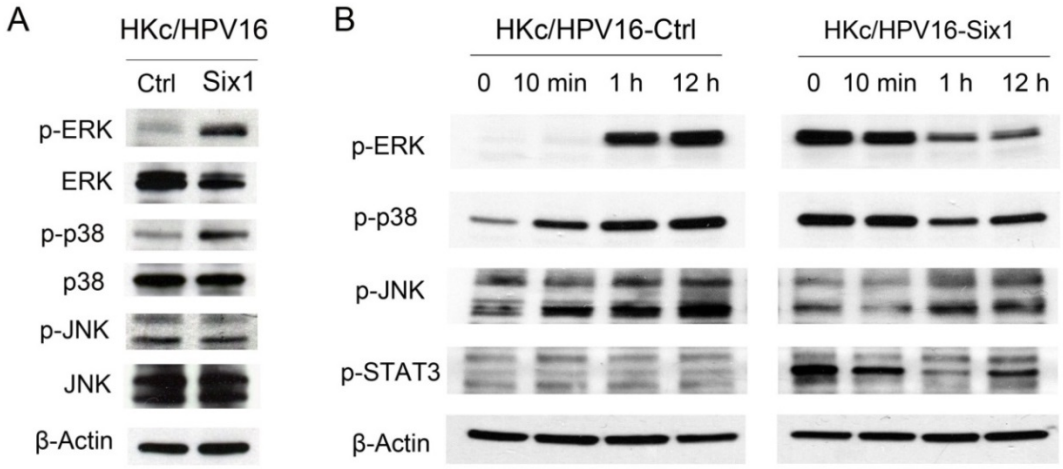

Figure 4.8 Six1 overexpression in HKc/HPV16 modulates MAPK signaling. (A) Protein levels of p-ERK, ERK, p-p38, p38, p-JNK and JNK were determined by western blotting of cell lysates prepared from HKc/HPV16-Ctrl and HKc/HPV16-Six1. (B) Western blot of p-ERK, p-p38, p-JNK and p-STAT3 in HKc/HPV16-Ctrl and HKc/HPV16-Six1 that were cultured in 1 mM Ca^{2+} medium for the indicated times. β-actin was used as control for protein equal loading.

4.2.6 THE ACTIVATION OF ERK AND P38 MAPK IS CRITICAL FOR SIX1-INDUCED EMT

We treated HKc/HPV16-Six1 with MAPK inhibitors to explore the role of MAPK activation in Six1 induction of EMT. Treatment of HKc/HPV16-Six1 with the p-ERK inhibitor U0126 and p38 inhibitor SB202190 almost completely blocked the expression of fibronectin (Figure 4.9). HKc/HPV16-Six1 treated with SB202190, but not U0126 or SP600125 increased E-cadherin protein level (Figure 4.9). Moreover, HKc/HPV16-Six1 treated with SB202190 and U0126, but not SP600125, lost some of their fibroblastic appearance (Figure 4.10A). Lastly, similar to what we observed in HKc/DR, Six1-overexpressing HKc/HPV16 treated with SB202190 exhibited a decreased ability to invade through Matrigel (Figure 4.10B). Given the minimal changes in JNK activity in response to Six1-overexpression in HKc/HPV16, we conclude that ERK and p38 MAPK signaling plays an important role in promoting EMT in Six1 overexpressing HKc/HPV16.

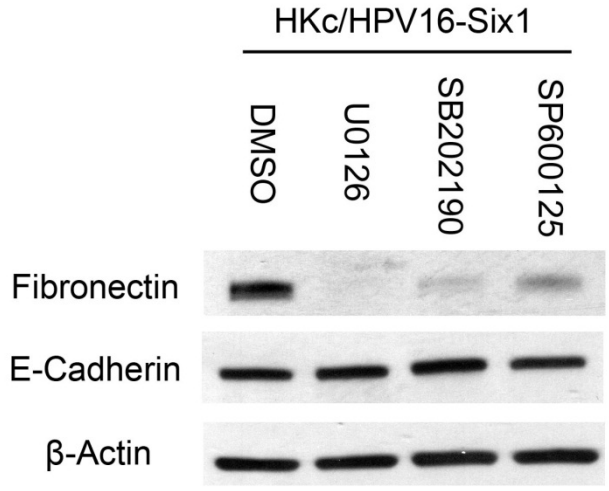

Figure 4.9 Western blot analysis for E-cadherin, fibronectin and β-actin (loading control). HKc/HPV16-Six1 were treated for 48 h with the ERK inhibitor U0126 (10 μM), the p38 inhibitor SB202190 (10 μM), the JNK inhibitor SP600125 (10 μM) or DMSO.

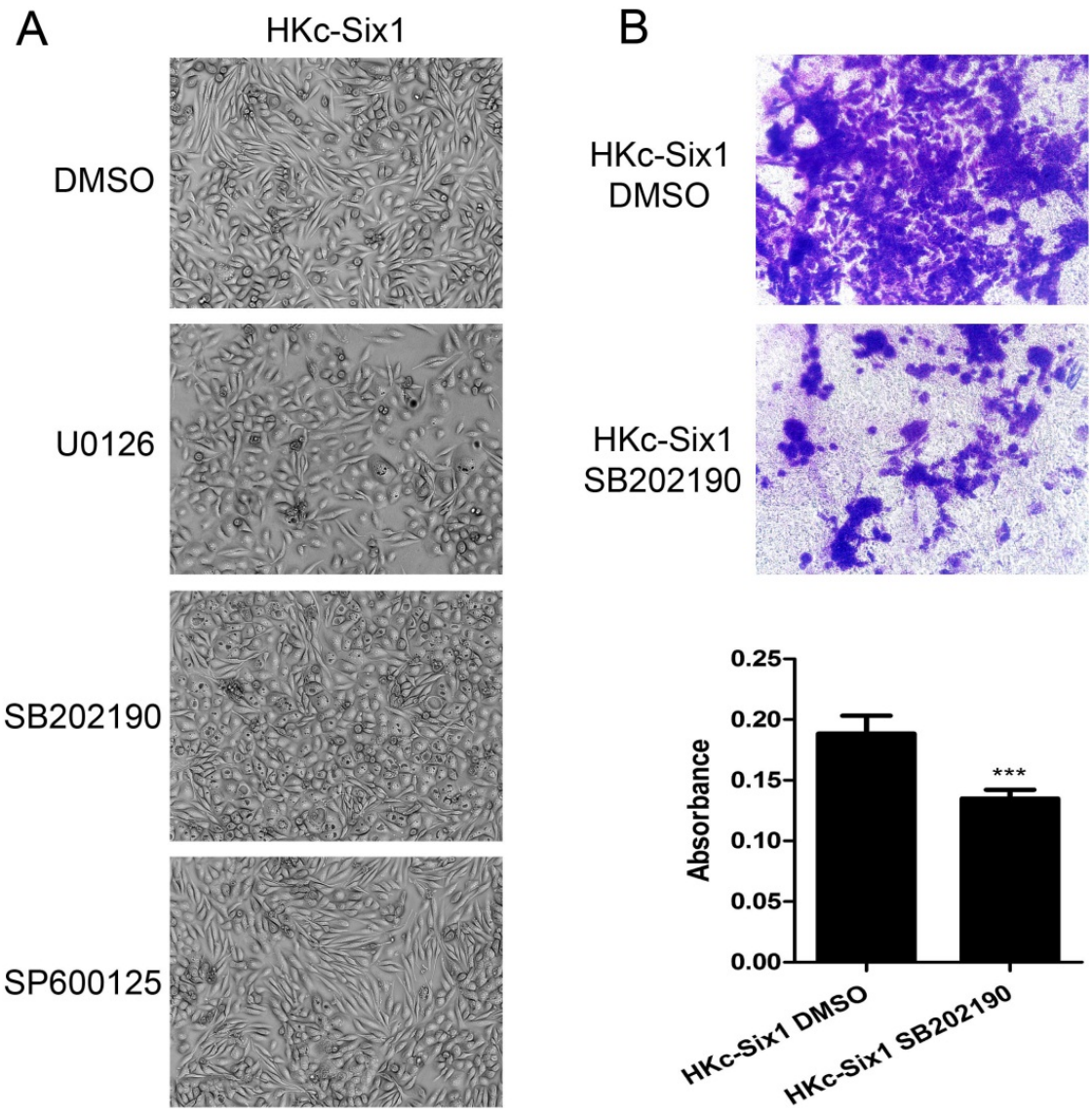

Figure 4.10 Inhibition of ERK and p38 reverses Six1-meditated EMT. (A) phase-contrast photographs of HKc/HPV16-Six1 (HKc-Six1) treated with the ERK inhibitor U0126 (10 μM), the p38 inhibitor SB202190 (10 μM), the JNK inhibitor SP600125 (10 uM) or DMSO for 48 h. Images are shown at 100× magnification. (B) Invasion assays for DR-Six1 treated with DMSO or SB202190 (10 μM for 24 h). Cell invasion was determined by a Matrigel invasion assay. The number of invading cells was quantified after crystal violet staining. Images are shown at 100× magnification. Crystal violet was extracted with ethanol and the absorbance determined in a spectrophotometer. Quantification of the invasion assay is presented in the bar graph next to the photographs. Each column represents the mean of three repeats.

4.3 DISCUSSION

Accumulating evidence has determined that inappropriate expression of homeobox genes in cancer contributes to tumorigenesis and tumor progression (Abate-Shen, 2002). The Six1 homeoprotein is essential for embryonic development, and also contributes to cancer cell proliferation and survival. The overexpression of Six1 has been found in various cancers, and is associated with increased tumor progression and metastasis, and decreased survival (Christensen et al., 2008). Our previous work determined that SIX1 mRNA expression increased during *in vitro* progression of HPV16-immortalized HKc and that Six1 protein was overexpressed in cervical cancer tissues, which strongly suggests that Six1 might play an important role in the progression of premalignant cervical lesions initiated by HPV infection (Wan et al., 2008). In the current study, we focused on the role of Six1 at early stages of HPV16-mediated transformation. We demonstrated that that Six1 overexpression promotes EMT and resistance to serum and high calcium-induced differentiation in HKc/HPV16. We further showed decreased TGF-β-Smad2/3 signaling, alterations in the expression of TGF-β receptors and the activation of ERK and p38 MAPK in association with Six1 overexpression in HKc/HPV16.

Immortality, decreased requirements for growth factors and lack of response to differentiation stimuli are characteristics of a transformed phenotype. In our *in vitro* model system of HPV16-mediated transformation, HKc/HPV16 immortalized cells resistant to calcium and serum-induced differentiation (HKc/DR) were selected from growth factor independent HKc/HPV16 (HKc/GFI). (Pirisi et al., 1988). Here we demonstrate that Six1 overexpression in HKc/HPV16 induces resistance to calcium and

serum -induced differentiation, suggesting that Six1 can promote progression during the early stages of HPV16-mediated transformation.

TGF-β signaling plays a dual role in tumor progression and dysregulation of TGF-β signaling is believed to be associated with progression of premalignant cervical lesions to cervical cancer (Baritaki et al., 2007; Noordhuis et al., 2011). TGF-β acts as a potent tumor suppressor since it strongly inhibits the proliferation of normal and early neoplastic cells. However, at late stages of tumorigenesis, tumors become resistant to TGF-β mediated growth inhibition and exploit TGF-β signaling to facilitate tumor metastasis and invasion (Meulmeester and Ten Dijke, 2011). In our *in vitro* model system, HKc/DR exhibit decreased expression of TβRI, which results in resistance to the antiproliferative effects of TGF-β (Mi et al., 2000). In this study, we found that Six1 overexpression dramatically reduced Smad-dependent signaling in response to TGF-β1. Decreased Smad-dependent signaling may contribute to the enhanced proliferation we observed in HKc/HPV16-Six1. On the contrary, we previously showed that Six1 overexpression decreased cell growth in HKc/DR (Xu et al., 2014). The different growth response to Six1 overexpression in HKc/HPV16 and HKc/DR may be explained by the different expression of TGF-β receptors and TGF-β signaling. Moreover, TGF-β is one of the primary serum factors responsible for inducing keratinocytes to undergo terminal differentiation (Bertolero et al., 1986). Thus, the decreased Smad signaling found in HKc/HPV16-Six1 likely plays a role in the resistance of these cells to serum-induced differentiation.

EMT allows immotile and polarized epithelial cells to acquire a motile, apolar and fibroblastoid phenotype, and has been considered being a critical step in mediating tumor

progression, metastasis as well as cancer stem cell properties (Christiansen and Rajasekaran, 2006; Mani et al., 2008). TGF-β can induce EMT through Smad-dependent and non-Smad signaling (Lamouille, Xu, and Derynck, 2014; Zhang, 2009). In our study, we found increased expression of TβRII and TβRIII in Six1-overexpressing HKc/HPV16, but we did not find any increase in Smad-dependent signaling. After examining typical non-Smad TGF-β pathways, we showed a significant activation of ERK and p38 MAPK in response to Six1 overexpression in HKc/HPV16. Inhibition of ERK and p38 MAPK activity in HKc/HPV16-Six1 significantly decreases the expression of fibronectin (a mesenchymal marker) and the cells also lose their fibroblastic appearance. These findings are consistent with our observation in HKc/DR, in which Six1 overexpression activates MAPK and MAPK activation is critical for Six1-induced EMT (Xu et al., 2014). Taken together, our data suggest that the MAPK activation is responsible for Six1-induced EMT in both HKc/HPV16 and HKc/DR.

Besides the association with EMT, MAPKs are vital for the regulation of keratinocyte differentiation (Eckert et al., 2002). For example: p38 MAPK functions to promote HKc differentiation by regulating the expression of involucrin, a marker of keratinocyte differentiation (Dashti, Efimova, and Eckert, 2001). High calcium induces a transient, peak-like activation of ERK in HKc, and calcium-induced differentiation can be blocked by MEK inhibition, which suggests an important role of the MEK/ERK pathway in the early stages of keratinocyte differentiation (Schmidt et al., 2000). In our study, we showed that the level of phosphorylation of ERK and p38 increased in HKc/HPV16-Ctrl upon high calcium treatment. In contrast, the activity of ERK and p38 decreased in HKc/HPV16-Six1 following treatment with high calcium. STAT3 also has

been known to play an important role in keratinocyte differentiation. Constitutive activation of Stat3 in mouse epidermis results in partial loss of the keratinocyte differentiation markers K10 and filaggrin and enhances malignant progression (Chan et al., 2008). STAT3 knock-down induces immature terminal differentiation of HKc (Saeki et al., 2012). Our study showed a significant activation of STAT3 in Six1-overexpressing HKc/HPV16. STAT3 overexpression in HKc/HPV16-Six1 may in fact retard differentiation even though these cells express high levels of p-ERK and p-p38.

In summary, Six1 overexpression in HKc/HPV16 induces cell proliferation, invasion, migration, and EMT and induces resistance to calcium/serum-induced differentiation. Although TβRII and TβRIII levels are increased in HKc/HPV16-Six1, Smad-dependent TGF-β signaling is reduced, while MAPK is activated. Activation of MAPK in HKc/HPV16 overexpressing Six1 is associated with resistance to calcium-induced terminal differentiation, although the precise mechanism remains to be determined.

CHAPTER 5

SIX1 PROMOTES COLORECTAL CANCER GROWTH AND METASTASIS BY STIMULATING ANGIOGENESIS AND RECRUITING TUMOR-ASSOCIATED MACROPHAGES

5.1 INTRODUCTION

Colorectal cancer (CRC) is the third most common malignancy and the third leading cause of cancer-related death in men and women in the United States. According to statistics from the American Cancer Society, in 2014 an estimated 71,830 men and 65,000 women will be diagnosed with colorectal cancer; and 26,270 men and 24,040 women will die of the disease (Siegel, Desantis, and Jemal, 2014).

The Six1 homeoprotein, a member of the Six family of homeodomain transcription factors, is essential for the development of numerous organs (Ikeda et al., 2010; Xu et al., 2003; Zheng et al., 2003). Six1 overexpression has been found in various human cancers and is associated with increased tumor progression and metastasis, and decreased survival (Christensen et al., 2008). Recently, Six1 overexpression has been found to be significantly associated with poorer overall survival in advanced-stage CRC (stages III and IV), where cancer metastasis to regional lymph nodes or distant organs has occurred (Wong et al., 2014). However, there is no statistically significant correlation between the extent of Six1 expression and prognosis in patients with CRC at all stages (Ono et al., 2012). Studies using RNA interference have demonstrated that inhibition of

Six1 expression suppresses CRC cell growth and invasion (Li et al., 2014). Together these findings suggest that Six1 overexpression may promote CRC progression and metastasis. Therefore, in this study, we investigated the role of Six1 on tumor progression and metastasis in mouse and human CRC cell lines. We find that overexpression of Six1 dramatically promotes CRC tumor growth and metastasis *in vivo*, increases features of cancer stem cells (CSCs), and stimulates angiogenesis by up-regulating the expression of vascular endothelial growth factor (VEGF). Furthermore, we determined that Six1 overexpression results in the recruitment of tumor-associated macrophages (TAM) by increasing the expression of macrophage-specific colony-stimulating factor (CSF-1), chemokine (C-C motif) ligand 2/5 (CCL2/5) and VEGF, which further facilitates CRC tumor growth and metastasis.

5.2 RESULTS

5.2.1 THE OVEREXPRESSION OF SIX1 ENHANCES CRC TUMOR GROWTH AND METASTASIS

To explore the association between Six1 overexpression and CRC development, we examined the expression of Six1 mRNA in the intestines from C57BL/6 mice, intestines from C57BL/6-APC$^{Min/+}$ mice and tumors from C57BL/6-APC$^{Min/+}$ mice. We observed increased expression of Six1 in the intestines from C57BL/6-APC$^{Min/+}$ mice compared to that from wild type C57BL/6 mice, and the mRNA level of Six1 was dramatically increased in tumors from C57BL/6-APC$^{Min/+}$ mice Figure 5.1). Next, we chose as a model system the tumorigenic but poorly metastatic mouse colon cancer cell line MC38 to investigate CRC progression in response to Six1 overexpression (Smith et

al., 2010). A surgical orthotopic homograft mouse model was used to explore the role of Six1 on tumor behavior *in vivo* by injecting MC38 vector control cells (MC38-Ctrl) and MC38 cells overexpressing Six1 (two independently-derived clones, MC38-Six1-1 and MC38-Six1-2) into the cecal subserosa of syngeneic C57BL/6 mice. As shown in Figure 5.2A and 5.2B, Six1-overexpressing MC38 cells formed primary tumors in 75% of implanted mice (15 out of 20), and the average tumor weight was ~420 mg. In contrast, MC38-Ctrl cells formed tumors in only 25% of the injected mice (5 out of 20), and the average tumor weight was ~132 mg. Thus, Six1-overexpression in MC38 cells significantly increased both tumor incidence and growth *in vivo* compared to MC38-Ctrl.

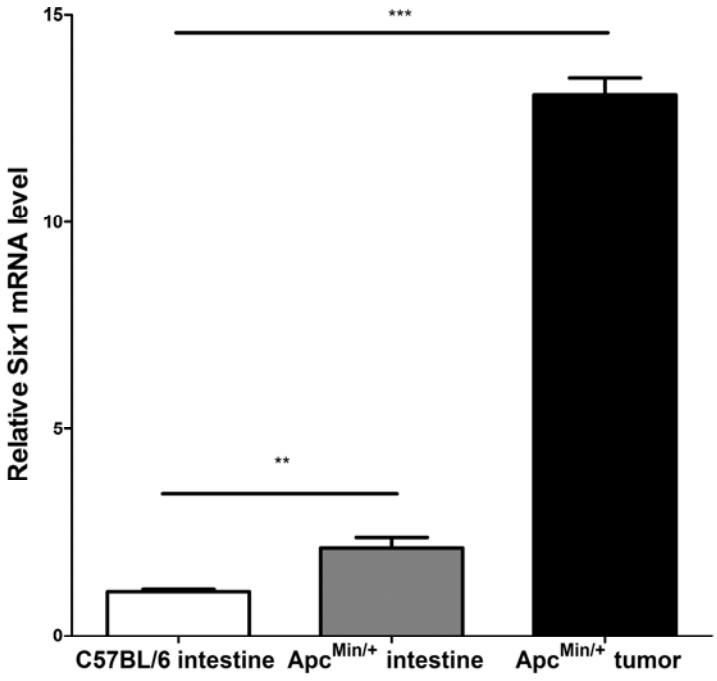

Figure 5.1 mRNA levels of Six1 increases during $APC^{Min}/^{+}$ mice tumorigenesis. The expression of Six1 mRNA was detected by real time PCR in intestines from C57BL/6 mice, intestines from C57BL/6-$APC^{Min}/^{+}$ mice and tumors from C57BL/6-$APC^{Min}/^{+}$ mice.

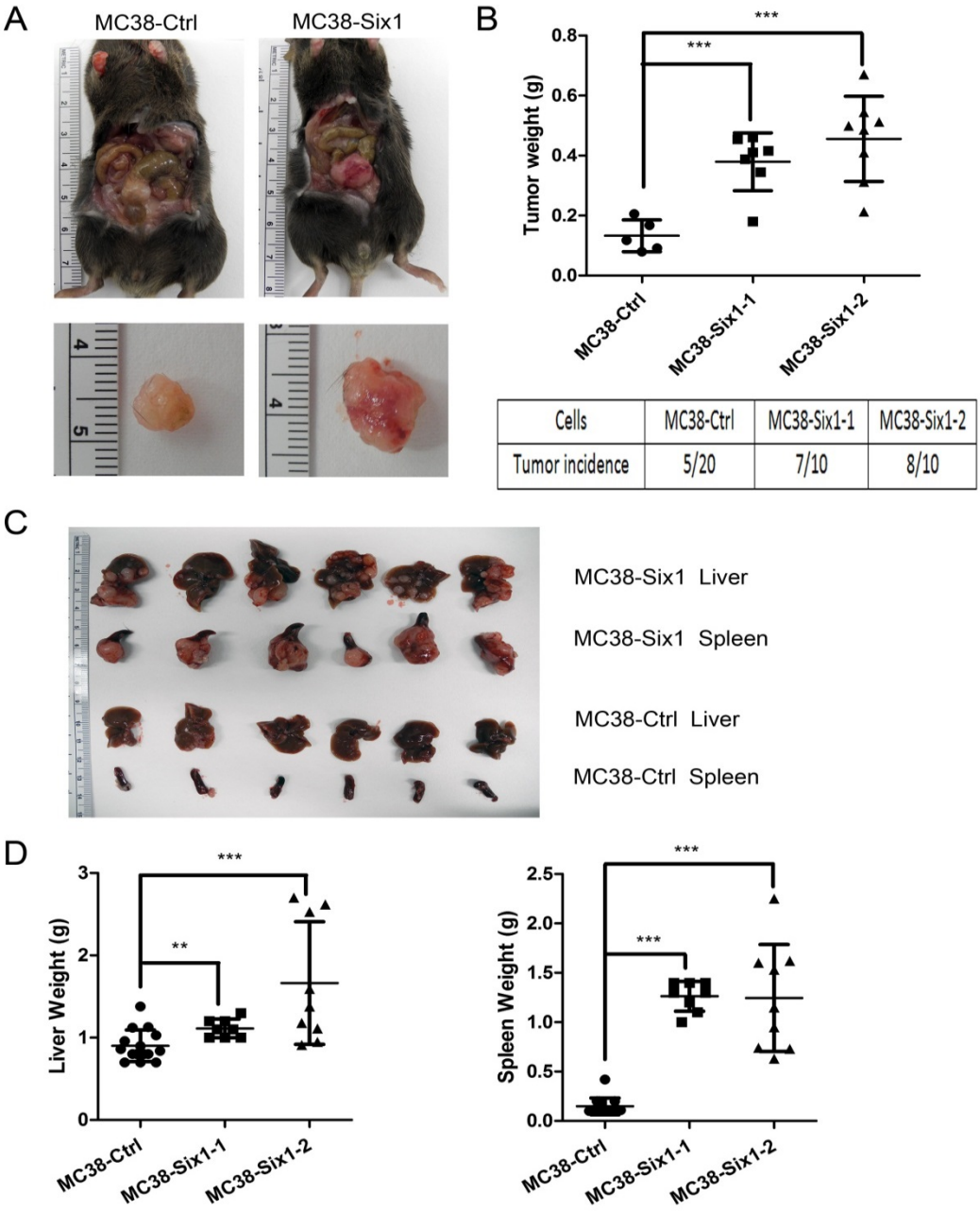

Figure 5.2 Six1 overexpression increases CRC tumor growth and metastasis *in vivo*. (A) Six1-overexpressing MC38 (MC38-Six1) or controls (MC38-Ctrl) were orthotopically injected into the cecum subserosa of C57BL/6 mice and 6 weeks later the mice were sacrificed. Left panels: tumors from MC38-Ctrl. Right panels: tumors from MC38-Six1. (B) The weight of tumors and tumor incidence in mice injected in the cecum with MC38-Ctrl or isolates of MC38-Six1 cells. (C) Upper panel: livers and spleens from Six1-overexpressing MC38 (MC38-Six1) tumor-bearing mice. Lower panel: livers and spleens from MC38-Ctrl tumor-bearing mice. (D) The weight of livers (left panel) and spleens (right panel) from Six1-overexpressing MC38 (MC38-Six1) or MC38-Ctrl tumor-bearing mice.

The liver is one of the most common sites of metastatic spread of CRC, and autopsies have found that up to 70% of colon cancer patients had liver metastasis at the time of death (Schima et al., 2005). To determine whether Six1 is involved in CRC metastasis, we used a splenic injection model to compare liver metastasis in MC38-Six1 to MC38-Ctrl. We found that mice injected with MC38-Six1 cells formed larger tumor burdens in the spleen and developed more metastases in the liver compared to those injected with MC38-Ctrl cells. However, interestingly the size of primary tumors in the spleen did not correlate to the extent of metastasis in the liver in either the MC38-Ctrl or MC38-Six1 groups (Figure 5.2C). We used liver weight as an indicator for the degree of liver metastases, and spleen weight as an indicator for the size of tumor in the spleen. As shown in Figure 5.2D, mice injected with Six1-overexpressing MC38 cells showed significantly increased spleen and liver weight as compared to those injected with MC38-Ctrl cells, suggesting that Six1 overexpression increased primary tumor growth and metastatic spread. Taken together, our results suggest that the overexpression of Six1 promoted CRC growth and metastasis.

5.2.2 SIX1 INCREASES FEATURES OF CANCER STEM CELLS (CSCS) IN COLORECTAL CANCER

We next sought to explore how Six1 overexpression promotes CRC growth and metastatic spread. We analyzed several properties of tumors in the cecum arising from mice injected with either MC38-Ctrl or MC38-Six1 cells. Since the increased tumor size found in MC38-Six1 cells could be the result of increased proliferation or decreased apoptosis, we used immunohistochemistry to compare the cell proliferation marker Ki67

and the apoptosis marker cleaved caspase-3 in MC38-Ctrl and MC38-Six1 tumors. Tumors overexpressing Six1 (MC38-Six1) showed increased levels of Ki67 positive cells but we found no marked difference in the percentage of cleaved caspase-3 positive cells compared to the controls (MC38-Ctrl) (Figure 5.3A), suggesting the effect of Six1 on tumor growth is associated with increased cell proliferation rather than alterations in the rates of apoptosis. However, when we compare cell proliferation *in vitro*, Six1 overexpression slightly suppressed cell growth in MC38 (Figure 5.3B) rather than increasing cell proliferation as we found in the *in vivo* cecal model studies. Moreover, we analyzed by Western blot the levels of several proteins involved in cell proliferation, such as c-Myc, PCNA, cyclin D1, and cyclin E, and found that none of them were up-regulated in Six1-overexpressing MC38 cells compared to the control cells (Figure 5.3C), indicating again that Six1 overexpression did not increase cell proliferation *in vitro* as it did *in vivo*. This observation, coupled with our previous finding that Six1 is associated with an increased CSCs population during HPV16-mediated transformation (Xu et al., 2014), led us to examine whether Six1 could enhance CSCs characteristics in MC38, thereby promoting CRC tumor progression. To this end, we determined the expression of ALDH1 in MC38-Ctrl and MC38-Six1 in tumors and in lysates from cultured MC38 cells. We found that the protein level of ALDH1 increased dramatically in tumors derived from MC38 cells overexpressing Six1 and in cultured MC38-Six1 cells compared to MC38-Ctrl (Figure 5.3A, C). Cell surface antigens $CD44^+$ and $CD166^+$ have been considered as CRC CSCs markers (Dalerba et al., 2007; Levin et al., 2010). We thus measured $CD44^+/CD166^+$ populations in MC38-Ctrl and MC38-Six1 by flow cytometry. Six1-overexpressing MC38 cells had a markedly increased $CD44^+/CD166^+$ population

(41.3% in MC38-Six1 versus 3.8% in MC38-Ctrl) (Figure 5.3D). Furthermore, we examined tumorsphere formation ability of MC38-Ctrl and MC38-Six1. As shown in Figure 5.3E, increased number of tumorspheres was observed in MC38-Six1 as compared to MC38-Ctrl. In all, our findings demonstrate that Six1 overexpression increases the cancer stem cell-like cell population in CRC cells.

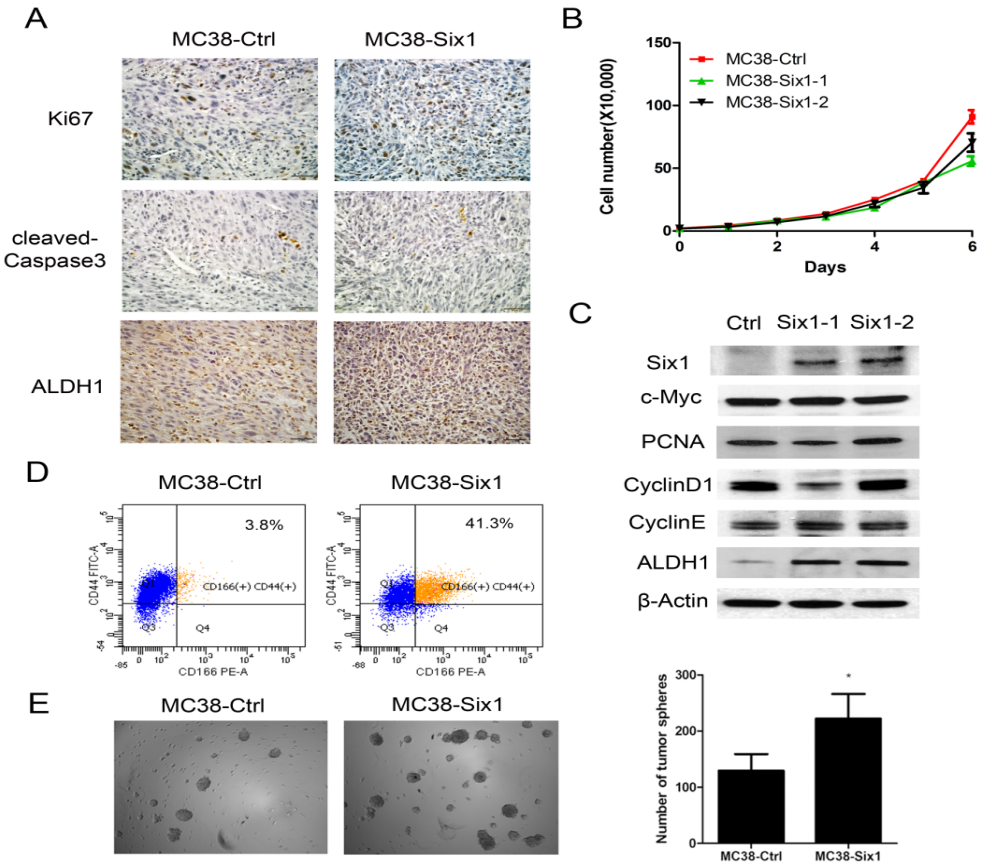

Figure 5.3 Six1 overexpression in MC38 cells increases CSC characteristics. (A) The expression of Ki67, cleaved caspase-3 and ALDH1 in tumors arising from mice injected in the cecum with MC38-Ctrl and MC38-Six1 as detected by immunohistochemistry. (X400) (B) Cell proliferation was determined by directly counting cells at the days indicated in MC38-Six1 and MC38-Ctrl. (C) Western blots for Six1, c-Myc, PCNA, cyclin D1, cyclin E and ALDH1 in MC38-Ctrl and two isolates of MC38 overexpressing Six-1 (MC38-Six1). β-actin was used as a loading control. (D) Analysis by flow cytometry of CD166 and CD44 expression in MC38 overexpressing Six1 (MC38-Six1) or MC38 controls (MC38-Ctrl). (E) Tumorsphere formation ability in MC38-Ctrl and MC38-Six1. Bars indicate SD and * indicates p values < 0.05.

5.2.3 SIX1 OVEREXPRESSION STIMULATES ANGIOGENESIS IN CRC TUMORS

Histopathological analysis showed a hyper-cellular solid carcinoma with high grade atypia and frequent mitosis in both Six1-overexpressing and control tumors (Figure 5.4A). Interestingly, we noted that in Six1-overexpressing tumors (MC38-Six1), there were more vessels, especially blood vessels, located within the tumor mass as compared to control tumors (MC38-Ctrl) (Figure 5.4A). CD31 and α-SMA staining was used to demonstrate the presence of vascular endothelial cells and pericytes in blood vessels. Tumors arising form MC38-Six1 cells had greater numbers of CD31 and α-SMA positive cells compared to that from MC38-Ctrl cells (Figure 5.4A), indicating that Six1 overexpression promotes tumor angiogenesis. In addition, we analyzed the levels of proteins that are related to tumor angiogenesis and metastasis in sera from MC38-Six1 and MC38-Ctrl tumor-bearing mice. We found that the protein levels of VEGF, MMP9 and lysyl oxidase (LOX) increased, and that of MMP2 remained the same in sera of MC38-Six1 tumor-bearing mice as compared to MC38-Ctrl mice (Figure 5.4B). Furthermore, immunohistochemical analyses demonstrated increased protein levels of MMP9, VEGF and LOX in MC38-Six1 compared to MC38-Ctrl tumors (Figure 5.4C). These results support that the increased accumulation of MMP9, VEGF and LOX we observed in the serum of tumor-bearing mice was due at least in part to the increased expression of these proteins in MC38-Six1 tumors rather than the larger size of the MC38-Six1 tumors compared to MC38-Ctrl. Taken together these data indicate that Six1 overexpression in CRC tumors stimulates angiogenesis and metastasis by increasing the expression of VEGF, LOX and MMP9.

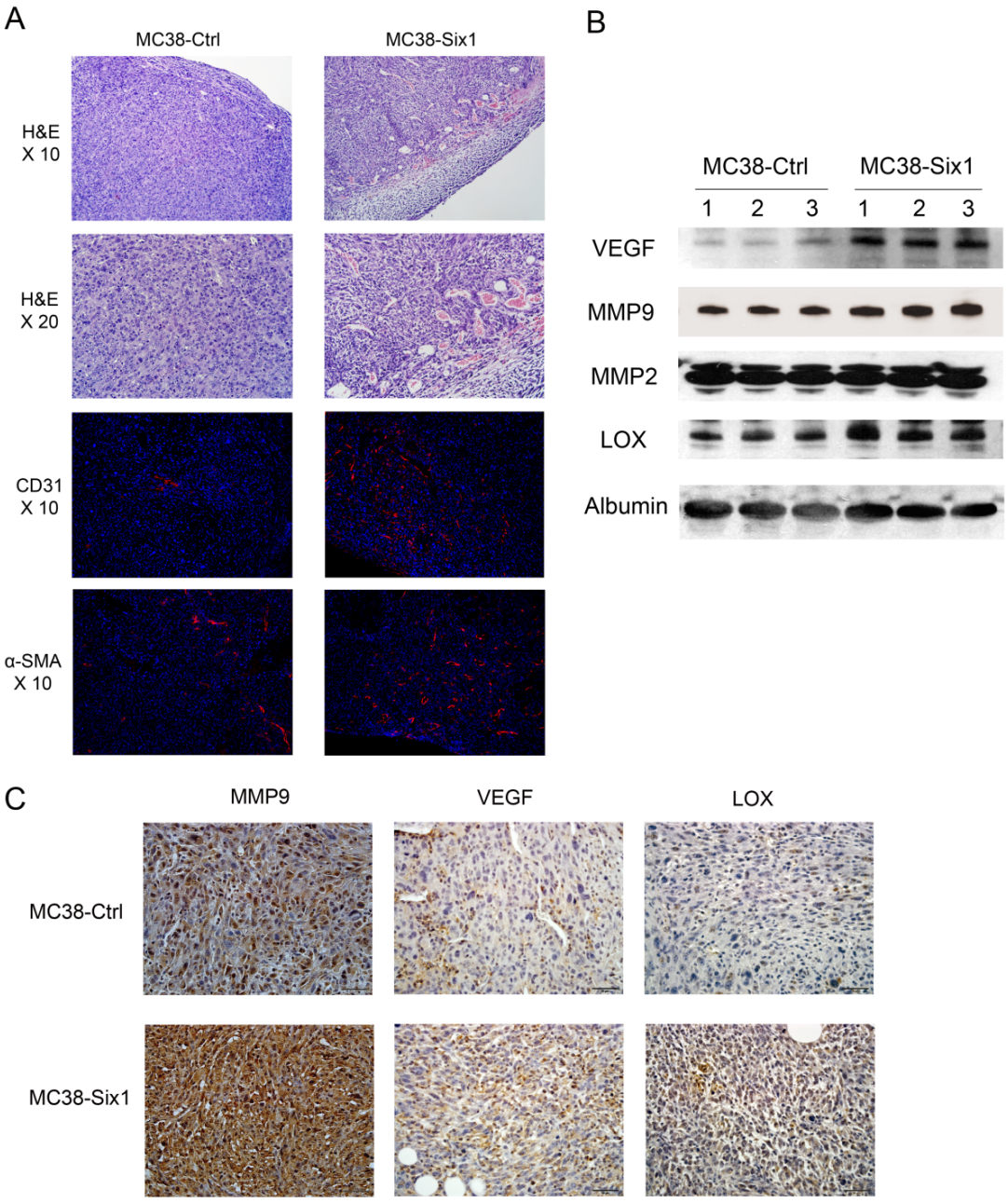

Figure 5.4 Six1 overexpression promotes angiogenesis. (A) Upper panels: H&E staining of primary tumors formed in the cecum of mice from MC38-Ctrl and MC38-Six1. Lower panels: immunofluorescent staining of CD31 (red) and α-SMA (red) merged with nuclei (blue) in MC38-Ctrl and MC38-Six1 tumors. Images are shown at the indicated magnification. (B) Western blots for VEGF, MMP2, MMP9 and LOX in sera from Six1-overexpressing MC38 tumor-bearing mice (MC38-Six1) and control mice (MC38-Ctrl). Albumin was used as a loading control. (C) The expression of MMP9, VEGF and LOX in MC38-Six1 and MC38-Ctrl tumors as assessed by immunohistochemistry (X400).

5.2.4 SIX1 OVEREXPRESSION PROMOTES MC38 CELL MIGRATION AND INVASION *IN VITRO*.

Since Six1 overexpression in MC38 cells enhanced tumor progression and metastasis *in vivo*, we sought to identify changes in cell behavior associated with Six1 overexpression. In a wound healing assay, MC38 overexpressing Six1 (MC38-Six1) exhibited enhanced cell migration compared to MC38 control cells (MC38-Ctrl) (Figure 5.5A).

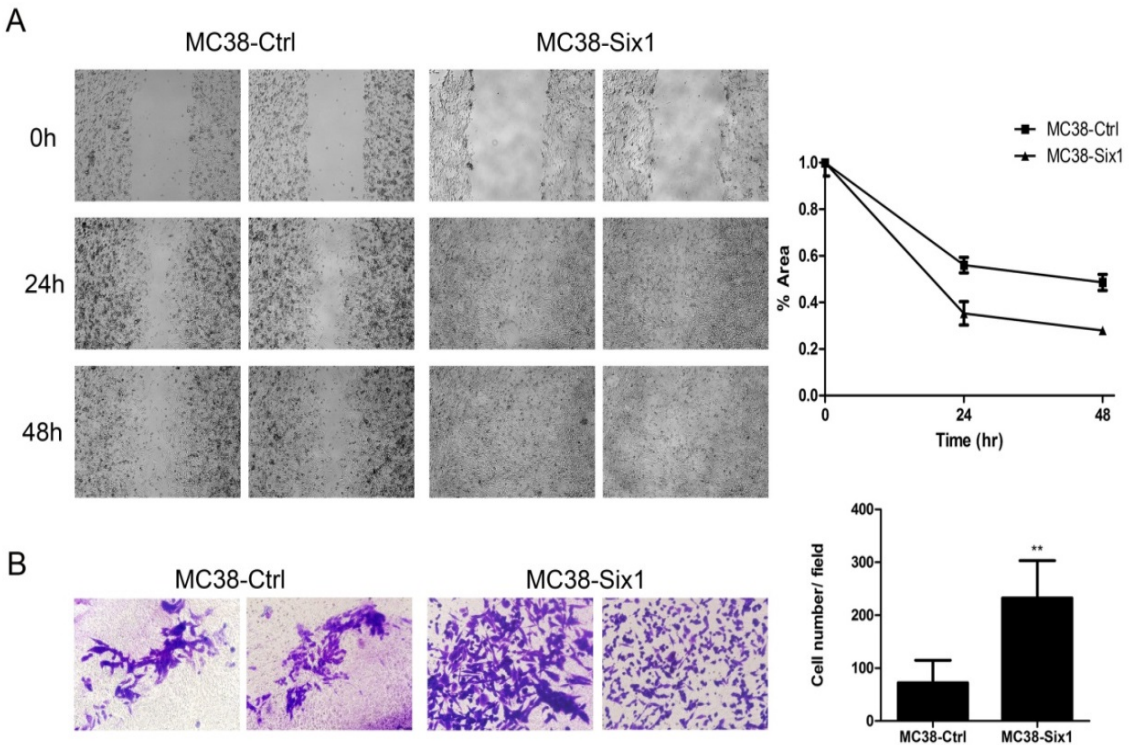

Figure 5.5 Six1 overexpression in MC38 increases migration and invasion *in vitro*. (A) Cell migration was determined by a wound healing assay. Microscopic images are at 100X magnification. The area of the wound is quantified to determine the extent of wound repair. (B) Cell invasion was determined by a Matrigel invasion assay. Images are shown at 400X magnification. The number of invading cells was quantified after crystal violet staining. Each column represents the mean of five different fields. Bars indicate SD and ** indicates p values < 0.01.

MC38-Six1 also showed ~3.2-fold increase in cell invasion through Matrigel compared to MC38-Ctrl (Figure 5.5B). Consistent with what we found in tumor tissue

and in MC38-Six1 tumor-bearing mice, MC38-Six1 cells *in vitro* displayed increased protein levels of MMP9 and VEGF, but not MMP2 compared to MC38-Ctrl cells (Figure 5.6A). These results show that Six1 increases MC38 cell migration and invasion *in vitro*.

5.2.5 SIX1 OVEREXPRESSION ACTIVATES ERK AND P38 MAPK IN MOUSE AND HUMAN CRC CANCER CELL LINES

Epithelial-mesenchymal transition (EMT) enables polarized epithelial cells to acquire enhanced migratory capacity and invasiveness, and has been considered as a critical step in mediating tumor progression, metastasis as well as stem cell properties (Christiansen and Rajasekaran, 2006; Mani et al., 2008). Six1-induced EMT has been elucidated in various cancers (Micalizzi et al., 2009; Ono et al., 2012; Xu et al., 2014). We compared the expression of typical EMT-related genes in MC38-Six1 to MC38-Ctrl cells by Western blotting. Surprisingly, we only observed a small decrease in E-cadherin and no marked change in vimentin or β-catenin (Figure 5.6A) levels; suggesting EMT is not an important cellular response to Six1 overexpression in MC38. In HPV16 immortalized human keratinocytes, we previously reported that Six1 overexpression leads to activation of MAPK signaling, especially phosphorylation of ERK and p38 MAPK (Xu et al., 2014). Similarly, the phosphorylation of p38 and ERK, but not JNK, increased considerably in Six1-overexpressing MC38 compared to MC38-Ctrl (Figure 5.6A).

We also compared some of the molecular changes associated with Six1 overexpression in mouse MC38 to Six1 overexpressing human CRC cell lines HT29 and SW480. Protein levels of PCNA and cleaved caspase-3 remained the same in Six1-overexpressing and control cells, indicating that Six1 overexpression had no major

impact on human CRC cell proliferation and apoptosis *in vitro* (Figure 5.6B). Six1 overexpression significantly decreased the expression of E-cadherin in SW480, and only slightly decreased E-cadherin in HT29. Interestingly, ERK and p38 MAPK phosphorylation was dramatically increased in Six1-overexpressing SW480 and HT29 compared to their corresponding controls (Figure 5.6B). Combining the results from MC38 and human CRC cells, we conclude that Six1 overexpression does not promote EMT or affect CRC cell growth and apoptosis *in vitro* but Six1 overexpression does activate the ERK and p38 MAPK pathway.

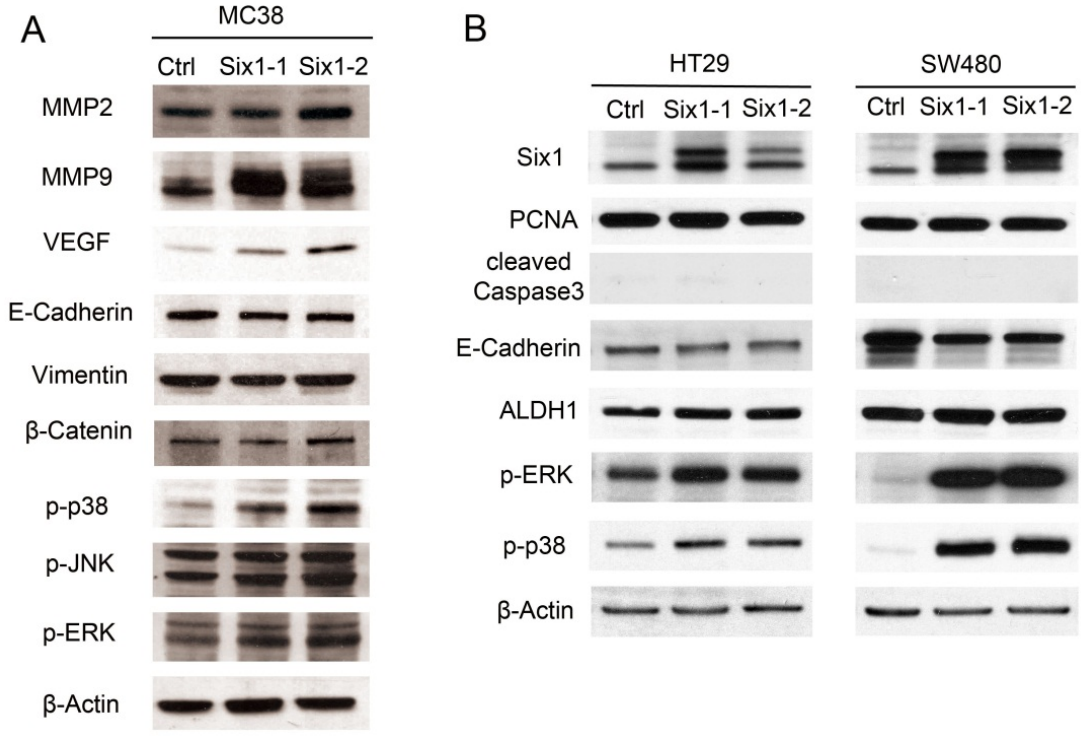

Figure 5.6 The overexpression of Six1 activates ERK and p38 MAPK in human and mouse CRC cell lines. (A) Western blots for MMP2, MMP9, VEGF, E-cadherin, vimentin, β-catenin, p-p38, p-JNK and p-ERK in two different isolates of MC38 overexpressing Six1 (MC38-Six1) and controls (MC38-Ctrl). (B) Western blots for Six1, PCNA, cleaved caspase-3, E-cadherin, ALDH1, p-ERK and p-p38 in two different isolates of Six1-overexpressing HT29 (HT29-Six1) and SW480 (SW480-Six1) and corresponding controls (HT29-Ctrl and SW480-Ctrl). β-actin was used as a loading control.

5.2.6 THE OVEREXPRESSION OF SIX1 IN MC38 ENHANCES THE RECRUITMENT OF TUMOR-ASSOCIATED MACROPHAGES (TAM)

In contrast to the results obtained from the orthotopic CRC model, in which MC38-Six1 tumors were significantly larger than MC38-Ctrl tumors in the cecum, in the subcutaneous injection model, Six1-overexpressing MC38 cells formed larger tumors in the flanks of C57BL/6 mice in some animals, but the increase in tumor weight was not statistically significant (Figure 5.7A).

This observation, along with some of our results with MC38 cells in culture, suggested that the tumor microenvironment is critical for Six1-induced tumor progression. The tumor microenvironment, also referred to as the tumor-associated stroma, is composed of non-neoplastic cells such as fibroblasts, infiltrating immune cells, endothelial cells and structural components (Hanahan and Coussens, 2012). In CRC, tumor-infiltrating immune cells, cytokines and other immune mediators are involved in almost all steps of colon tumorigenesis, including initiation, promotion, progression and metastasis (Terzic et al., 2010). For this reason, we investigated whether Six1 overexpression was associated with systemic inflammation, by examining the peripheral white blood cell (WBC) count. As shown in Figure 5.7B, the peripheral WBC count from MC38-Six1 and MC38-Ctrl tumor-bearing mice both fall within the normal range (gray zone), and there was no significant difference between them. We then analyzed the percentage of lymphocytes, monocytes and neutrophils in peripheral WBC, and none of them showed significant differences in C57BL/6 mice bearing MC38-Six1 tumors in their cecum compare to control mice (Figure 5.7C). We also examined the protein levels

of three proinflammatory cytokines (IL-1β, IL-6 and TNF-α) in the sera of these mice, and found no consistent differences (Figure 5.7D).

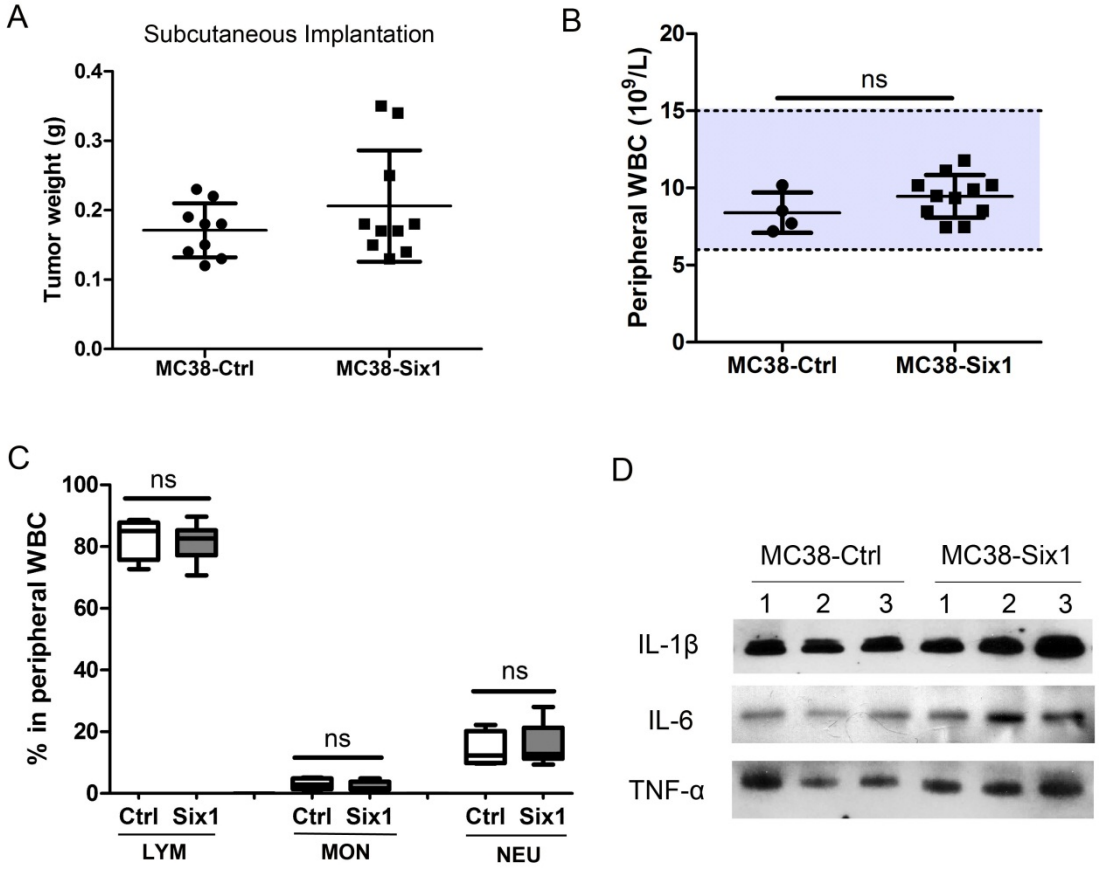

Figure 5.7 Six1 overexpression does not induce systemic inflammation. (A) Six1-overexpressing MC38 (MC38-Six1) or controls (MC38-Ctrl) were injected into the flank of C57BL/6 mice and the mice sacrificed 6 weeks later (n = 9-10). The weight of tumors formed from MC38-Ctrl and MC38-Six1 is shown. (B) Peripheral white blood cell (WBC) count from MC38-Six1 and MC38-Ctrl tumor-bearing mice (cecal implantation). (C) Percentage of lymphocytes, monocytes and neutrophils in peripheral WBC from MC38-Six1 and MC38-Ctrl tumor-bearing mice (cecal implantation). (D) The protein levels of IL-1β, IL-6 and TNF-α in sera from Six1-overexpressing MC38 tumor-bearing mice (MC38-Six1) and control mice (MC38-Ctrl) (cecal implantation).

Like other solid tumors, CRC tumors are infiltrated by various types of immune cells, including T cells, neutrophils, mast cells, natural killer (NK) cells and TAM (Terzic et al., 2010). To identify the altered population of immune cells, we performed flow

cytometry analyses to detect major immune cell types, using a combination of immunostaining and found low numbers or small changes in B cells, T cells, mast cells or natural killer cells (data not shown) A significant increase in the $CD11b^{+}/F4/80^{+}$ cell population was observed in MC38-Six1 tumors compared to MC38-Ctrl (28.8% ± 5 in MC38-Six1 versus 11.8% ± 1.9 in MC38-Ctrl), indicating Six1 overexpression in MC38 increased macrophage infiltration (Figure 5.8A). We also observed a reduction in $CD11b^{+}/Gr1^{+}$ population (a marker for neutrophils) in some Six1-overexpressing tumors when compared with control tumors, but the reduction was not statistically significant (Figure 5.8A).

We also detected the F4/80 positive cells in tumor samples by immunohistochemistry. Large clusters of F4/80 positive macrophages were observed in Six1-overexpressing tumors (MC38-Six1) but infrequently found in control tumors (MC38-Ctrl) (Figure 5.8B). Furthermore, we used immunofluorescence to visualize VEGF and F4/80 positive cells in MC38-Six1 tumor sections. Consistent with what we showed in Figure 5.4C, in which some small stromal cells were strongly positive for VEGF, we observed colocalization of VEGF-positive cells and F4/80 positive cells (Figure 5.9), suggesting TAM expressed VEGF to further facilitate tumor angiogenesis. These results suggest that Six1 overexpression in MC38 recruits TAM and further promotes tumor angiogenesis, and this increase in the TAM population in the tumor is most likely due to the recruitment of TAM by tumor cells, not due to the systemic inflammation.

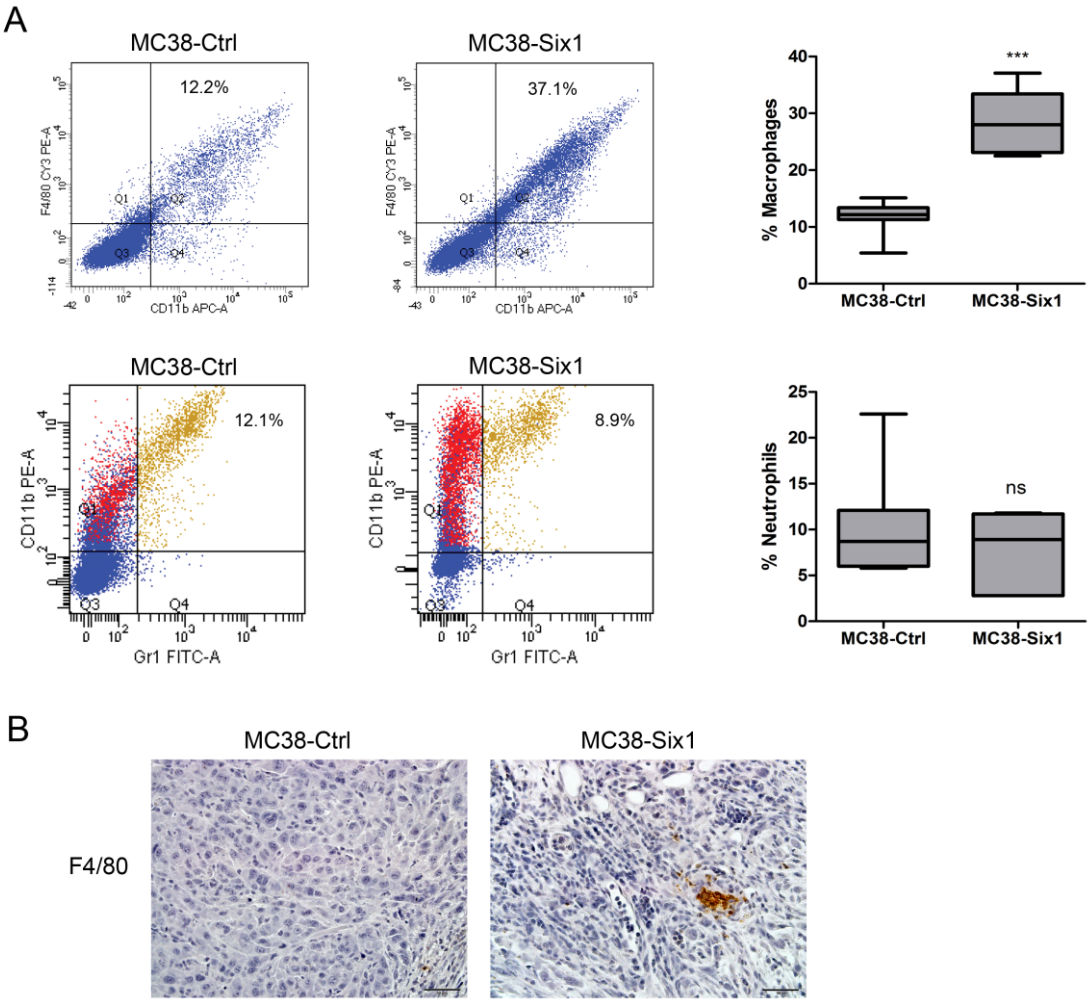

Figure 5.8 MC38 cells overexpressing Six-1 recruit macrophages to tumors. (A) Left panels: Flow cytometric analysis of the expression of CD11b, F4/80 and Gr1 in Six1-overexpressing MC38 tumors (MC38-Six1) and control tumors (MC38-Ctrl). Right panels: the percentage of total cells positive for either $CD11b^{+}F4/80^{+}$ (marker for macrophages) or $CD11b^{+}Gr1^{+}$ (marker for neutrophils) cells. Results are representative of seven independent experiments. (B) Immunohistochemical analysis of the expression of F4/80 in MC38-Ctrl and MC38-Six1 derived tumors (X400).

5.2.7 SIX1 INCREASES THE EXPRESSION OF CSF-1 AND CCL2/5, AND THEREBY AUGMENTS THE RECRUITMENT OF TAM

It is now generally accepted that TAM, through the secretion of cytokines, chemokines, and growth factors, exert pro-tumor functions by promoting tissue remodeling and angiogenesis rather than cytotoxic activity (Qian and Pollard, 2010).

TAM can be recruited to CRC tumor sites by several molecules, including CCL2 and CCL5, VEGF and CSF-1 (Erreni, Mantovani, and Allavena, 2011). We determined that the mRNA expression of CSF-1, CCL2, CCL5, and VEGF was increased in MC38 overexpressing Six1 compared to MC38-Ctrl (Figure 5.10A).

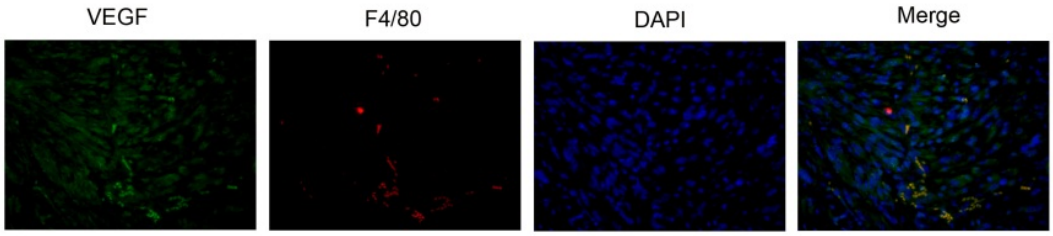

Figure 5.9 Immunofluorescent staining of VEGF (green), F4/80 (red) and merged with nuclei (blue) in MC38-Six1 derived tumors. In the merged image the yellow color indicates colocalization of VEGF and F4/80. Images are shown at 400× magnification.

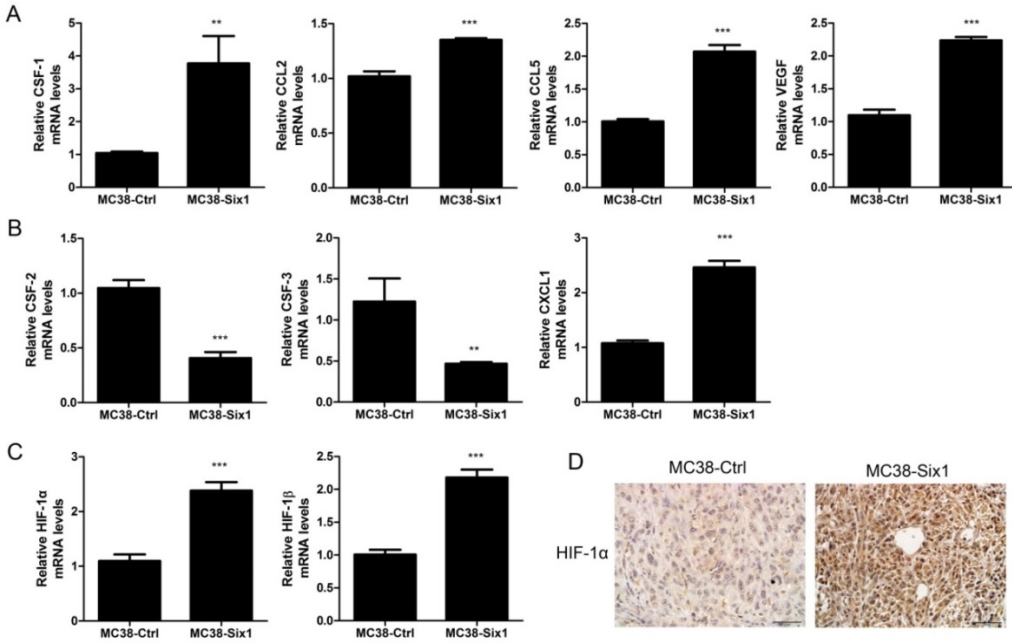

Figure 5.10 Six1 overexpression in MC38 increases the expression of molecules that induce chemotaxis of TAM. (A) mRNA expression of CSF-1, CCL2, CCL5 and VEGF were detected by real time PCR in MC38-Ctrl and MC38-Six1. (B) mRNA levels of CSF-2, CSF-3 and CXCL1 was determined by real time PCR in MC38-Ctrl and MC38-Six1. (C) mRNA expression of HIF-1α and HIF-1β was determined by real time PCR in MC38-Ctrl and MC38-Six1. Real time PCR data were normalized to β-actin expression. Bars indicate SD, and ** and *** indicate p values < 0.01 and 0.001 respectively. (D) Protein levels of HIF-1α were examined by immunohistochemistry (X400) in MC38-Ctrl and MC38-Six1 derived tumors.

We also explored mRNA expression of cytokines related to the recruitment of neutrophils to tumors, including granulocyte-macrophage colony-stimulating factor-2 (CSF-2), granulocyte colony-stimulating factor-3 (CSF-3) and CXCL1. We found decreased expression of CSF-2 and CSF-3 in MC38-Six1, and increased expression of CXCL1 (Figure 5.10B). This may help explain the wide variation in the proportion of neutrophils in tumors in the same group, and our finding that there was no difference in the neutrophils in tumors overexpressing Six1 and controls (Figure 5.8A). Since TAM can be recruited into tumors and accumulate in areas of hypoxia (Lewis and Murdoch, 2005), we analyzed the expression of HIF-1α and HIF-1β mRNA in MC38-Ctrl and MC38-Six1. An increase in mRNA for both HIF-1α and HIF-1 β was observed in MC38-Six1 (Figure 5.9C). Increased protein levels of HIF-1α was observed in MC38-Six1 tumors compared to control tumors (Figure 5.10D). Furthermore, we detected the expression of cytokines related to the recruitment of macrophages in response to Six1 overexpression in HCT116 and HT29. We observed increased mRNA of VEGF, CCL2, CCL5, CSF-1 and CSF-2 in HCT116-Six1, and increased CCL2, CCL5, CSF-1 and CSF-2 in HT29-Six1 when compared to their corresponding controls (Figure 5.11).

Although the expression of the cytokines did not follow same pattern, all these results supporting the conclusion that Six1 overexpression in CRC tumor cells recruit macrophage. Taken together, our data suggest that Six1 increases the expression of cytokines that elicit macrophage infiltration into the tumor, which results in CRC tumor growth, progression and metastasis.

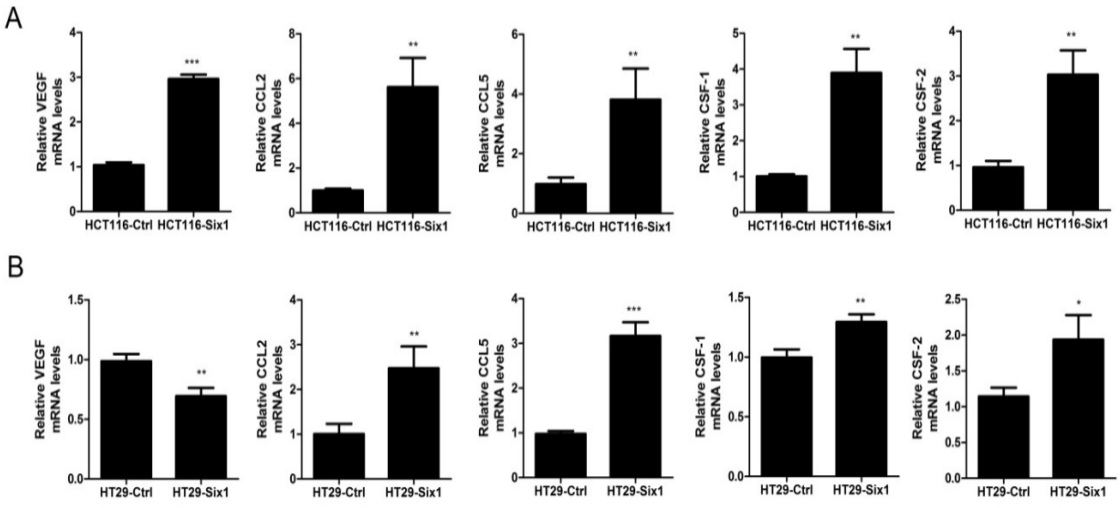

Figure 5.11 mRNA expressions of VEGF, CCL2, CCL5, CSF-1 and CSF-2 were detected by real time PCR in HCT116-Ctrl and HCT116-Six1 (A), and HT29-Ctrl and HT29-Six1 (B).

5.3 DISCUSSION

The Six1 homeoprotein plays an important role in the development of numerous organs. Inappropriate activation of Six1 expression has been found in various human cancers, and is associated with increased tumor progression and metastasis, and poor prognosis (Christensen et al., 2008). Recent studies have shown that the overexpression of Six1 is associated with decreased survival in advanced-stage CRC, which was related to EMT, growth and invasion (Li et al., 2014; Ono et al., 2012). In addition, we observed increased expression of Six1 in the intestines from C57BL/6-APC^{Min}/$^{+}$ mice compared to that from wild type C57BL/6 mice, and dramatically increased expression of Six1 in tumors from C57BL/6-APC^{Min}/$^{+}$ mice, indicating Six1 overexpression may be involved in early stages of CRC as well. In the present study, we determined that overexpression of Six1 in the mouse colon cancer cell line MC38 dramatically enhanced CRC tumor growth and metastasis *in vivo*. We then found that Six1 increased the population of CSCs

and stimulated angiogenesis to promote CRC progression. Moreover, we identified that Six1 overexpression induced macrophage chemotaxis most likely by increasing the expression of CSF-1, CCL2/5 and VEGF, thereby further facilitating CRC tumor growth and metastasis.

An important component of the tumor microenvironment is stromal cells. Stromal cells can be recruited by molecular signals from the cancer cells and cooperate with the cancer cells to support tumor progression, by enhancing primary tumor growth as well as enabling metastatic spread (Hanahan and Coussens, 2012). For example, tumor cells produce VEGF, a potent angiogenic factor, to induce endothelial cell proliferation and migration and promote angiogenesis. These new blood vessels help satisfy the oxygen and other metabolic needs of the tumor, provides a potential escape route for cancer cells, and thereby facilitates tumor progression and metastasis (Woodhouse, Chuaqui, and Liotta, 1997; Xu et al., 2006). To explore the role of Six1overexpression in CRC progression, we used an orthotopic CRC mouse model, in which tumor cells grow in the cecum of immunocompetent mice. We discovered that Six1 overexpression not only affects tumor cell malignancy by increasing CSC-like characteristics, but also promotes remodeling of the tumor stroma by stimulating angiogenesis and recruiting TAM.

Metastasis is the spread of cancer cells from the primary tumor site to distant organs and is the leading cause of death for CRC patients (Society, 2013; Steeg, 2006). The liver is one of the most common sites of CRC metastasis (Schima et al., 2005). Cancer cell metastasis involves the following steps: local invasion, intravasation, travel through the circulation, arrest and extravasation and proliferation at the distant site

(Reymond, d'Agua, and Ridley, 2013). To investigate the role of Six1 in CRC metastasis, we used a splenic injection model to estimate liver metastasis. We chose this model because spontaneous liver metastasis in the orthotopic CRC model is very rare and not adequate to assess whether Six1 contributes to metastasis. The splenic injection model mimics spontaneous liver metastasis by recapitulating early dissemination and later extravasation and colonization of the liver (Lavilla-Alonso et al., 2011). Using this model, we demonstrate a dramatic increase in liver metastasis of CRC in Six1-overexpressing tumor-bearing mice compared to the control mice, suggesting that Six1 facilitates CRC metastasis.

EMT has been considered a critical step in mediating tumor metastasis (Christiansen and Rajasekaran, 2006) and a loss of E-cadherin has been shown to lead to early metastasis (Perl et al., 1998). The correlation between Six1 overexpression and EMT has been established in breast and colon cancer (Micalizzi et al., 2009; Ono et al., 2012). In addition, our previous results showed Six1 induced EMT during HPV16-mediated transformation (Xu et al., 2014). In this study, we observed a significant decrease of E-cadherin in SW480 cells overexpressing Six1; but surprisingly, only a slight decrease was observed in MC38 and HCT116 cells overexpressing Six1. Overall these observations indicate that EMT may be important for the increase of CRC cell migration and invasion found associated with Six1 overexpression, but the extent of the mesenchymal phenotype is different among the different CRC cell lines. Furthermore, we showed increased expression of VEGF and MMP9 in response to Six1 overexpression, which promotes tumor angiogenesis and metastasis (Egeblad and Werb, 2002; Hanrahan

et al., 2003; Lopez-Otin and Matrisian, 2007; Martin and Matrisian, 2007), and may explain how Six1 promotes CRC progression.

Ample clinical and experimental evidence has demonstrated the promotive role of TAM on tumorigenesis (Qian and Pollard, 2010). During the early stages of tumor development macrophages promote an inflammatory environment in the tumor. During later stages of tumor progression, macrophages stimulate angiogenesis, enhance tumor cell migration and invasion, and regulate anti-tumor immunity. For example, clinical studies have shown that overexpression of CSF-1, the major regulator of macrophages, is associated with poor prognosis in various cancers, including CRC (Mroczko et al., 2007). Macrophages produce epidermal growth factor (EGF), which activates migration in tumor cells. Moreover, macrophages accumulate in hypoxic areas of the tumor and constitutively express HIF-1α, which regulates the transcription of genes associated with angiogenesis, including VEGF. Tumor cells stimulate the production of MMP9 by macrophages, which disrupts extra-cellular matrix (ECM), and thus promotes cell invasion (reviewed in (Qian and Pollard, 2010)). In our study, we discovered that the overexpression of Six1 in CRC grown as orthotopic tumor induces TAM infiltration by enhancing the expression of CSF-1, CCL2/5 and VEGF. The recruited TAM reciprocally secrete molecules that are beneficial for the tumors, such as VEGF and MMP9, and further promote tumor angiogenesis and metastasis.

Enhanced MAPK signaling is a common event in tumors, and the link between MAPK signaling and cancer cell survival, angiogenesis and metastasis is well established (Fang and Richardson, 2005; Mansour et al., 1994). For example, studies based on human CRC samples indicate a significant correlation between VEGF expression and ERK

activation (Cassano et al., 2002). The p38 MAPK pathway regulates the expression of MMP9, which is critical for the migration and invasion of various cancers, including CRC (Ringshausen et al., 2004; Simon et al., 2001; Wei et al., 2013). The activation of p38 is essential for the expression of HIF-1α and VEGF, which promotes tumor angiogenesis (Duyndam et al., 2003; Yoshino et al., 2006). In addition, activation of p38 signaling results in an increase in the CSC population found under hypoxia conditions and serum depletion (Lin et al., 2012). Similarly, ERK-dependent signaling pathway regulates MMP9 mediated cell invasion (Lakka et al., 2002). Epidermal growth factor receptor (EGFR)-mediated ERK activation propagates human prostate CSCs (Rybak, Ingram, and Tang, 2013). Moreover, we have previously found that Six1overexpression results in differentiation resistance, promotes EMT and induces features of CSC in HPV16-immortalized HKc by the activation of MAPK signaling ((Xu et al., 2014) and our unpublished data). *Iwanaga* et al. found that Six1 significantly correlates with phosphorylated ERK in human breast cancers, and Six1 overexpression increases tumor initiating cells by activation of ERK (Iwanaga et al., 2012). Here, we demonstrate that the overexpression of Six1 induces the activation of ERK and p38 in both mouse and human CRC cell lines. Thus, we propose that the MAPK activation may be a common mechanism leading to tumor progression in Six1-overexpressing tumors and inhibiting the MAPK pathway could be a potential therapeutic approach for the treatment of these malignancies.

REFERENCES

Abate-Shen, C. (2002). Deregulated homeobox gene expression in cancer: cause or consequence? Nat Rev Cancer 2(10), 777-85.

Akerman, G. S., Tolleson, W. H., Brown, K. L., Zyzak, L. L., Mourateva, E., Engin, T. S., Basaraba, A., Coker, A. L., Creek, K. E., and Pirisi, L. (2001). Human papillomavirus type 16 E6 and E7 cooperate to increase epidermal growth factor receptor (EGFR) mRNA levels, overcoming mechanisms by which excessive EGFR signaling shortens the life span of normal human keratinocytes. Cancer Res 61(9), 3837-43.

Bakin, A. V., Rinehart, C., Tomlinson, A. K., and Arteaga, C. L. (2002). p38 mitogen-activated protein kinase is required for TGFbeta-mediated fibroblastic transdifferentiation and cell migration. J Cell Sci 115(Pt 15), 3193-206.

Bakin, A. V., Tomlinson, A. K., Bhowmick, N. A., Moses, H. L., and Arteaga, C. L. (2000). Phosphatidylinositol 3-kinase function is required for transforming growth factor beta-mediated epithelial to mesenchymal transition and cell migration. J Biol Chem 275(47), 36803-10.

Baritaki, S., Sifakis, S., Huerta-Yepez, S., Neonakis, I. K., Soufla, G., Bonavida, B., and Spandidos, D. A. (2007). Overexpression of VEGF and TGF-beta1 mRNA in Pap smears correlates with progression of cervical intraepithelial neoplasia to cancer: implication of YY1 in cervical tumorigenesis and HPV infection. Int J Oncol 31(1), 69-79.

Behbakht, K., Qamar, L., Aldridge, C. S., Coletta, R. D., Davidson, S. A., Thorburn, A., and Ford, H. L. (2007). Six1 overexpression in ovarian carcinoma causes resistance to TRAIL-mediated apoptosis and is associated with poor survival. Cancer Res 67(7), 3036-42.

Bertolero, F., Kaighn, M. E., Camalier, R. F., and Saffiotti, U. (1986). Effects of serum and serum-derived factors on growth and differentiation of mouse keratinocytes. *In vitro* Cell Dev Biol 22(7), 423-8.

Bhowmick, N. A., Chytil, A., Plieth, D., Gorska, A. E., Dumont, N., Shappell, S., Washington, M. K., Neilson, E. G., and Moses, H. L. (2004). TGF-beta signaling in fibroblasts modulates the oncogenic potential of adjacent epithelia. Science 303(5659), 848-51.

Bhowmick, N. A., Ghiassi, M., Bakin, A., Aakre, M., Lundquist, C. A., Engel, M. E., Arteaga, C. L., and Moses, H. L. (2001a). Transforming growth factor-beta1 mediates epithelial to mesenchymal transdifferentiation through a RhoA-dependent mechanism. Mol Biol Cell 12(1), 27-36.

Bhowmick, N. A., Zent, R., Ghiassi, M., McDonnell, M., and Moses, H. L. (2001b). Integrin beta 1 signaling is necessary for transforming growth factor-beta activation of p38MAPK and epithelial plasticity. J Biol Chem 276(50), 46707-13.

Borger, D. R., Mi, Y., Geslani, G., Zyzak, L. L., Batova, A., Engin, T. S., Pirisi, L., and Creek, K. E. (2000). Retinoic acid resistance at late stages of human papillomavirus type 16-mediated transformation of human keratinocytes arises despite intact retinoid signaling and is due to a loss of sensitivity to transforming growth factor-beta. Virology 270(2), 397-407.

Bos, P. D., Zhang, X. H., Nadal, C., Shu, W., Gomis, R. R., Nguyen, D. X., Minn, A. J., van de Vijver, M. J., Gerald, W. L., Foekens, J. A., and Massague, J. (2009). Genes that mediate breast cancer metastasis to the brain. Nature 459(7249), 1005-9.

Boyce, S. T., and Ham, R. G. (1983). Calcium-regulated differentiation of normal human epidermal keratinocytes in chemically defined clonal culture and serum-free serial culture. J Invest Dermatol 81(1 Suppl), 33s-40s.

Buck, M. B., and Knabbe, C. (2006). TGF-beta signaling in breast cancer. Ann N Y Acad Sci 1089, 119-26.

Cassano, A., Bagala, C., Battelli, C., Schinzari, G., Quirino, M., Ratto, C., Landriscina, M., and Barone, C. (2002). Expression of vascular endothelial growth factor, mitogen-activated protein kinase and p53 in human colorectal cancer. Anticancer Res 22(4), 2179-84.

Chan, K. S., Sano, S., Kataoka, K., Abel, E., Carbajal, S., Beltran, L., Clifford, J., Peavey, M., Shen, J., and Digiovanni, J. (2008). Forced expression of a constitutively active form of Stat3 in mouse epidermis enhances malignant progression of skin tumors induced by two-stage carcinogenesis. Oncogene 27(8), 1087-94.

Chen, L., Mayer, J. A., Krisko, T. I., Speers, C. W., Wang, T., Hilsenbeck, S. G., and Brown, P. H. (2009). Inhibition of the p38 kinase suppresses the proliferation of human ER-negative breast cancer cells. Cancer Res 69(23), 8853-61.

Chen, R. H., Su, Y. H., Chuang, R. L., and Chang, T. Y. (1998). Suppression of transforming growth factor-beta-induced apoptosis through a phosphatidylinositol 3-kinase/Akt-dependent pathway. Oncogene 17(15), 1959-68.

Christensen, K. L., Patrick, A. N., McCoy, E. L., and Ford, H. L. (2008). The six family of homeobox genes in development and cancer. Adv Cancer Res 101, 93-126.

Christiansen, J. J., and Rajasekaran, A. K. (2006). Reassessing epithelial to mesenchymal transition as a prerequisite for carcinoma invasion and metastasis. Cancer Res 66(17), 8319-26.

Coletta, R. D., Christensen, K., Reichenberger, K. J., Lamb, J., Micomonaco, D., Huang, L., Wolf, D. M., Muller-Tidow, C., Golub, T. R., Kawakami, K., and Ford, H. L. (2004). The Six1 homeoprotein stimulates tumorigenesis by reactivation of cyclin A1. Proc Natl Acad Sci U S A 101(17), 6478-83.

Coletta, R. D., Christensen, K. L., Micalizzi, D. S., Jedlicka, P., Varella-Garcia, M., and Ford, H. L. (2008). Six1 overexpression in mammary cells induces genomic instability and is sufficient for malignant transformation. Cancer Res 68(7), 2204-13.

Conery, A. R., Cao, Y., Thompson, E. A., Townsend, C. M., Jr., Ko, T. C., and Luo, K. (2004). Akt interacts directly with Smad3 to regulate the sensitivity to TGF-beta induced apoptosis. Nat Cell Biol 6(4), 366-72.

Creek, K. E., Geslani, G., Batova, A., and Pirisi, L. (1995). Progressive loss of sensitivity to growth control by retinoic acid and transforming growth factor-beta at late stages of human papillomavirus type 16-initiated transformation of human keratinocytes. Adv Exp Med Biol 375, 117-35.

Creek, K. E., Jenkins, G. R., Khan, M. A., Batova, A., Hodam, J. R., Tolleson, W. H., and Pirisi, L. (1994). Retinoic acid suppresses human papillomavirus type 16 (HPV16)-mediated transformation of human keratinocytes and inhibits the expression of the HPV16 oncogenes. Adv Exp Med Biol 354, 19-35.

Dai, J. L., Turnacioglu, K. K., Schutte, M., Sugar, A. Y., and Kern, S. E. (1998). Dpc4 transcriptional activation and dysfunction in cancer cells. Cancer Res 58(20), 4592-7.

Dalerba, P., Dylla, S. J., Park, I. K., Liu, R., Wang, X., Cho, R. W., Hoey, T., Gurney, A., Huang, E. H., Simeone, D. M., Shelton, A. A., Parmiani, G., Castelli, C., and Clarke, M. F. (2007). Phenotypic characterization of human colorectal cancer stem cells. Proc Natl Acad Sci U S A 104(24), 10158-63.

Dashti, S. R., Efimova, T., and Eckert, R. L. (2001). MEK6 regulates human involucrin gene expression via a p38alpha - and p38delta -dependent mechanism. J Biol Chem 276(29), 27214-20.

Datto, M. B., Li, Y., Panus, J. F., Howe, D. J., Xiong, Y., and Wang, X. F. (1995). Transforming growth factor beta induces the cyclin-dependent kinase inhibitor p21 through a p53-independent mechanism. Proc Natl Acad Sci U S A 92(12), 5545-9.

Davies, M., Robinson, M., Smith, E., Huntley, S., Prime, S., and Paterson, I. (2005). Induction of an epithelial to mesenchymal transition in human immortal and malignant keratinocytes by TGF-beta1 involves MAPK, Smad and AP-1 signalling pathways. J Cell Biochem 95(5), 918-31.

de Sanjose, S., Quint, W. G., Alemany, L., Geraets, D. T., Klaustermeier, J. E., Lloveras, B., Tous, S., Felix, A., Bravo, L. E., Shin, H. R., Vallejos, C. S., de Ruiz, P. A., Lima, M. A., Guimera, N., Clavero, O., Alejo, M., Llombart-Bosch, A., Cheng-Yang, C., Tatti, S. A., Kasamatsu, E., Iljazovic, E., Odida, M., Prado, R., Seoud, M., Grce, M., Usubutun, A., Jain, A., Suarez, G. A., Lombardi, L. E., Banjo, A., Menendez, C., Domingo, E. J., Velasco, J., Nessa, A., Chichareon, S. C., Qiao, Y. L., Lerma, E., Garland, S. M., Sasagawa, T., Ferrera, A., Hammouda, D., Mariani, L., Pelayo, A., Steiner, I., Oliva, E., Meijer, C. J., Al-Jassar, W. F., Cruz, E., Wright, T. C., Puras, A., Llave, C. L., Tzardi, M., Agorastos, T., Garcia-Barriola, V., Clavel, C., Ordi, J., Andujar, M., Castellsague, X., Sanchez, G. I., Nowakowski, A. M., Bornstein, J., Munoz, N., and Bosch, F. X. (2010). Human papillomavirus genotype attribution in invasive cervical cancer: a retrospective cross-sectional worldwide study. Lancet Oncol 11(11), 1048-56.

Derynck, R., and Zhang, Y. E. (2003). Smad-dependent and Smad-independent pathways in TGF-beta family signalling. Nature 425(6958), 577-84.

Descargues, P., Sil, A. K., Sano, Y., Korchynskyi, O., Han, G., Owens, P., Wang, X. J., and Karin, M. (2008). IKKalpha is a critical coregulator of a Smad4-independent TGFbeta-Smad2/3 signaling pathway that controls keratinocyte differentiation. Proc Natl Acad Sci U S A 105(7), 2487-92.

Duyndam, M. C., Hulscher, S. T., van der Wall, E., Pinedo, H. M., and Boven, E. (2003). Evidence for a role of p38 kinase in hypoxia-inducible factor 1-independent induction of vascular endothelial growth factor expression by sodium arsenite. J Biol Chem 278(9), 6885-95.

Dyson, N., Howley, P. M., Munger, K., and Harlow, E. (1989). The human papilloma virus-16 E7 oncoprotein is able to bind to the retinoblastoma gene product. Science 243(4893), 934-7.

Eckert, R. L., Efimova, T., Dashti, S. R., Balasubramanian, S., Deucher, A., Crish, J. F., Sturniolo, M., and Bone, F. (2002). Keratinocyte survival, differentiation, and death: many roads lead to mitogen-activated protein kinase. J Investig Dermatol Symp Proc 7(1), 36-40.

Edlund, S., Landstrom, M., Heldin, C. H., and Aspenstrom, P. (2002). Transforming growth factor-beta-induced mobilization of actin cytoskeleton requires signaling by small GTPases Cdc42 and RhoA. Mol Biol Cell 13(3), 902-14.

Egeblad, M., and Werb, Z. (2002). New functions for the matrix metalloproteinases in cancer progression. Nat Rev Cancer 2(3), 161-74.

Elliott, R. L., and Blobe, G. C. (2005). Role of transforming growth factor Beta in human cancer. J Clin Oncol 23(9), 2078-93.

Erreni, M., Mantovani, A., and Allavena, P. (2011). Tumor-associated Macrophages (TAM) and Inflammation in Colorectal Cancer. Cancer Microenviron 4(2), 141-54.

Fang, J. Y., and Richardson, B. C. (2005). The MAPK signalling pathways and colorectal cancer. Lancet Oncol 6(5), 322-7.

Faridi, R., Zahra, A., Khan, K., and Idrees, M. (2011). Oncogenic potential of Human Papillomavirus (HPV) and its relation with cervical cancer. Virol J 8, 269.

Galliher, A. J., and Schiemann, W. P. (2006). Beta3 integrin and Src facilitate transforming growth factor-beta mediated induction of epithelial-mesenchymal transition in mammary epithelial cells. Breast Cancer Res 8(4), R42.

Galliher, A. J., and Schiemann, W. P. (2007). Src phosphorylates Tyr284 in TGF-beta type II receptor and regulates TGF-beta stimulation of p38 MAPK during breast cancer cell proliferation and invasion. Cancer Res 67(8), 3752-8.

Ganguly, N., and Parihar, S. P. (2009). Human papillomavirus E6 and E7 oncoproteins as risk factors for tumorigenesis. J Biosci 34(1), 113-23.

Grady, W. M., Myeroff, L. L., Swinler, S. E., Rajput, A., Thiagalingam, S., Lutterbaugh, J. D., Neumann, A., Brattain, M. G., Chang, J., Kim, S. J., Kinzler, K. W., Vogelstein, B., Willson, J. K., and Markowitz, S. (1999). Mutational inactivation of transforming growth factor beta receptor type II in microsatellite stable colon cancers. Cancer Res 59(2), 320-4.

Grainge, M. J., Seth, R., Guo, L., Neal, K. R., Coupland, C., Vryenhoef, P., Johnson, J., and Jenkins, D. (2005). Cervical human papillomavirus screening among older women. Emerg Infect Dis 11(11), 1680-5.

Grifone, R., Demignon, J., Houbron, C., Souil, E., Niro, C., Seller, M. J., Hamard, G., and Maire, P. (2005). Six1 and Six4 homeoproteins are required for Pax3 and Mrf expression during myogenesis in the mouse embryo. Development 132(9), 2235-49.

Gu, W., Yeo, E., McMillan, N., and Yu, C. (2011). Silencing oncogene expression in cervical cancer stem-like cells inhibits their cell growth and self-renewal ability. Cancer Gene Ther 18(12), 897-905.

Gumbiner, B. M. (2005). Regulation of cadherin-mediated adhesion in morphogenesis. Nat Rev Mol Cell Biol 6(8), 622-34.

Haglund, K., and Dikic, I. (2005). Ubiquitylation and cell signaling. EMBO J 24(19), 3353-9.

Hanahan, D., and Coussens, L. M. (2012). Accessories to the crime: functions of cells recruited to the tumor microenvironment. Cancer Cell 21(3), 309-22.

Hannon, G. J., and Beach, D. (1994). p15INK4B is a potential effector of TGF-beta-induced cell cycle arrest. Nature 371(6494), 257-61.

Hanrahan, V., Currie, M. J., Gunningham, S. P., Morrin, H. R., Scott, P. A., Robinson, B. A., and Fox, S. B. (2003). The angiogenic switch for vascular endothelial growth factor (VEGF)-A, VEGF-B, VEGF-C, and VEGF-D in the adenoma-carcinoma sequence during colorectal cancer progression. J Pathol 200(2), 183-94.

Hartsough, M. T., and Mulder, K. M. (1995). Transforming growth factor beta activation of p44mapk in proliferating cultures of epithelial cells. J Biol Chem 270(13), 7117-24.

Ikeda, K., Kageyama, R., Suzuki, Y., and Kawakami, K. (2010). Six1 is indispensable for production of functional progenitor cells during olfactory epithelial development. Int J Dev Biol 54(10), 1453-64.

Iwanaga, R., Wang, C. A., Micalizzi, D. S., Harrell, J. C., Jedlicka, P., Sartorius, C. A., Kabos, P., Farabaugh, S. M., Bradford, A. P., and Ford, H. L. (2012). Expression of Six1 in luminal breast cancers predicts poor prognosis and promotes increases in tumor initiating cells by activation of extracellular signal-regulated kinase and transforming growth factor-beta signaling pathways. Breast Cancer Res 14(4), R100.

Jaffe, A. B., and Hall, A. (2005). Rho GTPases: biochemistry and biology. Annu Rev Cell Dev Biol 21, 247-69.

Jang, C. W., Chen, C. H., Chen, C. C., Chen, J. Y., Su, Y. H., and Chen, R. H. (2002). TGF-beta induces apoptosis through Smad-mediated expression of DAP-kinase. Nat Cell Biol 4(1), 51-8.

Jiang, F., Jia, Y., and Cohen, I. (2002). Fibronectin- and protein kinase C-mediated activation of ERK/MAPK are essential for proplateletlike formation. Blood 99(10), 3579-84.

Kawakami, K., Sato, S., Ozaki, H., and Ikeda, K. (2000). Six family genes--structure and function as transcription factors and their roles in development. Bioessays 22(7), 616-26.

Kim, M. S., Lee, E. J., Kim, H. R., and Moon, A. (2003). p38 kinase is a key signaling molecule for H-Ras-induced cell motility and invasive phenotype in human breast epithelial cells. Cancer Res 63(17), 5454-61.

Kong, W., Yang, H., He, L., Zhao, J. J., Coppola, D., Dalton, W. S., and Cheng, J. Q. (2008). MicroRNA-155 is regulated by the transforming growth factor beta/Smad pathway and contributes to epithelial cell plasticity by targeting RhoA. Mol Cell Biol 28(22), 6773-84.

Kowli, S., Velidandla, R., Creek, K. E., and Pirisi, L. (2013). TGF-beta regulation of gene expression at early and late stages of HPV16-mediated transformation of human keratinocytes. Virology 447(1-2), 63-73.

Kretzschmar, M., Doody, J., Timokhina, I., and Massague, J. (1999). A mechanism of repression of TGFbeta/ Smad signaling by oncogenic Ras. Genes Dev 13(7), 804-16.

Kumar, J. P. (2009). The sine oculis homeobox (SIX) family of transcription factors as regulators of development and disease. Cell Mol Life Sci 66(4), 565-83.

Laclef, C., Hamard, G., Demignon, J., Souil, E., Houbron, C., and Maire, P. (2003a). Altered myogenesis in Six1-deficient mice. Development 130(10), 2239-52.

Laclef, C., Souil, E., Demignon, J., and Maire, P. (2003b). Thymus, kidney and craniofacial abnormalities in Six 1 deficient mice. Mech Dev 120(6), 669-79.

Lakka, S. S., Jasti, S. L., Gondi, C., Boyd, D., Chandrasekar, N., Dinh, D. H., Olivero, W. C., Gujrati, M., and Rao, J. S. (2002). Downregulation of MMP-9 in ERK-mutated stable transfectants inhibits glioma invasion *in vitro*. Oncogene 21(36), 5601-8.

Lamouille, S., and Derynck, R. (2007). Cell size and invasion in TGF-beta-induced epithelial to mesenchymal transition is regulated by activation of the mTOR pathway. J Cell Biol 178(3), 437-51.

Lamouille, S., Xu, J., and Derynck, R. (2014). Molecular mechanisms of epithelial-mesenchymal transition. Nat Rev Mol Cell Biol 15(3), 178-96.

Larder, R., Clark, D. D., Miller, N. L., and Mellon, P. L. (2011). Hypothalamic dysregulation and infertility in mice lacking the homeodomain protein Six6. J Neurosci 31(2), 426-38.

Lavilla-Alonso, S., Abo-Ramadan, U., Halavaara, J., Escutenaire, S., Tatlisumak, T., Saksela, K., Kanerva, A., Hemminki, A., and Pesonen, S. (2011). Optimized mouse model for the imaging of tumor metastasis upon experimental therapy. PLoS One 6(11), e26810.

Lavoie, J. N., L'Allemain, G., Brunet, A., Muller, R., and Pouyssegur, J. (1996). Cyclin D1 expression is regulated positively by the p42/p44MAPK and negatively by the p38/HOGMAPK pathway. J Biol Chem 271(34), 20608-16.

Lee, M. K., Pardoux, C., Hall, M. C., Lee, P. S., Warburton, D., Qing, J., Smith, S. M., and Derynck, R. (2007). TGF-beta activates Erk MAP kinase signalling through direct phosphorylation of ShcA. EMBO J 26(17), 3957-67.

Levin, T. G., Powell, A. E., Davies, P. S., Silk, A. D., Dismuke, A. D., Anderson, E. C., Swain, J. R., and Wong, M. H. (2010). Characterization of the intestinal cancer stem cell marker CD166 in the human and mouse gastrointestinal tract. Gastroenterology 139(6), 2072-2082 e5.

Lewis, C., and Murdoch, C. (2005). Macrophage responses to hypoxia: implications for tumor progression and anti-cancer therapies. Am J Pathol 167(3), 627-35.

Li, C. M., Guo, M., Borczuk, A., Powell, C. A., Wei, M., Thaker, H. M., Friedman, R., Klein, U., and Tycko, B. (2002). Gene expression in Wilms' tumor mimics the earliest committed stage in the metanephric mesenchymal-epithelial transition. Am J Pathol 160(6), 2181-90.

Li, X., Oghi, K. A., Zhang, J., Krones, A., Bush, K. T., Glass, C. K., Nigam, S. K., Aggarwal, A. K., Maas, R., Rose, D. W., and Rosenfeld, M. G. (2003). Eya protein phosphatase activity regulates Six1-Dach-Eya transcriptional effects in mammalian organogenesis. Nature 426(6964), 247-54.

Li, Z., Tian, T., Hu, X., Zhang, X., Li, L., Nan, F., Chang, Y., Wang, X., Sun, Z., Lv, F., and Zhang, M. (2014). Targeting Six1 by lentivirus-mediated RNA interference inhibits colorectal cancer cell growth and invasion. Int J Clin Exp Pathol 7(2), 631-9.

Li, Z., Tian, T., Lv, F., Chang, Y., Wang, X., Zhang, L., Li, X., Li, L., Ma, W., Wu, J., and Zhang, M. (2013). Six1 promotes proliferation of pancreatic cancer cells via upregulation of cyclin D1 expression. PLoS One 8(3), e59203.

Lin, S. P., Lee, Y. T., Wang, J. Y., Miller, S. A., Chiou, S. H., Hung, M. C., and Hung, S. C. (2012). Survival of cancer stem cells under hypoxia and serum depletion via decrease in PP2A activity and activation of p38-MAPKAPK2-Hsp27. PLoS One 7(11), e49605.

Liu, Y., Nandi, S., Martel, A., Antoun, A., Ioshikhes, I., and Blais, A. (2012). Discovery, optimization and validation of an optimal DNA-binding sequence for the Six1 homeodomain transcription factor. Nucleic Acids Res 40(17), 8227-39.

Lopez-Otin, C., and Matrisian, L. M. (2007). Emerging roles of proteases in tumour suppression. Nat Rev Cancer 7(10), 800-8.

Mani, S. A., Guo, W., Liao, M. J., Eaton, E. N., Ayyanan, A., Zhou, A. Y., Brooks, M., Reinhard, F., Zhang, C. C., Shipitsin, M., Campbell, L. L., Polyak, K., Brisken, C., Yang, J., and Weinberg, R. A. (2008). The epithelial-mesenchymal transition generates cells with properties of stem cells. Cell 133(4), 704-15.

Mansour, S. J., Matten, W. T., Hermann, A. S., Candia, J. M., Rong, S., Fukasawa, K., Vande Woude, G. F., and Ahn, N. G. (1994). Transformation of mammalian cells by constitutively active MAP kinase kinase. Science 265(5174), 966-70.

Markowitz, S., Wang, J., Myeroff, L., Parsons, R., Sun, L., Lutterbaugh, J., Fan, R. S., Zborowska, E., Kinzler, K. W., Vogelstein, B., and et al. (1995). Inactivation of the type II TGF-beta receptor in colon cancer cells with microsatellite instability. Science 268(5215), 1336-8.

Martin, M. D., and Matrisian, L. M. (2007). The other side of MMPs: protective roles in tumor progression. Cancer Metastasis Rev 26(3-4), 717-24.

Matsumoto, K., Hashimoto, K., Hashiro, M., Yoshimasa, H., and Yoshikawa, K. (1990). Modulation of growth and differentiation in normal human keratinocytes by transforming growth factor-beta. J Cell Physiol 145(1), 95-101.

Meng, E., Long, B., Sullivan, P., McClellan, S., Finan, M. A., Reed, E., Shevde, L., and Rocconi, R. P. (2012). $CD44^{+}$/CD24- ovarian cancer cells demonstrate cancer stem cell properties and correlate to survival. Clin Exp Metastasis 29(8), 939-48.

Meulmeester, E., and Ten Dijke, P. (2011). The dynamic roles of TGF-beta in cancer. J Pathol 223(2), 205-18.

Mi, Y., Borger, D. R., Fernandes, P. R., Pirisi, L., and Creek, K. E. (2000). Loss of transforming growth factor-beta (TGF-beta) receptor type I mediates TGF-beta resistance in human papillomavirus type 16-transformed human keratinocytes at late stages of *in vitro* progression. Virology 270(2), 408-16.

Micalizzi, D. S., Christensen, K. L., Jedlicka, P., Coletta, R. D., Baron, A. E., Harrell, J. C., Horwitz, K. B., Billheimer, D., Heichman, K. A., Welm, A. L., Schiemann, W. P., and Ford, H. L. (2009). The Six1 homeoprotein induces human mammary carcinoma cells to undergo epithelial-mesenchymal transition and metastasis in mice through increasing TGF-beta signaling. J Clin Invest 119(9), 2678-90.

Micalizzi, D. S., Wang, C. A., Farabaugh, S. M., Schiemann, W. P., and Ford, H. L. (2010). Homeoprotein Six1 increases TGF-beta type I receptor and converts TGF-beta signaling from suppressive to supportive for tumor growth. Cancer Res 70(24), 10371-80.

Minn, A. J., Gupta, G. P., Padua, D., Bos, P., Nguyen, D. X., Nuyten, D., Kreike, B., Zhang, Y., Wang, Y., Ishwaran, H., Foekens, J. A., van de Vijver, M., and Massague, J. (2007). Lung metastasis genes couple breast tumor size and metastatic spread. Proc Natl Acad Sci U S A 104(16), 6740-5.

Minn, A. J., Kang, Y., Serganova, I., Gupta, G. P., Giri, D. D., Doubrovin, M., Ponomarev, V., Gerald, W. L., Blasberg, R., and Massague, J. (2005). Distinct organ-specific metastatic potential of individual breast cancer cells and primary tumors. J Clin Invest 115(1), 44-55.

Missero, C., Calautti, E., Eckner, R., Chin, J., Tsai, L. H., Livingston, D. M., and Dotto, G. P. (1995). Involvement of the cell-cycle inhibitor Cip1/WAF1 and the E1A-associated p300 protein in terminal differentiation. Proc Natl Acad Sci U S A 92(12), 5451-5.

Missero, C., Di Cunto, F., Kiyokawa, H., Koff, A., and Dotto, G. P. (1996). The absence of p21Cip1/WAF1 alters keratinocyte growth and differentiation and promotes ras-tumor progression. Genes Dev 10(23), 3065-75.

Mroczko, B., Groblewska, M., Wereszczynska-Siemiatkowska, U., Okulczyk, B., Kedra, B., Laszewicz, W., Dabrowski, A., and Szmitkowski, M. (2007). Serum macrophage-colony stimulating factor levels in colorectal cancer patients

correlate with lymph node metastasis and poor prognosis. Clin Chim Acta 380(1-2), 208-12.

Munoz, N., Bosch, F. X., de Sanjose, S., Herrero, R., Castellsague, X., Shah, K. V., Snijders, P. J., and Meijer, C. J. (2003). Epidemiologic classification of human papillomavirus types associated with cervical cancer. N Engl J Med 348(6), 518-27.

Myeroff, L. L., Parsons, R., Kim, S. J., Hedrick, L., Cho, K. R., Orth, K., Mathis, M., Kinzler, K. W., Lutterbaugh, J., Park, K., and et al. (1995). A transforming growth factor beta receptor type II gene mutation common in colon and gastric but rare in endometrial cancers with microsatellite instability. Cancer Res 55(23), 5545-7.

Ng, K. T., Lee, T. K., Cheng, Q., Wo, J. Y., Sun, C. K., Guo, D. Y., Lim, Z. X., Lo, C. M., Poon, R. T., Fan, S. T., and Man, K. (2010). Suppression of tumorigenesis and metastasis of hepatocellular carcinoma by shRNA interference targeting on homeoprotein Six1. Int J Cancer 127(4), 859-72.

Ng, K. T., Man, K., Sun, C. K., Lee, T. K., Poon, R. T., Lo, C. M., and Fan, S. T. (2006). Clinicopathological significance of homeoprotein Six1 in hepatocellular carcinoma. Br J Cancer 95(8), 1050-5.

Noordhuis, M. G., Fehrmann, R. S., Wisman, G. B., Nijhuis, E. R., van Zanden, J. J., Moerland, P. D., Ver Loren van Themaat, E., Volders, H. H., Kok, M., ten Hoor, K. A., Hollema, H., de Vries, E. G., de Bock, G. H., van der Zee, A. G., and Schuuring, E. (2011). Involvement of the TGF-beta and beta-catenin pathways in pelvic lymph node metastasis in early-stage cervical cancer. Clin Cancer Res 17(6), 1317-30.

Ohgushi, M., Kuroki, S., Fukamachi, H., O'Reilly, L. A., Kuida, K., Strasser, A., and Yonehara, S. (2005). Transforming growth factor beta-dependent sequential activation of Smad, Bim, and caspase-9 mediates physiological apoptosis in gastric epithelial cells. Mol Cell Biol 25(22), 10017-28.

Ono, H., Imoto, I., Kozaki, K., Tsuda, H., Matsui, T., Kurasawa, Y., Muramatsu, T., Sugihara, K., and Inazawa, J. (2012). SIX1 promotes epithelial-mesenchymal transition in colorectal cancer through ZEB1 activation. Oncogene 31(47), 4923-34.

Ozdamar, B., Bose, R., Barrios-Rodiles, M., Wang, H. R., Zhang, Y., and Wrana, J. L. (2005). Regulation of the polarity protein Par6 by TGFbeta receptors controls epithelial cell plasticity. Science 307(5715), 1603-9.

Peralta-Zaragoza, O., Bermudez-Morales, V. H., Perez-Plasencia, C., Salazar-Leon, J., Gomez-Ceron, C., and Madrid-Marina, V. (2012). Targeted treatments for cervical cancer: a review. Onco Targets Ther 5, 315-28.

Perl, A. K., Wilgenbus, P., Dahl, U., Semb, H., and Christofori, G. (1998). A causal role for E-cadherin in the transition from adenoma to carcinoma. Nature 392(6672), 190-3.

Pirisi, L., Batova, A., Jenkins, G. R., Hodam, J. R., and Creek, K. E. (1992). Increased sensitivity of human keratinocytes immortalized by human papillomavirus type 16 DNA to growth control by retinoids. Cancer Res 52(1), 187-93.

Pirisi, L., Creek, K. E., Doniger, J., and DiPaolo, J. A. (1988). Continuous cell lines with altered growth and differentiation properties originate after transfection of human keratinocytes with human papillomavirus type 16 DNA. Carcinogenesis 9(9), 1573-9.

Pirisi, L., Yasumoto, S., Feller, M., Doniger, J., and DiPaolo, J. A. (1987). Transformation of human fibroblasts and keratinocytes with human papillomavirus type 16 DNA. J Virol 61(4), 1061-6.

Pon, Y. L., Zhou, H. Y., Cheung, A. N., Ngan, H. Y., and Wong, A. S. (2008). p70 S6 kinase promotes epithelial to mesenchymal transition through snail induction in ovarian cancer cells. Cancer Res 68(16), 6524-32.

Qian, B. Z., and Pollard, J. W. (2010). Macrophage diversity enhances tumor progression and metastasis. Cell 141(1), 39-51.

Rao, Q. X., Yao, T. T., Zhang, B. Z., Lin, R. C., Chen, Z. L., Zhou, H., Wang, L. J., Lu, H. W., Chen, Q., Di, N., and Lin, Z. Q. (2012). Expression and functional role of ALDH1 in cervical carcinoma cells. Asian Pac J Cancer Prev 13(4), 1325-31.

Reichenberger, K. J., Coletta, R. D., Schulte, A. P., Varella-Garcia, M., and Ford, H. L. (2005). Gene amplification is a mechanism of Six1 overexpression in breast cancer. Cancer Res 65(7), 2668-75.

Reymond, N., d'Agua, B. B., and Ridley, A. J. (2013). Crossing the endothelial barrier during metastasis. Nat Rev Cancer 13(12), 858-70.

Ringshausen, I., Dechow, T., Schneller, F., Weick, K., Oelsner, M., Peschel, C., and Decker, T. (2004). Constitutive activation of the MAPkinase p38 is critical for MMP-9 production and survival of B-CLL cells on bone marrow stromal cells. Leukemia 18(12), 1964-70.

Ritchie, M. E., Silver, J., Oshlack, A., Holmes, M., Diyagama, D., Holloway, A., and Smyth, G. K. (2007). A comparison of background correction methods for two-colour microarrays. Bioinformatics 23(20), 2700-7.

Ruf, R. G., Xu, P. X., Silvius, D., Otto, E. A., Beekmann, F., Muerb, U. T., Kumar, S., Neuhaus, T. J., Kemper, M. J., Raymond, R. M., Jr., Brophy, P. D., Berkman, J., Gattas, M., Hyland, V., Ruf, E. M., Schwartz, C., Chang, E. H., Smith, R. J., Stratakis, C. A., Weil, D., Petit, C., and Hildebrandt, F. (2004). SIX1 mutations cause branchio-oto-renal syndrome by disruption of EYA1-SIX1-DNA complexes. Proc Natl Acad Sci U S A 101(21), 8090-5.

Rybak, A. P., Ingram, A. J., and Tang, D. (2013). Propagation of human prostate cancer stem-like cells occurs through EGFR-mediated ERK activation. PLoS One 8(4), e61716.

Sadot, E., Simcha, I., Shtutman, M., Ben-Ze'ev, A., and Geiger, B. (1998). Inhibition of beta-catenin-mediated transactivation by cadherin derivatives. Proc Natl Acad Sci U S A 95(26), 15339-44.

Saeki, Y., Nagashima, T., Kimura, S., and Okada-Hatakeyama, M. (2012). An ErbB receptor-mediated AP-1 regulatory network is modulated by STAT3 and c-MYC during calcium-dependent keratinocyte differentiation. Exp Dermatol 21(4), 293-8.

Sanggaard, K. M., Rendtorff, N. D., Kjaer, K. W., Eiberg, H., Johnsen, T., Gimsing, S., Dyrmose, J., Nielsen, K. O., Lage, K., and Tranebjaerg, L. (2007). Branchio-oto-renal syndrome: detection of EYA1 and SIX1 mutations in five out of six Danish families by combining linkage, MLPA and sequencing analyses. Eur J Hum Genet 15(11), 1121-31.

Saslow, D., Solomon, D., Lawson, H. W., Killackey, M., Kulasingam, S. L., Cain, J., Garcia, F. A., Moriarty, A. T., Waxman, A. G., Wilbur, D. C., Wentzensen, N., Downs, L. S., Jr., Spitzer, M., Moscicki, A. B., Franco, E. L., Stoler, M. H.,

Schiffman, M., Castle, P. E., and Myers, E. R. (2012). American Cancer Society, American Society for Colposcopy and Cervical Pathology, and American Society for Clinical Pathology screening guidelines for the prevention and early detection of cervical cancer. CA Cancer J Clin 62(3), 147-72.

Schima, W., Kulinna, C., Langenberger, H., and Ba-Ssalamah, A. (2005). Liver metastases of colorectal cancer: US, CT or MR? Cancer Imaging 5 Spec No A, S149-56.

Schmidt, M., Goebeler, M., Posern, G., Feller, S. M., Seitz, C. S., Brocker, E. B., Rapp, U. R., and Ludwig, S. (2000). Ras-independent activation of the Raf/MEK/ERK pathway upon calcium-induced differentiation of keratinocytes. J Biol Chem 275(52), 41011-7.

Schmitt, M., Depuydt, C., Benoy, I., Bogers, J., Antoine, J., Arbyn, M., and Pawlita, M. (2013). Prevalence and viral load of 51 genital human papillomavirus types and three subtypes. Int J Cancer 132(10), 2395-403.

Schock, F., and Perrimon, N. (2002). Molecular mechanisms of epithelial morphogenesis. Annu Rev Cell Dev Biol 18, 463-93.

Self, M., Lagutin, O. V., Bowling, B., Hendrix, J., Cai, Y., Dressler, G. R., and Oliver, G. (2006). Six2 is required for suppression of nephrogenesis and progenitor renewal in the developing kidney. EMBO J 25(21), 5214-28.

Seoane, J., Le, H. V., Shen, L., Anderson, S. A., and Massague, J. (2004). Integration of Smad and forkhead pathways in the control of neuroepithelial and glioblastoma cell proliferation. Cell 117(2), 211-23.

Sheridan, C., Kishimoto, H., Fuchs, R. K., Mehrotra, S., Bhat-Nakshatri, P., Turner, C. H., Goulet, R., Jr., Badve, S., and Nakshatri, H. (2006). $CD44^{+}$/CD24- breast cancer cells exhibit enhanced invasive properties: an early step necessary for metastasis. Breast Cancer Res 8(5), R59.

Shin, I., Bakin, A. V., Rodeck, U., Brunet, A., and Arteaga, C. L. (2001). Transforming growth factor beta enhances epithelial cell survival via Akt-dependent regulation of FKHRL1. Mol Biol Cell 12(11), 3328-39.

Shipitsin, M., Campbell, L. L., Argani, P., Weremowicz, S., Bloushtain-Qimron, N., Yao, J., Nikolskaya, T., Serebryiskaya, T., Beroukhim, R., Hu, M., Halushka, M. K.,

Sukumar, S., Parker, L. M., Anderson, K. S., Harris, L. N., Garber, J. E., Richardson, A. L., Schnitt, S. J., Nikolsky, Y., Gelman, R. S., and Polyak, K. (2007). Molecular definition of breast tumor heterogeneity. Cancer Cell 11(3), 259-73.

Siegel, P. M., and Massague, J. (2003). Cytostatic and apoptotic actions of TGF-beta in homeostasis and cancer. Nat Rev Cancer 3(11), 807-21.

Siegel, R., Desantis, C., and Jemal, A. (2014). Colorectal cancer statistics, 2014. CA Cancer J Clin 64(2), 104-17.

Simon, C., Simon, M., Vucelic, G., Hicks, M. J., Plinkert, P. K., Koitschev, A., and Zenner, H. P. (2001). The p38 SAPK pathway regulates the expression of the MMP-9 collagenase via AP-1-dependent promoter activation. Exp Cell Res 271(2), 344-55.

Smith, J. J., Deane, N. G., Wu, F., Merchant, N. B., Zhang, B., Jiang, A., Lu, P., Johnson, J. C., Schmidt, C., Bailey, C. E., Eschrich, S., Kis, C., Levy, S., Washington, M. K., Heslin, M. J., Coffey, R. J., Yeatman, T. J., Shyr, Y., and Beauchamp, R. D. (2010). Experimentally derived metastasis gene expression profile predicts recurrence and death in patients with colon cancer. Gastroenterology 138(3), 958-68.

Society, A. C. (2013). "Cancer Facts and Figures 2013." American Cancer Society, Atlanta.

Sorrentino, A., Thakur, N., Grimsby, S., Marcusson, A., von Bulow, V., Schuster, N., Zhang, S., Heldin, C. H., and Landstrom, M. (2008). The type I TGF-beta receptor engages TRAF6 to activate TAK1 in a receptor kinase-independent manner. Nat Cell Biol 10(10), 1199-207.

Spitz, F., Demignon, J., Porteu, A., Kahn, A., Concordet, J. P., Daegelen, D., and Maire, P. (1998). Expression of myogenin during embryogenesis is controlled by Six/sine oculis homeoproteins through a conserved MEF3 binding site. Proc Natl Acad Sci U S A 95(24), 14220-5.

Staller, P., Peukert, K., Kiermaier, A., Seoane, J., Lukas, J., Karsunky, H., Moroy, T., Bartek, J., Massague, J., Hanel, F., and Eilers, M. (2001). Repression of p15INK4b expression by Myc through association with Miz-1. Nat Cell Biol 3(4), 392-9.

Steeg, P. S. (2006). Tumor metastasis: mechanistic insights and clinical challenges. Nat Med 12(8), 895-904.

Tan, J., Zhang, C., and Qian, J. (2011). Expression and significance of Six1 and Ezrin in cervical cancer tissue. Tumour Biol 32(6), 1241-7.

Terzic, J., Grivennikov, S., Karin, E., and Karin, M. (2010). Inflammation and colon cancer. Gastroenterology 138(6), 2101-2114 e5.

Toft, L., Tolstrup, M., Muller, M., Sehr, P., Bonde, J., Storgaard, M., Ostergaard, L., and Sogaard, O. S. (2014). Comparison of the immunogenicity of Cervarix and Gardasil human papillomavirus vaccines for oncogenic non-vaccine serotypes HPV-31, HPV-33, and HPV-45 in HIV-infected adults. Hum Vaccin Immunother 10(5).

Wagner, E. F., and Nebreda, A. R. (2009). Signal integration by JNK and p38 MAPK pathways in cancer development. Nat Rev Cancer 9(8), 537-49.

Walboomers, J. M., Jacobs, M. V., Manos, M. M., Bosch, F. X., Kummer, J. A., Shah, K. V., Snijders, P. J., Peto, J., Meijer, C. J., and Munoz, N. (1999). Human papillomavirus is a necessary cause of invasive cervical cancer worldwide. J Pathol 189(1), 12-9.

Wan, F., Miao, X., Quraishi, I., Kennedy, V., Creek, K. E., and Pirisi, L. (2008). Gene expression changes during HPV-mediated carcinogenesis: a comparison between an *in vitro* cell model and cervical cancer. Int J Cancer 123(1), 32-40.

Wang, C. A., Jedlicka, P., Patrick, A. N., Micalizzi, D. S., Lemmer, K. C., Deitsch, E., Casas-Selves, M., Harrell, J. C., and Ford, H. L. (2012). SIX1 induces lymphangiogenesis and metastasis via upregulation of VEGF-C in mouse models of breast cancer. J Clin Invest 122(5), 1895-906.

Wei, S. C., Tsao, P. N., Weng, M. T., Cao, Z., and Wong, J. M. (2013). Flt-1 in colorectal cancer cells is required for the tumor invasive effect of placental growth factor through a p38-MMP9 pathway. J Biomed Sci 20, 39.

Wendt, M. K., Allington, T. M., and Schiemann, W. P. (2009). Mechanisms of the epithelial-mesenchymal transition by TGF-beta. Future Oncol 5(8), 1145-68.

Werness, B. A., Levine, A. J., and Howley, P. M. (1990). Association of human papillomavirus types 16 and 18 E6 proteins with p53. Science 248(4951), 76-9.

Wettenhall, J. M., and Smyth, G. K. (2004). limmaGUI: a graphical user interface for linear modeling of microarray data. Bioinformatics 20(18), 3705-6.

Wilkes, M. C., Mitchell, H., Penheiter, S. G., Dore, J. J., Suzuki, K., Edens, M., Sharma, D. K., Pagano, R. E., and Leof, E. B. (2005). Transforming growth factor-beta activation of phosphatidylinositol 3-kinase is independent of Smad2 and Smad3 and regulates fibroblast responses via p21-activated kinase-2. Cancer Res 65(22), 10431-40.

Wilkes, M. C., Murphy, S. J., Garamszegi, N., and Leof, E. B. (2003). Cell-type-specific activation of PAK2 by transforming growth factor beta independent of Smad2 and Smad3. Mol Cell Biol 23(23), 8878-89.

Wong, C., Law, W. L., Wan, Y. F., Poon, J. T., and Lam, C. L. (2014). Health-related quality of life and risk of colorectal cancer recurrence and All-cause death among advanced stages of colorectal cancer 1-year after diagnosis. BMC Cancer 14(1), 337.

Woodhouse, E. C., Chuaqui, R. F., and Liotta, L. A. (1997). General mechanisms of metastasis. Cancer 80(8 Suppl), 1529-37.

Xie, Z., and Bikle, D. D. (2007). The recruitment of phosphatidylinositol 3-kinase to the E-cadherin-catenin complex at the plasma membrane is required for calcium-induced phospholipase C-gamma1 activation and human keratinocyte differentiation. J Biol Chem 282(12), 8695-703.

Xu, H., Zhang, Y., Altomare, D., Pena, M. M., Wan, F., Pirisi, L., and Creek, K. E. (2014). Six1 promotes epithelial-mesenchymal transition and malignant conversion in human papillomavirus type 16-immortalized human keratinocytes. Carcinogenesis.

Xu, L., Cochran, D. M., Tong, R. T., Winkler, F., Kashiwagi, S., Jain, R. K., and Fukumura, D. (2006). Placenta growth factor overexpression inhibits tumor growth, angiogenesis, and metastasis by depleting vascular endothelial growth factor homodimers in orthotopic mouse models. Cancer Res 66(8), 3971-7.

Xu, P. X., Zheng, W., Huang, L., Maire, P., Laclef, C., and Silvius, D. (2003). Six1 is required for the early organogenesis of mammalian kidney. Development 130(14), 3085-94.

Yamaguchi, K., Shirakabe, K., Shibuya, H., Irie, K., Oishi, I., Ueno, N., Taniguchi, T., Nishida, E., and Matsumoto, K. (1995). Identification of a member of the MAPKKK family as a potential mediator of TGF-beta signal transduction. Science 270(5244), 2008-11.

Yamashita, M., Fatyol, K., Jin, C., Wang, X., Liu, Z., and Zhang, Y. E. (2008). TRAF6 mediates Smad-independent activation of JNK and p38 by TGF-beta. Mol Cell 31(6), 918-24.

Yao, T., Chen, Q., Zhang, B., Zhou, H., and Lin, Z. (2011). The expression of ALDH1 in cervical carcinoma. Med Sci Monit 17(8), HY21-26.

Yi, J. Y., Shin, I., and Arteaga, C. L. (2005). Type I transforming growth factor beta receptor binds to and activates phosphatidylinositol 3-kinase. J Biol Chem 280(11), 10870-6.

Yoshino, Y., Aoyagi, M., Tamaki, M., Duan, L., Morimoto, T., and Ohno, K. (2006). Activation of p38 MAPK and/or JNK contributes to increased levels of VEGF secretion in human malignant glioma cells. Int J Oncol 29(4), 981-7.

Yu, L., Hebert, M. C., and Zhang, Y. E. (2002). TGF-beta receptor-activated p38 MAP kinase mediates Smad-independent TGF-beta responses. EMBO J 21(14), 3749-59.

Yu, Y., Davicioni, E., Triche, T. J., and Merlino, G. (2006). The homeoprotein six1 transcriptionally activates multiple protumorigenic genes but requires ezrin to promote metastasis. Cancer Res 66(4), 1982-9.

Yu, Y., Khan, J., Khanna, C., Helman, L., Meltzer, P. S., and Merlino, G. (2004). Expression profiling identifies the cytoskeletal organizer ezrin and the developmental homeoprotein Six-1 as key metastatic regulators. Nat Med 10(2), 175-81.

Zhang, Y., Feng, X. H., and Derynck, R. (1998). Smad3 and Smad4 cooperate with c-Jun/c-Fos to mediate TGF-beta-induced transcription. Nature 394(6696), 909-13.

Zhang, Y. E. (2009). Non-Smad pathways in TGF-beta signaling. Cell Res 19(1), 128-39.

Zheng, W., Huang, L., Wei, Z. B., Silvius, D., Tang, B., and Xu, P. X. (2003). The role of Six1 in mammalian auditory system development. Development 130(17), 3989-4000.

Zheng, X. H., Liang, P. H., Guo, J. X., Zheng, Y. R., Han, J., Yu, L. L., Zhou, Y. G., and Li, L. (2010). Expression and clinical implications of homeobox gene Six1 in cervical cancer cell lines and cervical epithelial tissues. Int J Gynecol Cancer 20(9), 1587-92.

Zyzak, L. L., MacDonald, L. M., Batova, A., Forand, R., Creek, K. E., and Pirisi, L. (1994). Increased levels and constitutive tyrosine phosphorylation of the epidermal growth factor receptor contribute to autonomous growth of human papillomavirus type 16 immortalized human keratinocytes. Cell Growth Differ 5(5), 537-47.